Exploring the pathophysiological cell signalling pathways induced by the osteoblast protein BRIL

Vincent Maranda

Department of Human Genetics

McGill University

Montréal, Québec, Canada

August 2019

A thesis submitted to McGill University in partial fulfillment of the requirements of the degree of Master of Science

ABSTRACT

Osteogenesis imperfecta (OI) is a heritable disorder that affects bones and leads to overall skeletal fragility and frequent fractures in children. The genetic cause of OI type V is a recurrent heterozygous c.-14C>T point mutation in the 5'-UTR of the BRIL gene. It causes a novel in-frame translation start site (ATG) that adds 5 amino acids (MALEP) onto the N-terminus of the BRIL osteoblast-specific membrane protein. Another dominant *BRIL* mutation, introducing a single amino acid change (serine to leucine) at position 40 of the protein (S40L-BRIL), was found to cause atypical OI type VI. It is hypothesized that the two mutant forms of BRIL have different mechanisms which lead to distinct forms of OI. The specific mechanisms by which the mutant proteins cause these disorders has yet to be ascertained, although a gain-of-function has been proposed. We hypothesize that the mutant BRIL proteins act by activating intracellular signalling pathway(s) leading to perturbed osteoblast function. To explore this possibility, prior to the beginning of the project, a screen was performed by transient transfection in MC3T3 osteoblasts whether BRIL could activate luciferase (Luc) reporters driven by multimerized copies of binding sites for 20 individual transcription factors. Starting from there, we found that BRIL robustly activated MEF2-Luc and NFATC-Luc in MC3T3 and MLO-A5. Induction of MEF2-Luc by BRIL was also detected in human SaOS-2 and rat UMR106 osteosarcoma cells, but not in HEK293 and NIH3T3 cells, thereby demonstrating that BRIL's activity is limited to cells of bone origin. The activity elicited by BRIL were comparable to those induced by expression of MEF2C and NFATc1 and in the case of MEF2C, acted synergistically when combined with BRIL. MEF2-Luc activation by BRIL was dose-dependent and could be suppressed by

co-expression of the MEF2 antagonist HDAC4. As compared to WT-BRIL, MALEP-BRIL showed consistently high induction levels in MLO-A5 cells, while S40L-BRIL significantly lower induction levels. In MLO-A5 cells, upregulation of *Ptgs2* (COX2) and *Nr4a3* was detected as well as induction of a Ptgs2-Luc reporter following MALEP-BRIL transfections. Mechanistically, BRIL did not affect MEF2 or NFATC gene expression. Modulation experiments using factors involved in the Ca^{2+}-calcineurin-NFAT signaling pathway as well as FK506 revealed a potential axis by which BRIL's effect is transmitted downstream to transcription factors. Structure-function studies showed that disruption of BRIL first five amino acids, whether by the presence of tags, amino acid deletion or alanine scanning resulted in inhibition of MEF2C and NFAT's inductions, thereby pointing to BRIL's function at its N-terminal. High amino acid conservation also hints at the same region of the protein having an important function. Specifically, disruption of D2, T3 and Y5 showed the greatest effect on luciferase readouts in MC3T3 cells. In sum, it is now possible to include MEF2, NFAT and COX2 as candidates for interaction with BRIL, which has clarified BRIL's function, and is of value to elucidate the functions specific to MALEP-BRIL and S40L-BRIL. Considering many questions remain in regard to the BRIL protein in general and its two mutant forms, further elucidating these functions could serve as new avenues to therapeutic applications for OI type V and atypical type VI.

RÉSUMÉ

L'ostéogenèse imparfaite (OI) est un trouble héréditaire qui affecte les os et conduit à la fragilité générale du squelette et à de fréquentes fractures chez les enfants. La cause génétique de l'OI de type V est une mutation hétérozygote récurrente ponctuelle C-14C> T dans la séquence 5'-UTR du gène BRIL. Il crée un nouveau site d'initiation de la traduction (ATG) qui ajoute 5 acides aminés (MALEP) à l'extrémité N-terminale de la protéine membranaire spécifique des ostéoblastes BRIL. Une autre mutation dominante de BRIL, introduisant un seul changement d'acide aminé (sérine en leucine) à la position 40 de la protéine (S40L-BRIL), s'est avérée causer une OI atypique de type VI. On suppose que les deux formes mutantes de BRIL ont des mécanismes différents qui conduisent à des formes distinctes d'OI. Les mécanismes spécifiques par lesquels les protéines mutantes sont à l'origine de ces troubles doivent encore être déterminés, bien qu'un gain de fonction ait été proposé. Nous émettons l'hypothèse que les protéines BRIL mutantes agissent en activant une ou plusieurs voies de signalisation intracellulaires conduisant à une perturbation de la fonction des ostéoblastes. Pour explorer cette possibilité, avant le début du projet, un crible a été réalisé par transfection transitoire dans les ostéoblastes MC3T3 pour savoir si BRIL pouvait activer des rapporteurs de luciférase (Luc) sous le contrôle de copies multimérisées de sites de liaison pour 20 facteurs de transcription individuels. À partir de là, nous avons constaté que BRIL avait activé de manière robuste MEF2-Luc et NFATC-Luc dans les MC3T3 et MLO-A5. L'induction de MEF2-Luc par BRIL a également été détectée dans les cellules humaines et de rat d'ostéosarcome SaOS-2 et UMR106 respectivement, mais pas dans les cellules HEK293 et NIH3T3, démontrant

ainsi que l'activité de BRIL est limitée aux cellules osseuses. Les activités induites par BRIL étaient comparables à celles induites par l'expression de MEF2C et NFATc1 et, dans le cas de MEF2C, agissait en synergie lorsqu'elle était combinée avec BRIL. L'activation de MEF2-Luc par BRIL était dépendante de la dose et pouvait être supprimée par la co-expression de HDAC4, un antagoniste de MEF2. Par rapport au WT-BRIL, MALEP-BRIL a affiché des niveaux d'induction systématiquement élevés dans les cellules MLO-A5, tandis que le S40L-BRIL générait des niveaux d'induction bas. Dans les cellules MLO-A5, une régulation à la hausse de *Ptgs2* (COX2) et de *Nr4a3* a été détectée ainsi que l'induction d'un rapporteur Ptgs2-Luc à la suite de transfections MALEP-BRIL. De plus, BRIL n'a pas affecté l'expression des gènes MEF2 ou NFATC. Des expériences de modulation utilisant des facteurs impliqués dans la voie de signalisation de la Ca^{2+}-calcineurine-NFAT ainsi que du FK506 ont révélé un axe potentiel par lequel l'effet de BRIL est transmis en aval aux facteurs de transcription. Des études de structure-fonction ont montré que la perturbation des cinq premiers acides aminés de BRIL, que ce soit par la présence d'étiquettes, la suppression d'acides aminés ou le balayage d'alanine, entraînait une inhibition des inductions de MEF2C et de NFAT, indiquant ainsi la fonction de BRIL à son extrémité N-terminale. Une conservation élevée en acides aminés fait également allusion à la même région de la protéine ayant une fonction importante. Plus précisément, la perturbation de D2, T3 et Y5 a eu le plus grand effet sur la lecture de la luciférase dans les cellules MC3T3. En résumé, il est maintenant possible d'inclure MEF2, NFAT et COX2 en tant que candidats à une interaction avec BRIL, ce qui a clarifié la fonction de BRIL et est utile pour élucider les fonctions spécifiques à MALEP-BRIL et S40L-BRIL. Considérant que

de nombreuses questions subsistent en ce qui concerne la protéine BRIL en général et ses deux formes mutantes, une élucidation plus poussée de ces fonctions pourrait constituer une nouvelle voie pour des applications thérapeutiques des OI de types V et atypiques de type VI.

TABLE OF CONTENTS

LIST OF ABBREVIATIONS

Actb	Gene encoding mouse β-actin
AdipoQ	Gene encoding mouse adiponectin, C1Q
ALPL	Gene encoding human alkaline phosphatase, biomineralization associated
ANOVA	Analysis of variance
AP1	Activator protein 1
B2m	Gene encoding mouse β(2)-microglobulin
BGLAP	Gene encoding human bone gamma carboxyglutamate protein
Bglap	Gene encoding mouse bone gamma carboxyglutamate protein
BMP1	Bone morphogenetic protein 1
bp	Base pair
BRIL	Bone-restricted Ifitm-like protein, AKA IFITM5
BRIL	Gene encoding human bone-restricted Ifitm-like protein, AKA IFITM5
Bril	Gene encoding mouse bone-restricted Ifitm-like protein, AKA Ifitm5
Bril	Gene encoding mouse bone-restricted Ifitm-like
Bts2	Gene encoding mouse bone marrow stromal cell antigen 2
C	Carboxyl
Ca^{2+}	Calcium
cAMP	Cyclic adenosine monophosphate
CD225	Cluster of differentiation 225
CD81	Cluster of differentiation 81
CD9	Cluster of differentiation 9

cDNA	Complimentary deoxyribonucleic acid
CMV	Cytomegalovirus
Cn-A	Calcineurin, subunit α
COL1A1	Gene encoding human collagen type 1 α1 chain
Col1a1	Gene encoding mouse collagen type 1 α1 chain
COL1A2	Gene encoding human collagen type 1 α2 chain
Col2-Sox9	Collagen type II / SRY-box 9
COPII	Coat protein complex II
CRTAP	Cartilage-associated protein
DAPI	4′,6-diamidino-2-phenylindole
DNA	Deoxyribonucleic acid
E	Embryonic day
EDTA	Ethylenediaminetetraacetic acid
ERK	Extracellular signal-regulated kinase
Fabp4	Gene encoding mouse fatty acid binding protein 4
FK506	Tacrolimus / Fujimycin
FKBP	FK506 binding protein
FOXO	Forkhead box
FPRP	F2 receptor negative regulator
GFP	Green fluorescent protein
GLI1	GLI family zinc finger 1
GLI2	GLI family zinc finger 2
GLI3	GLI family zinc finger 3

Hdac1	Gene encoding mouse histone deacetylase 1
HDAC1	Histone deacetylase 1
Hdac2	Gene encoding mouse histone deacetylase 2
HDAC2	Histone deacetylase 2
Hdac3	Gene encoding mouse histone deacetylase 3
HDAC3	Histone deacetylase 3
Hdac4	Gene encoding mouse histone deacetylase 4
HDAC4	Histone deacetylase 4
Hdac5	Gene encoding mouse histone deacetylase 5
HDAC5	Histone deacetylase 5
Hdac7	Gene encoding mouse histone deacetylase 7
HDAC7	Histone deacetylase 7
HEK293	Human embryonic kidney cells
IBSP	Gene encoding human integrin binding sialoprotein
Ibsp	Gene encoding mouse integrin binding sialoprotein
Ifit3	Gene encoding mouse interferon-induced protein with tetratricopeptide repeats 3
IFITM	Interferon induced transmembrane protein family
Ifitm	Interferon induced transmembrane gene family
IFITM1	Gene encoding human interferon induced transmembrane protein 1
Ifitm1	Gene encoding mouse interferon induced transmembrane protein 1
IFITM10	Interferon induced transmembrane protein 10
IFITM2	Gene encoding human interferon induced transmembrane protein 2

Ifitm2	Gene encoding mouse interferon induced transmembrane protein 2
IFITM3	Gene encoding human interferon induced transmembrane protein 3
Ifitm3	Gene encoding mouse interferon induced transmembrane protein 3
IFITM5	Interferon induced transmembrane protein 5, (BRIL)
IFITM5	Gene encoding human interferon induced transmembrane protein 5, (*BRIL*)
Ifitm5	Gene encoding mouse interferon induced transmembrane protein 5, (*Bril*)
Ifitm6	Gene encoding mouse interferon induced transmembrane protein 6
Ifitm7	Gene encoding mouse interferon induced transmembrane protein 7
IFN	Interferon
IFN-α	Interferon alpha
IFN-γ	Interferin gamma
IL-2	Interleukin-2
Irgm	Gene encoding mouse interferon inducible protein 1
JNK	c-Jun N-terminal kinase
kb	Kilobase
kDa	KiloDalton
KDEL	Lysine-Aspartic acid-Glutamic acid-Leucine
KI	Knock-in
KO	Knockout
LEPRE1	Prolyl 3-hydroxylase 1
MALEP-BRIL	Bone-restricted IFITM-like protien with mutant MALEP amino acid extension

MAPK	Mitogen-activated protein kinase
MC3T3	Mouse osteoblast cell line
Mef2a	Gene encoding mouse myocyte enhancer factor 2A
MEF2A	Myocyte enhancer factor 2A
Mef2b	Gene encoding mouse myocyte enhancer factor 2B
MEF2B	Myocyte enhancer factor 2B
Mef2c	Gene encoding mouse myocyte enhancer factor 2C
MEF2C	Myocyte enhancer factor 2C
Mef2d	Gene encoding mouse myocyte enhancer factor 2D
MEF2D	Myocyte enhancer factor 2D
Mhc	Gene encoding mouse histocompatibility complex
MLO-A5	Murine long bone osteocyte A5
MLO-Y4	Murine long bone osteocyte Y4
N	Amino
NFAT	Nuclear factor of activated T-cells
Nfatc1	Gene encoding mouse nuclear factor of activated T cells 1
NFATc1	Nuclear factor of activated T-cells 1
Nfatc2	Gene encoding mouse nuclear factor of activated T cells 2
NIH3T3	Mouse embryonic fibroblast cells
NR4A1	Nuclear Receptor Subfamily 4 Group A Member 1
NR4A2	Nuclear Receptor Subfamily 4 Group A Member 2
Nr4a3	Gene encoding mouse nuclear receptor subfamily 4 group A member 3
NR4A3	Nuclear Receptor Subfamily 4 Group A Member 3

Ocn	Gene encoding mouse osteocalcin
OI	Osteogenesis imperfecta
Osterix / Sp7	Sp7 Transcription factor
PEDF	Pigment epithelium-derived factor
PG	Prostaglandins
PKA	Protein kinase A
PPIase	Peptidylprolyl cis/trans isomerase
PPIB	Cyclophilin B
Ptgs2	Gene encoding mouse prostaglandin-endoperoxide synthase 2
COX2	Cyclooxygenase II
PTH	Parathyroid hormone
RBP-Jk	Recombining binding protein suppressor of hairless
RCAN1	Regulator of calcineurin 1
rER	Rough endoplasmic reticulum
RNA	Ribonucleic acid
RT-qPCR	Reverse transcription - quantitative polymerase chain reaction
RUNX2	Runt-related transcription factor 2
Runx2	Gene encoding mouse runt-related transcription factor 2
S40L-BRIL	Bone-restricted IFITM-like protien with mutant S40L amino acid replacement
SaOS-2	Human osteosarcoma cells
SD	Standard deviation
SE	Standard error

SERPINF1	Gene encoding human pigment epithelium-derived factor
Serpinf1	Gene encoding mouse serpin family F member 1
SERPINH1	Heat-shock protein 47
Sfrp2	Secreted Frizzled Related Protein 2
Sfrp3	Secreted Frizzled Related Protein 3
Sost	Gene encoding mouse sclerostin
Sp1	Specific protein 1
Sp3	Specific protein 3
SPP1	Gene encoding human secreted phosphoprotein 1
STAT3	Signal transducer and activator of transcription 3
TFX	Transfection
TRAP	Tartrate-resistant phosphatase
UMR106	Rat osteosarcoma cell line
UTR	Untranslated region
W	Well
Wnt	Wingless
WNT1	Wingless family member 1
WT	Wild-type
ZFP354C	Zinc finger protein 354c

LIST OF FIGURES

LIST OF TABLES

ACKNOWLEDGEMENTS

I would like to begin by thanking my supervisor, Dr. Pierre Moffatt, for being a phenomenal guide and mentor throughout my master's degree. He was always there to discuss results, answer questions and help with report redactions, poster and oral presentation and overall everyday work, and for this I am grateful. His inspiring work ethic, patience and passion have allowed me to grow as a student and scientist.

I also thank the members of my supervisory committee, Dr. René St-Arnaud and Dr. Xiang-Jiao Yang, for their wise suggestions and feedback critical for the progression and completion of my project.

I express my gratitude to the past and present members of the lab, notably Marie-Hélène Gaumond, Lisa Lamplugh, Samantha Robinson and Iliana Palenzuela, for the endless willingness to help with any laboratory work. A special thanks goes to Marie-Hélène, who dedicated many hours to train and guide me for two years. I am also very grateful to all lab members, as well as Barb Small and Paul Richard, for creating such a pleasant work environment.

I would like the thank the Réseau de recherche en santé buccodentaire et osseuse (RSBO) and the McGill University Human Genetics Department for funding and awards. I thank the McGill University Department of Human Genetics for providing me with various learning and networking opportunities.

Lastly, I would like to thank my family and my fiancée for their endless support and encouragement, to whom I owe all my accomplishments and success.

Chapter 1: INTRODUCTION

1.1. Bone-restricted IFITM-like protein

1.1.1. Discovery of BRIL

BRIL (bone-restricted Ifitm-like) was discovered using a signal trap screening assay [1] of cDNAs in the UMR106 rat osteosarcoma cell line [2]. A later *in silico* analysis of the 309 base pair cDNA fragment identified homology with the Interferon inducible transmembrane 5 (*Ifitm5)* gene, which is part of the interferon-induced transmembrane (IFITM) gene family, a group of interferon (IFN) inducible genes. *Ifitm5/Bril* was detected in parallel by a DNA microarray analysis of the MC3T3 mouse osteoblast cell line and was characterized as an osteoblast marker [3].

Analysis of rat and mouse tissue samples showed that *Bril* has a bone-restricted expression [2, 4]. Specifically, it is found only in osteoblasts from both intramembranous and endochondral ossification origins [2]. *Bril* is present as early as embryonic day 14.5 (E14.5) in long bones at the metaphyseal/epiphyseal region and at the bone collar of the developing diaphysis. Around E16.5, BRIL can be detected in newly formed trabecular bone, specifically in osteoblasts. BRIL's expression is persistent, albeit decreasingly, until mice are 8 months old [2]. BRIL was also found during physiological and mechanically induced tooth movement of young adult mice, specifically in the cellular cementum and regions of alveolar bone of jaw bones [5].

Through cell culture differentiation *in vitro* studies, the expression of BRIL was linked with osteoblast differentiation and matrix production. BRIL was not detected in either MLO-Y4 mouse osteocyte cells or osteoclasts from mouse bone marrow cells.

However, specifically in MC3T3 osteoblasts, BRIL expression was noted from day 4 onwards until day 27, peaking at day 21 [2]. These expression patterns and traits markedly distinguish BRIL from the initial IFITM family it was identified as being part of, as detailed in the following section.

1.1.2. *Ifitm* family

BRIL was initially categorised in the IFITM family due to its proximity and its homology with other members of the family. The IFITM gene family are a group of IFN inducible genes, discovered by screening human neuroblastoma cells [6]. The screen was conducted in 1984 and identified *IFITM1*, *IFITM2* and *IFITM3*, which have later shown to have antiviral activities [7]. Later, it was also identified that *IFITM1/Ifitm1*, *IFITM2/Ifitm2*, *IFITM3/Ifitm3* and *IFITM5/Ifitm5* reside contiguously on a 23kb or 60kb DNA segment on the human or mouse chromosome 11p15.5 and 7F5 respectively [8]. IFITM1, IFITM2 and IFITM3 were categorised into the first of three clades, classifying IFITM family members [8]. Clade I also include murine orthologs, as well as *Ifitm6* and *Ifitm7*, the latter being encoded by a processed gene derived from the *Ifitm1* gene. Apart from *Ifitm7*, all IFITM genes have an intron flanked by two coding exons [8, 9]. Clade II and III both only have one member: IFITM5 (BRIL) and IFITM10 respectively, neither of which are interferon inducible nor have an antiviral function.

Prediction analyses grouped the IFITM genes together for a conserved CD225 domain and two projected transmembrane domains, though these do not necessarily translate to physiological functional domains [10]. Each human *IFITM1-3* contain IFN response elements in their promoter regions, and are induced by IFN-α and IFN-γ [11].

However, in mice, only *Ifitm3* was responsive to IFNs. As such, IFITM1-3 are all antiviral proteins due to their induction in response to viral infection. They restrict viral entry and heighten cellular resistance against many viral pathogens, which include Marburg and Ebola filoviruses, influenza A, West Nile virus, Dengue virus, human immunodeficiency virus-1 and severe acute respiratory syndrome coronavirus [12-15]. IFITM1-3 are also all ubiquitous proteins and are involved in various physiological functions like cell adhesion, apoptosis and tumor progression. Although BRIL (IFITM5) has a certain structural homology with the IFITM family, it markedly distinguishes itself in function and in structure, specifically at the N- and C-termini of the protein. BRIL sequence identity matches 52%, 48% and 53% to IFITM1, IFITM2 and IFITM3 respectively, while the protein sequence similarity amongst each IFITM1, IFITM2 and IFITM3 is nearer to 90% [2]. The antiviral functions of IFITM1-3 are not seen with BRIL (IFITM5) and, as previously outlined in Section 1.1.1., are replaced by bone-restricted activities in osteoblasts, which differentiate BRIL from the IFITM family members [2, 8].

1.1.3. BRIL gene regulation, topology and localization

The regulation of the human, mouse and rat *Bril/BRIL* gene was studied by Kasaai et al. [16]. BRIL's promoter region was found around 250 bp upstream of the coding ATG start site. However, high variability between human, mouse and rat 5'-UTR regions of the *Bril/BRIL* gene offers various unique alternative transcription start sites. All in all, in UMR106 and MC3T3 cells, through the use of luciferase reporter assays, *Bril* was found to be activated through the binding of several GC-rich boxes by Sp1 and Sp3, transcription factors that are part of the ubiquitously expressed specific protein

(Sp) family [16, 17]. Two TATA boxes were also found within the human, mouse and rat promoter regions, which appear to be essential for the activity of Sp family members. Another member of the Sp family, Sp7, or osterix, was investigated for its role in the differentiation of mesenchymal precursor cells into osteoblasts and eventually osteocytes [18]. Although osterix alone was found to be a weak activator, the combination of Sp1 and osterix yielded greater than additive, or synergistic, induction of the *Bril* promoter. GLI2, a GLI transcription factor part of the hedgehog signalling pathway and involved in osteoblast differentiation, was also found to be an activator of *BRIL*, which concurrently contains a canonical GLI binding site in its promoter region [19]. GLI transcription factors are found downstream of Patched and Smoothened, both hedgehog pathway transmembrane proteins, and have an effect on a wide array of genes. Although GLI1 and GLI3 were also found to somewhat upregulated *BRIL*, *BRIL* seemed most responsive to GLI2. GLI2 likely had a direct interaction with the *BRIL* gene, considering the treatment of MC3T3 cells with Indian hedgehog signaling pathway agonists resulted in *BRIL* upregulation in a concentration dependent manner [16].

The *Bril/BRIL* gene can also be negatively modulated by other factors. The zinc finger protein ZFP354C was identified as such a factor considering the *Bril/BRIL* promoter contains several consensus binding sites for zine finger proteins. The presence of ZFP354C downregulated the *Bril/BRIL* gene in all species in a dose dependent way, even when co-expressed with Sp1. ZFP354 has been linked to osteoblast differentiation in UMR106 cells and therefore a bone cell context, and this by reducing the activation of the *osteocalcin* promoter via RUNX2 [20]. Another factor

negatively affecting the modulation of *Bril/BRIL* is its methylation status. Both rat and mouse *Bril* and human *BRIL* promoters contain CpG dinucleotides, which, when unmethylated or methylated, allow or restrict transcription respectively. These CpG dinucleotides in the *Bril* promoter were found to be methylated (thereby silenced) in proliferating MC3T3 cells, which do not express *Bril* [16]. Similarly, when *Bril* is expressed in differentiating MC3T3 cells, demethylation was noted. Methylation was therefore suggested as being a form of regulation of the *Bril/BRIL* gene.

BRIL is a 132 amino acid transmembrane protein and has a molecular weight of 14.8kDa [2]. Originally, the IFITM family was projected to have a type III protein orientation, where both N- and C-termini would be found outside the cell. However, re-evaluations of IFITM topological conformations suggest a type II orientation for IFITM1, IFITM3 and BRIL [21-23], the latter being illustrated in Figure 1. Specifically, for BRIL, this was confirmed with immunofluorescent staining of osteoblasts demonstrating the protein being mainly localized at the plasma membrane, where the N-terminus is cytoplasmic, and the C-terminus is either extracellular at the plasma membrane or luminal at the Golgi apparatus.

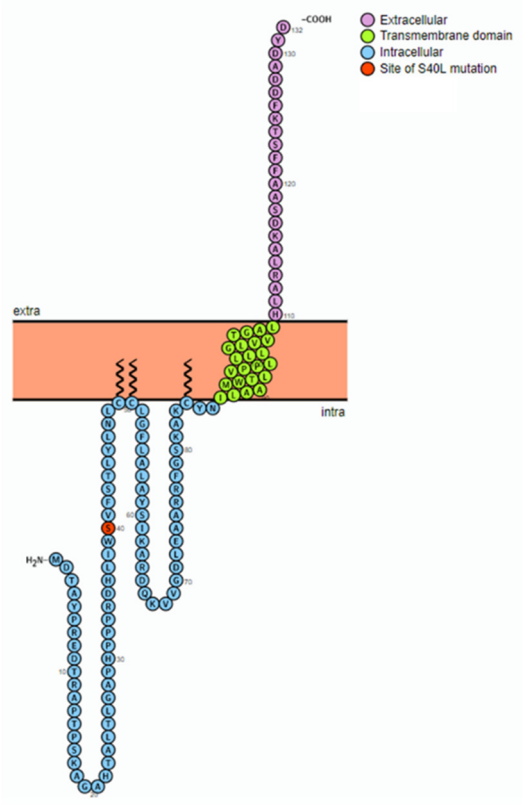

Figure 1. BRIL orientation and topology at the plasma membrane. Amino acids in the intracellular part of the protein colored in blue. Transmembrane domain denoted in green. Extracellular C-terminal end of the protein colored in purple. The three palmitoylated cysteines residues, essential for plasma membrane targeting, are indicted. Amino acid S40 is the site of the S40L mutation, discussed in section 1.2.3., and is colored in orange. Image generated by *Protter* tool for visualization of proteins [24].

BRIL's targeting to the plasma membrane is dependent on many intracellular mechanisms, biochemical alterations and specific sequence residues. In normal conditions, BRIL is first transported to the plasma membrane via targeting to the rough endoplasmic reticulum (rER) [21]. In order to be secreted, generally all proteins must go

through the rER as an entry point to the secretory pathway [25]. Considering BRIL does not harbor a signal peptide, and contains a single transmembrane domain located at the C-terminal end, it was suggested that BRIL is first targeted to the rER through tail-anchored machinery [21, 26]. Patoine et al. [21] also discusses that although BRIL was not significantly detected in the rER at steady state in transfected MC3T3 cells, the addition of a KDEL retention motif to the BRIL protein in the C-terminal end resulted in an exclusive rER immunostaining. The absence of significant rER BRIL at steady state conditions suggests that the rER-Golgi transport is rapid. BRIL therefore subsequently travels to the Golgi apparatus via coat protein complex II (COPII) vesicles to finally reach its destination of plasma membrane. In conditions where anterograde transport via the COPII pathway is unfeasible, BRIL remains in the rER [21]. Additionally, to reach the plasma membrane, BRIL requires palmitoylation at two cysteine residues (C52 and C53). Though BRIL contains three different cysteine residues heavily conserved throughout most species, only mutations in C52 and C53 significantly reduced stability and perturbed localization of the protein at the plasma membrane and Golgi apparatus. The C-terminal transmembrane region is also important to BRIL's expression and localization, as mutation of one residue leads to BRIL remaining in the cytoplasm of osteoblasts, and this at low levels of protein expression [21]. The observed effect is most likely related to the tail-anchored targeting property of BRIL, as disruption of the transmembrane domain may inhibit the protein being transported from the cytosol to the rER.

1.1.4. BRIL's known interactions with other factors

The literature provides limited information on BRIL's interactome, though some studies have been conducted to elucidate it. Using a co-immunoprecipitation and mass spectrometry approach, Hanagata et al. [4] found peptide fragments corresponding to BRIL after a pull-down for overexpressed FKBP19 in MC3T3. The FKBP family proteins are considered immunophilins that bind immunosuppressive drugs like FK506 and rapamycin, and show peptidylprolyl cis/trans isomerase (PPIase) activity [27-29]. The FKBP family have versatile biological functions, involved in protein folding, receptor signaling, protein trafficking, transcription and apoptosis [30]. Specifically, FKBP19 has been shown to associate with CD81, which in turn interacts with prostaglandin F2 receptor negative regulator (FPRP) and CD9 antigen, resulting in the multi-protein complex FKBP19-CD81-[FPRP/CD9] in MC3T3 osteoblasts [31]. Furthermore, BRIL's role was suggested to dissociate CD9 from the complex by interacting with FKBP19. Based on the abolition of the interaction with FKBP19 when BRIL's first transmembrane region harboring C52 and C53 is removed, the interaction with CD9 and FKBP19 is likely dependent on the palmitoylation status of BRIL's C52 and C53 [32]. The loss of interaction probably is caused by BRIL's aberrant localization and stability. However, it is unclear how and where the interaction with FKBP19 takes place, considering BRIL localizes to the plasma membrane while FKBP19's PPIase interaction domain localizes at rER facing the lumen. The biological significance of the FKBP19-BRIL interaction is still unclear, as our group was unable to reproduce these results (unpublished data). Further investigation into BRIL's interactome is required to elucidate the function of this osteoblast-restricted protein.

1.1.4. Function of BRIL *in vitro* and *in vivo*

Based on previously mentioned analyses of rat and mouse tissues, BRIL was characterized as being associated with bone formation, specifically in osteoblasts [2]. BRIL overexpression and knockdown assays *in vitro* in MC3T3 osteoblasts linked BRIL to mineralization. Specifically, BRIL overexpression in UMR106 cells led to increased mineralization, while knockdown in MC3T3 cells led to decreased mineralization. Furthermore, Hanagata and Li [31] proposed that BRIL could be a regulator of the skeletal immune system. In MC3T3 osteoblasts, an analysis of gene expression from a DNA microarray showed BRIL overexpression lead to several genes to be upregulated, including bone marrow stromal cell antigen 2 (*Bts2*), interferon inducible protein 1 (*Irgm*), interferon-induced protein with tetratricopeptide repeats 3 (*Ifit3*), β(2)-microglobulin (*B2m*) and the major histocompatibility complex (*MHC*) class I antigen gene [31]. All these genes are also induced by IFNs in osteoblasts, thereby suggesting BRIL may be involved in a pathway like that induced by IFNs.

Knowledge on BRIL's role *in vivo* in mice is also limited. First, a transgenic mouse model by Lietman et al. [33] overexpressing BRIL in osteoblasts showed no significant phenotype. Micro-computed tomography analyses of 3-month-old femurs and spines yielded no significant variation in the trabecular or cortical parameters. Only minor increases in bone volume density (BV/TV) and average trabecular number (Tb.N.) were observed. All in all, the overexpression of BRIL show no significant phenotype in both neonate and adult mouse bones [33]. A global knockout (KO) of BRIL in mice by Hanagata et al. [4], where the gene is absent in all tissues, yielded no alteration in osteoblast maturation as seen through comparable detected levels of

osteocalcin in femur bone sections. Furthermore, the presence of tartrate-resistant phosphatase (TRAP)-positives cells around calcified cartilage between KO and wild-type mice suggested normal osteoclastogenesis. The global KO mouse model did show a mild skeletal phenotype, characterized by shorter skeletons in newborn and adult mice [4]. Bone bending was noted in newborn mice but was corrected through mouse maturing. However, Patoine et al. [34] generated a new germline BRIL KO mouse model that showed no apparent differences between KO and WT littermates, and thereby concluding that BRIL is dispensable for bone development and homeostasis and has no link with mineralization in mice. Lastly, a deletion of the whole *Ifitm* gene cluster (*Ifitm1, Ifitm2, Ifitm3* and *Ifitm5*) by LoxP-mediated excision in mice showed no obvious skeletal phenotype [35]. These mice were of the same size, weight and had no apparent behavioural changes as WT mice throughout their life. *Ifitm* cluster KO mice did have increased sensitivity to viral infections and adult moderate metabolic syndrome, showing signs of greater adiposity, morphologically different hypothalamic microglia and high levels of leptin. In humans, only three probands with large genomic deletions spanning 8 to 24 genes that include BRIL have been identified and catalogued in the DECIPHER database [36]. Although signs of mild skeletal defects are described, there are no confirmation that these are directly linked to the loss of BRIL.

While information on BRIL's function both *in vitro* and *in vivo* have not yielded conclusive evidence, BRIL does have a special link with a well-known disease, osteogenesis imperfecta.

1.2. Osteogenesis imperfecta

1.2.1. Overview and types of osteogenesis imperfecta

Osteogenesis imperfecta (OI) is a heritable disorder that affects bones and leads to overall skeletal fragility [37]. The disease spans a wide range of clinical severity, from perinatal lethality to milder forms of the disease with few or no fractures [38]. However, since there are many causes that lead to osteogenesis imperfecta, the disease is broken down into various types. The majority of patients (85-90%) with OI are inherited in an autosomal dominant manner and are caused by mutations in the *COL1A1* and *COL1A2* genes, leading to quantitative or qualitative defects in type 1 collagen [39]. These were originally filtered into OI types I-IV, while other types were used to categorise mutations in non-collagenous genes leading to OI [40]. Recent advances in genetics have called for re-examination of the classification of OI [41, 42]. However, most recent classifications resemble the original Sillence classification and are outlined in Table 1.

Table 1. Main classification of osteogenesis imperfecta

Gene	Protein	Type	Pattern of inheritance
COL1A1	Collagen type 1 a1 chain	I, II, III, IV	Autosomal dominant
COL1A2	Collagen type 1 a2 chain	II, III, IV	Autosomal dominant
IFITM5	Bone-restricted Ifitm-like protein	V, atypical VI	Autosomal dominant
SERPINF1	Pigment epithelium-derived factor	VI	Autosomal recessive
CRTAP	Cartilage-associated protein	VII	Autosomal recessive
LEPRE1	Prolyl 3-hydroxylase 1	VIII	Autosomal recessive
PPIB	Cyclophilin B	IX	Autosomal recessive
SERPINH1	Heat-shock protein 47	X	Autosomal recessive
FKBP10	Peptidyl prolyl isomerase FKBP65	XI	Autosomal recessive
SP7	Osterix	XII	Autosomal recessive
BMP1	Bone morphogenetic protein 1	XIII	Autosomal recessive
TMEM38B	Trimeric intracellular cation channel subtype B	XIV	Autosomal recessive
WNT1	Wingless family member 1	XV	Autosomal recessive

One particular class of OI, type V, is inherited in an autosomal dominant fashion and clinically is similar to most types of OI, with respect to bone fragility and fractures,

but with some distinctions. First classified by Glorieux et al. [43], patients with OI type V had low trauma fractures, the absence of blue sclera and dentinogenesis imperfecta, as well as one of several unique phenotypes: the calcification of the forearm interosseous membrane, the tendency for episodes of hyperplastic calluses formation, a mesh-like collagen lamellation patterns, radial-head dislocation and/or a subphyseal metaphyseal radiodense line [43, 44]. The calcification of the interosseous membrane of the forearm (and irregularly of the tibia-fibula) is seen in most patients and appears to be caused by periosteal hyperostosis, leading to limited range of motion of the arm and radial head [45]. Additionally, although hyperplastic callus formation appears to be unique to OI type V patients, only a minority of fractures lead to patient's forming such calluses [46, 47]. The disease has been described as heterogeneous, where mild, moderate and severe cases of bone deformities, vertebral compression and fracture incidence exist, among some characteristics. The genetic cause of OI type V was established as being caused by a recurrent heterozygous mutation (c.-14C>T as described further in section 1.2.2) in the BRIL gene [48, 49].

Since the original discovery of the recurrent c.-14C>T mutation in patients with the classical clinical hallmarks of OI type V, another OI type named 'atypical type VI' was reported [50, 51]. The classification was proposed because of the histological features which resembled those observed in OI type VI caused by mutations in *SERPINF1*, namely the increased unmineralized osteoid visible upon Goldner staining and fish-scale lamellation pattern of a bone biopsy from the proband [50]. The genetic cause for this even rarer form is not due to recessive mutations in *SERPINF1*, but due to an autosomal dominant missense in the coding region of *IFITM5* (c.119C>T; p.S40L).

Only 7 case reports have been documented so far, all caused by the heterozygote c.119C>T de novo mutation and causing severe OI with deformities and fractures [50-56]. Notwithstanding, the clinical presentation of patients with the c.119C>T is severe and differs substantially from the classical OI type V, as well as from OI type VI. Bowing and shortening of long bones, fractures, and deformities of other skeletal elements have been observed in utero [53], as well as in some patients who have been followed for several years until adulthood [55].

1.2.2. MALEP-BRIL

Two groups independently identified that a single cytosine to thymine point mutation at position -14 of the 5'-UTR is the genetic cause of OI type V [48, 49]. The cytosine in question is a part of a CpG-dinucleotide and methylated in 100% of sperm cells and leukocytes, and in 80% for bone marrow cells and fibroblasts [57]. Methylated CpG-dinucleotides are popular candidates for deamination and consequent mutations, and the high methylation status of sperm cells may explain the *de novo* nature of the mutation causing OI type V [57]. The methylation status of BRIL at position -14 in sperm cells could also suggest a paternal age effect as a factor impacting the inheritance of OI type V. The presence of a methylated CpG-dinucleotide at position -14 may furthermore explain why this particular nucleotide is prone to mutations. The aforementioned C to T mutation leads to a novel in frame translation start site that adds 5 amino acids (Methionine-M, Alanine-A, Leucine-L, Glutamic acid-E, Proline-P) onto the N-terminus of the protein. This mutated form of BRIL is hereafter called MALEP-BRIL.

The MALEP-BRIL mutant has been studied both *in vitro* and *in vivo* (although limited by the perinatal lethality of all mouse models, as discussed later). Immunofluorescent staining of MC3T3 cells has confirmed that MALEP-BRIL localizes at the plasma membrane of osteoblasts in a type II topology, indistinguishable to the WT form of the protein (hereafter called WT-BRIL) [21]. Like WT-BRIL, MALEP-BRIL has its C52, C53 and C86 residues palmitoylated, in both mouse and human forms of the mutant. Studies were also conducted on primary cell cultures originating from a patient with OI type V [58]. Primary osteoblasts expressed differentiation markers like *ALPL*, *BGLAP*, *IBSP* and *SPP1* at higher levels, while *COL1A1* levels were lower. These osteoblasts had significantly increased mineralization but decreased cross-linked collagen in the matrix. Fibrils deposited in culture were also described as irregular. Reich et al. [58] therefore attributed these observations to a gain-of-function mechanism leading to overactive tissue mineralization and defective collagen incorporation. Another study by Farber et al. [50] used primary cell cultures of OI type V to show increased expression of *SERPINF1* (encoding the PEDF protein) and consequently greater secreted levels of PEDF in cultured osteoblasts. It was suggested that this could be the source of the hyperostosis phenotype associated with OI type V. MALEP-BRIL and OI type V have also been the subject of *in vivo* mouse models. Lietman et al. [33] generated a mouse model whereby MALEP-BRIL expression was controlled by the osteoblast-specific *Col1a1* promoter. However, mice expressing MALEP-BRIL exhibited perinatal lethality. Analyses of embryonic bone tissue showed delayed mineralization and skeletal defects. Lowered expression of differentiation markers like *Sp7*, *Col1a1* and *Ocn* were also noted in primary osteoblasts extracted from mice calvaria at E18.5.

A knock-in (KI) mouse model of OI type V by Rauch et al. [59] also led to perinatal lethality. KI mice had skeletal anomalies like a hypo-mineralized bones and frail and wavy ribs. Following gene expression analyses of E15.5 and E17.5 samples, it was found that *Bril* itself, *Bglap*, *Ibsp* and *Sost* were all downregulated, while *Nr4a3* and *Ptgs2* were upregulated. It was hypothesized that the latter markers were linked to an inflammatory response, while upregulation of *AdipoQ* and *Fabp4* in young primary cell cultures may be linked to shift in cell fate, from osteoblastogenesis to adipogenesis. All in all, the mechanism by which OI type V is caused by the MALEP-BRIL mutant remains largely elusive, and there is a need for further studies.

1.2.3. S40L-BRIL

As described above, another dominant BRIL mutation, introducing a single amino acid change (serine to leucine) at position 40 of the human protein and position 42 of the mouse protein (hereafter called S40L-BRIL), was found to cause atypical OI type VI, according to the original classification of OI. Similar to MALEP-BRIL, S40L-BRIL has been studied in both *in vitro and ex vivo* contexts. Initial analyses in MC3T3 cells of the S40L-BRIL mutant showed significant shifts in both protein localization and biochemistry. S40L-BRIL was poorly palmitoylated, which was established to be critical for its subcellular localization [21]. The S40L-BRIL mutant therefore remains trapped in the ER-Golgi network and has difficulty reaching the plasma membrane, as noted by immunofluorescent staining of MC3T3 osteoblasts. The cellular abundance of the S40L-BRIL mutant produced by overexpression in MC3T3 osteoblast is also significantly less than both WT-BRIL and MALEP-BRIL.

Findings originating from primary osteoblast cultures of a patient with the S40L mutation conflicted with observations in MC3T3 cultures. BRIL gene and protein expression were largely unaffected in the proband dermal fibroblasts and cultured osteoblasts, and the protein localized correctly to the plasma membrane in proband osteoblasts [50]. It was noted that *ALPL*, *BGLAP*, *COL1A1* and *SERPINF1* were all downregulated in proband osteoblasts, while *IBSP* and *SPP1* were both upregulated. Decreases of *SERPINF1* gene expression were of notice, considering a mutation in SERPINF1 is the cause of OI type VI, which resembles the atypical type VI. It was therefore hypothesized that decreased *SERPINF1* expression and consequent PEDF levels in conditioned media of proband cells lead to afflicted bone and poor mineralization phenotypes seen in patients with the S40L mutation in BRIL [50]. These results are in contrast to differentiating osteoblasts from a patient with OI type V which showed increased *SERPINF1* expression and PEDF secretion. The authors therefore suggested that BRIL and PEDF may have a relationship, linking both types of OI with bone mineralization. However, like OI type V and MALEP-BRIL, the mechanism by which S40L-BRIL still needs to be studied in order to pinpoint the nature of the relationship BRIL may have with other factors.

1.3. Project rationale and objectives

Given that KO mouse models have shown that BRIL is dispensable for bone development, it is hypothesized that the two mutant forms of BRIL that lead to OI operate through gain-of-function mechanisms [34]. It was also suggested that these negative effects are dominant as heterozygosity leads to the respective type of OI.

Although both MALEP-BRIL and S40L-BRIL are mutants forms of the same BRIL protein, the mechanism by which they act is likely different based on their palmitoylation status and their subsequent cellular localization as well as their expression levels. Based on the observations and hypotheses of Patoine et al. [21] following experiments with BRIL forms in MC3T3 cells, S40L-BRIL is poorly palmitoylated and is trapped in the ER-Golgi network, while this was not observed in the case of MALEP-BRIL. This suggests that both mutants are operative from within the intracellular compartment, but the mechanisms mostly likely differ in nature considering MALEP-BRIL and S40L-BRIL are differentially expressed and localized within the cell. The specific mechanisms by which the mutant proteins cause these disorders has yet to be ascertained and is the main aim of this research project.

The main objective of the project was to determine the mechanism by which the mutant forms MALEP-BRIL and S40L-BRIL, differ from the normal function of WT-BRIL, thereby causing OI type V and atypical type VI, respectively. The project also aimed to verify whether the studied BRIL forms could elicit signaling pathways within osteoblasts. We have opted to conduct the studies *in vitro* using two pertinent mouse cell lines, MC3T3, an osteoblast precursor line, and MLO-A5, a preosteocyte-like line. Since knock-out mouse models showed no significant differences between KO and WT mice, this leads to the conclusion that MALEP-BRIL's and S40L-BRIL's detrimental effects stem from aberrant gain-of-function mutations. Specifically, MC3T3 and MLO-A5 cells will be used to carry out several experiments; luciferase assays to determine pathways and cellular activity BRIL could potentially be involved in, RT-qPCR to assess the variations of gene expression that transfection of BRIL may cause, as well as Western

blots and immunofluorescence stains to confirm and evaluate the protein expression and localization respectively. Prior to the beginning of the project, a large screening assay was performed to determine if any of the three forms of BRIL (denoted WT-BRIL, MALEP-BRIL and S40L-BRIL) could activate intracellular pathways causing activation of luciferase reporters. This screen was carried out in both MC3T3 and MLO-A5 cells and will be outlined in section 3.1.1. The results of this screen were therefore used to pursue pertinent avenues, which will be explored throughout the project.

Elucidating these new functions of the two aberrant forms of BRIL are important in order to better understand how they impact osteoblast activity, and consequently lead to OI. Shedding light on the nature of these mechanisms could potentially lead to ways to suppress them and pave new avenues to therapeutic applications for OI.

Chapter 2: MATERIALS AND METHODS

2.1. Cell culture

A total of 6 different cell lines were used during this project, outlined in Table 1. Cell lines were subject to a maximum of 25 passages and were cultivated under the conditions found in Table 3 with the addition of a penicillin-streptomycin (PenStrep) mix at a concentration of 100units/mL Penicillin G Sodium and 100ug/mL Streptomycin Sulfate (Life Technologies). Media was changed every 2-3 days.

Table 2. List of cell lines used in tissue culture.

Cell line	Species	Tissue of origin
HEK293	Human	Embryonic kidney
MC3T3-E1	Mouse	Bone (calvaria)
MLO-A5	Mouse	Bone (long bone)
NIH3T3	Mouse	Embryonic
SaOS-2	Human	Osteosarcoma
UMR106	Rat	Osteosarcoma

Table 3. Conditions of maintenance of cell lines used in tissue culture.

	HEK293	MC3T3	MLO-A5	NIH3T3	SaOS-2	UMR106
Medium	DMEM + 10% FBS	α-MEM + 10% FBS	α-MEM + 5% FBS + 5% BCS	DMEM + 10% FBS	DMEM + 10% FBS	DMEM + 10% FBS
Trypsin	0.05%	0.05%	0.05%	0.05%	0.25%	0.25%
Trypsin time (min)	5	10	5	5	10	10
Dilution 4 days	1/12	1/5	1/20	1/12	1/5	1/20
Dilution 5 days	1/20	1/8	1/30	1/20	1/8	1/30

2.2. Cloning

Table 4 outlines plasmids used in the context of this project that were purchased or described elsewhere. All other plasmids were constructed in-house or described elsewhere. Point mutations and deletions were introduced by whole plasmid amplification using Phusion DNA polymerase (New England Biolabs) with phosphorylated primers covering the targeted codons. PCR products were resolved on an agarose gel, excised to isolate the desired band and subsequently purified on Minelute columns (QIAGEN). The product was then cloned into a pCMV-Neo backbone using the multiple cloning sites therein (with the exception of Empty (pCDNA), GFP (pQBI), MEF2C and MEF2D (pcDNA3.1(-))). The list of plasmids used previously in other works have been referenced in Table 4. All plasmids constructed in-house were Sanger-sequenced at the McGill University and Génome Québec Innovation Center to confirm correct sequence.

Table 4. List of plasmids used in other works or purchased and used for transfection experiments.

Plasmid name	Reference	Sources
Empty	-	Invitrogen
GFP	-	Quantum Biotechnology Inc.
WT-BRIL	Patoine et al, 2014 [21]	In-house
HA-BRIL	-	In-house
BRIL L101R	Patoine et al, 2014	In-house
BRIL KDEL	Patoine et al, 2014	In-house
BRIL C52A	Patoine et al, 2014	In-house
BRIL C53A	Patoine et al, 2014	In-house
BRIL C52A-C53A	Patoine et al, 2014	In-house
BRIL K118-STOP	Patoine et al, 2014	In-house
OSTN-BRIL	Patoine et al, 2014	In-house
BRIL A22N	Patoine et al, 2014	In-house
MALEP-BRIL	Patoine et al, 2014	In-house
S40L-BRIL	Patoine et al, 2014	In-house
mMEF2A	-	In-house

hMEF2C	Grégoire and Yang, 2005 [60]	-
hMEF2D	Grégoire and Yang, 2005	-
mNFATc1	Monticelli and Rao, 2002 [61]	Addgene 11100
hHDAC4	Wang et al, 1999 [62]	-
hHDAC4-mut	Wang et al, 1999	-
mCalcineurin A	Clipstone et al, 1994 [63]	Addgene 11785
mRCAN1	Liu et al, 2009 [64]	Addgene 65413
NFAT-luciferase reporter	Clipstone and Crabtree, 1992 [65]	Addgene 17870
MEF2-luciferase reporter	-	Cignal CCS-7024L
Ptgs2-luciferase reporter	-	In-house

2.3. Transient transfection

Transient transfection experiments were carried out in all cell types. Cells were seeded in accordance with Table 5 calculated to obtain approximately 70% confluency at the time of the transient transfection, 24 hours post-seeding. Transfections were carried out in 6-well, 12-well or 24-well plates (Sarstedt). FBS-free media (100µl of media per well for 6-well plates; 50µl of media per well for 12-well and 24-well plates) was mixed with Xtreme Gene 9 DNA Transfection Reagent (Sigma Aldrich) (3µl per 1µg of DNA for HEK293 cells; 6µl per 1µg of DNA for MC3T3, MLO-A5, NIH3T3, SaOS-2 and UMR106 cells) and vortexed for 10 seconds. Afterwards, DNA from the expression plasmid(s) of the gene(s) of interest (a combined total of 1µg of DNA per well for 6-well plates; 0.5µg of DNA per well for 12-well plates; 0.2ug of DNA per well for 24-well plates) was added to the mix, which was vortexed for 1 second and incubated for 20 minutes at room temperature. Medium covering the cells was changed for medium without PenStrep, followed by the addition of the transfection mix to the medium covering the cells.

Table 5. Seeding conditions and cell counts used in tissue culture.

	HEK293	MC3T3	MLO-A5	NIH3T3	SaOS-2	UMR106
# cell/6W for TFX	315 000	190 000	315 000	315 000	N/A	N/A
# cell/12W for TFX	125 000	75 000	80 000	125 000	N/A	N/A
# cell/24W for TFX	65 000	35 000	40 000	65 000	50 000	55 000

2.4. Luciferase assay

Luciferase assays were carried out 24 hours post-transfection. Medium was removed from cell layers, washed once with phosphate-buffered saline (PBS) and replaced with 100µL of Passive Lysis Buffer (Promega) to cover cells. Cultures were then rocked for 10 minutes. A 10µL sample of the lysed cells was mixed with 50µL Luciferase Assay Reagent (originating from Promega's Luciferase Assay System) dispensed in luminometer tubes. Light output was measured using a Berthold Sirius Luminometer programmed to perform a 2-second measurement delay followed by a 10-second measurement read for luciferase activity.

2.5. RNA extraction

RNA extractions were carried out 24 hours post-transfection. First, cells were washed thrice with PBS. Afterwards, 1mL (6-well) or 0.5mL (12-well) of Trizol was added to the cell layer. The cell lysates were pipetted up-and-down several times and transferred in a microtube. Cell lysates were homogenized by vortexing for approximately 1 minute. Chloroform was added to the homogenates, vortexed again for 1 minute and incubated at room temperature for 2-3 minutes. The samples were then

centrifuged for 15 minutes at 13,200rpm at 4℃. The upper aqueous phase was recovered, and RNA was precipitated with isopropanol then centrifuged at 13,200rpm for 10 minutes at 4℃. RNA pellets were washed using ethanol 70%, dried for 5-10 minutes and resuspended in 0.1% diethylpyrocarbonate (DEPC)-treated water. The purity of the sample was established with the 260/280nm absorbance, and the concentration was measured using the NanoDrop 1000 Spectrophotometer (Thermo Fisher Scientific) and stored at -20℃.

2.6. Protein extraction

Protein extractions were carried out 24 hours post-transfection. First, cells were washed thrice with PBS. Proteins were afterwards extracted from cultured cell layers using the following cell lysis buffer: 50mM Tris-HCl (pH 7.4), 150mM NaCl, 1mM EDTA, 1% (v/v) NP-40 (nonylphenoxypolyethoxyl-ethanol) with 1% of protease inhibitor cocktail (Sigma Aldrich). Cell layers were homogenized by collecting with a cell scraper, transferred to a microtube, incubated on ice for 10 minutes and vortexed at 5-minute intervals. Homogenates were centrifuged at 13,200rpm for 10 minutes at 4˚C. Soluble proteins from the homogenate supernatant were collected and combined with 4x Laemmli buffer (200 mM Tris-HCl pH 6.8, 8% SDS, 40% glycerol, 50mM EDTA, 0.08% bromophenol blue) with 5% β-mercaptoethanol, boiled for 5 minutes and stored at -20˚C.

Proteins were also occasionally extracted from the organic phase of the RNA extraction protocol. All traces of the aqueous phase were removed, followed by the addition of ethanol 100% to precipitate unwanted DNA and debris. Samples were

incubated for 2-3 minutes at room temperature, centrifuged at 2,000rpm for 5 minutes at 4˚C. The phenol-ethanol supernatant was recovered, to which isopropanol was added to precipitate proteins, and incubated for 10 minutes at room temperature. The pellet was thrice washed with 0.3M guanidine hydrochloride, incubated for 20 minutes and centrifuged at 3,000rpm for 5 minutes at 4˚C. The pellet was washed with ethanol 100%, re-suspended in the aforementioned cell lysis buffer, sonicated and crushed using manual homogenizers. Soluble proteins from the homogenate supernatant were again collected and combined with 4X Laemmli buffer (200 mM Tris-HCl pH 6.8, 8% SDS, 40% glycerol, 50mM EDTA, 0.08% bromophenol blue) with 5% β-mercaptoethanol, boiled for 10 minutes and stored at -20˚C

2.7. Real time quantitative PCR (RT-qPCR)

Complementary DNA (cDNA) was prepared from the extracted RNA samples using the High Capacity cDNA Reverse Transcription Kit (Applied Biosystems). Reactions of 20µl containing 2µg of RNA were prepared according to the manufacturer's protocol using the following conditions: 25℃ for 10 minutes, 37℃ for 120 minutes and 85℃ for 5 minutes. Resulting cDNA was diluted in Milli-Q water (Millipore) (1 in 5). Real-time PCR reactions of 20µl were prepared in duplicates in MicroAmp Optical 96-well Reaction Plates (Applied Biosystems) using TaqMan Fast Advanced Master Mix and TaqMan Gene Expression Assay Probes (Applied Biosystems) found in Table 6. Plates were run and analysed on a 7500 Real Time PCR System (Applied Biosystems) using the Relative Quantification (ddCt) plate assay

function of the 7500 Sequence Detection Software (SDS) v.1.3.0. Taqman probes for mouse β-actin (*Actb*) were used as endogenous gene controls.

Table 6. List of Taqman probes.

Gene symbol	Gene name	Taqman ID
Actb	Mouse β-actin	4352933-0808024
Mef2a	Mouse myocyte enhancer factor 2A	Mm01318991_m1
Mef2b	Mouse myocyte enhancer factor 2B	Mm00484956_g1
Mef2c	Mouse myocyte enhancer factor 2C	Mm01340842_m1
Mef2d	Mouse myocyte enhancer factor 2D	Mm00504931_m1
Hdac1	Mouse histone deacetylase 1	Mm02745760_g1
Hdac2	Mouse histone deacetylase 2	Mm00515108_m1
Hdac3	Mouse histone deacetylase 3	Mm 00515916_m1
Hdac4	Mouse histone deacetylase 4	Mm01304741_m1
Hdac5	Mouse histone deacetylase 5	Mm01246076_m1
Hdac7	Mouse histone deacetylase 7	Mm00469527_m1
Nfatc1	Mouse nuclear factor of activated T cells 1	Mm00479445_m1
Nfatc2	Mouse nuclear factor of activated T cells 2	Mm01240677_m1
Bril	Mouse bone-restricted Ifitm-like	Mm00804741_g1
Nr4a3	Mouse nuclear receptor subfamily 4 group A member 3	Mm00450071_g1
Ptgs2	Mouse prostaglandin-endoperoxide synthase 2	Mm00478374_m1
Serpinf1	Mouse serpin family F member 1	Mm00441270_m1
Sost	Mouse sclerostin	Mm04208528_m1

2.8. Western blot

Protein samples were loaded on 1mm thick SDS-polyacrylamide gel and migrated by electrophoresis (PAGE) (concentration varied depending on the protein of interest) in Tris-glycine SDS running buffer. Proteins were transferred to 0.45µm nitrocellulose membranes (BioRad Laboratories) post-migration. Membranes were blocked in PBS with 5% skim milk and 0.05% Tween for 1 hour and treated overnight with the corresponding primary antibody at 4°C. Membranes were washed thrice for 10 minutes with PBS-Tween 0.05% and treated with the secondary HRP-coupled antibody for 1 hour at room temperature. Detection was done using ECL Prime Western Blotting Detection Reagent (GE Healthcare). Antibodies used in the context of this project are

outlined in Table 7. Both primary and secondary antibodies were diluted in the blocking solution. Hybridization using a β-actin antibody was used as an endogenous control. Antibodies for anti-BRIL N-term and anti-BRIL C-term have been described in a previous publication by Patoine et al. (2014).

Table 7. List of primary and secondary antibodies.

Experiment type	Antibody	Species	Type	Dilution	Brand	Catalogue #
Primary antibodies	Anti-BRIL N-term	Rabbit	Polyclonal	1/2000	N/A	N/A
	Anti-BRIL C-term	Rabbit	Polyclonal	1/500	N/A	N/A
	Anti-IFITM3	Rabbit	Polyclonal		Abcam	Ab155992
	Anti-DKK / FLAG	Rabbit	Polyclonal	1/1000	Sigma-Aldrich	F7425
	Anti-HA	Rabbit	Polyclonal	1/1000	Sigma	H6909
	Anti-NFAT	Mouse	Monoclonal	1/100	DSHB	AB2152505
	Anti-Mef2a	Mouse	Monoclonal	1/250	DSHB	AB2618839
	Anti-Mef2c	Mouse	Monoclonal	1/250	DSHB	AB2722252
	Anti-B-actin	Mouse	Monoclonal	1/2000	Cell Signaling Technology	3700
	Anti-phospho-HDAC	Rabbit	Polyclonal	1/500	N/A	N/A
Secondary antibodies – Western blots	Anti-Mouse HRP	Sheep	Polyclonal	1/30000	Sigma	A6782
	Anti-Rabbit HRP	Donkey	Polyclonal	1/30000	GE Healthcare	NA934V
Secondary antibodies – Immuno-fluorescence staining	Anti-Mouse Alexa Fluor 488	Goat	Polyclonal	1/2000	Life Technologies	A11001
	Anti-Mouse Alexa Fluor 594	Goat	Polyclonal	1/2000	Life Technologies	A11005
	Anti-Rabbit Alexa Fluor 488	Goat	Polyclonal	1/2000	Life Technologies	A11008
	Anti-Rabbit Alexa Fluor 594	Goat	Polyclonal	1/2000	Life Technologies	A11012

2.9. Immunofluorescence staining

Cell layers were fixed for 15 minutes with 3% paraformaldehyde (PFA) diluted in PBS, and either treated with 0.1% Triton X-100 diluted in PBS for permeabilization or left non-permeabilized. Samples were then blocked for 1 hour in PBS with 2% skim milk

and 0.1% BSA. Primary antibodies were diluted in the blocking solution and incubated for 1 hour at room temperature. After the incubation, cells were washed thrice for 5 minutes with PBS, 0.1% BSA. Cells were incubated with the secondary antibodies in the dark as to not affect the fluorescent markers. Afterwards, cells were mounted with ProLongGold Antifade Reagent with DAPI (Life Technologies). Cells were imaged by epifluorescence microscopy using a Leica DMRB Microscope equipped with an Olympus DP70 digital camera. Antibodies used in the context of this project are outlined in Table 6.

2.10. Statistical analysis

Unless otherwise specified, data is expressed as averages and standard deviations (SD). Each experiment included two repeats (two independent wells), and biological replicates (independent experiments) range from 2 to 30, depending on the figure. Statistical significance was assessed using an ordinary one-way or two-way ANOVA, depending on the data, with no matching or pairing and assuming Gaussian distribution. This was followed by Tukey's multiple comparisons test, with a single pooled variance. The family-wise significance and confidence levels were set to 0.05 (95% confidence interval). Statistical analyses were performed utilizing GraphPad Prism 6 (GraphPad Software).

Chapter 3: RESULTS

3.1. BRIL in MC3T3-E1 cells

3.1.1. Luciferase reporter activity original screen

Prior to the beginning of this project, a large screening assay was performed to determine if any of the three forms of BRIL (denoted WT-BRIL, MALEP-BRIL and S40L-BRIL) could activate intracellular pathways causing activation of luciferase reporters. HEK293, MC3T3-E1 (hereafter denoted MC3T3) and MLO-A5 cells were co-transfected with plasmids encoding the three forms of BRIL and a wide range of luciferase reporters harboring responsive luciferase constructs. It is important to note that both MC3T3 and MLO-A5 cells do not express endogenous BRIL under the tested conditions. The responsive luciferase constructs encode a firefly luciferase reporter gene under the control of a minimal CMV promoter and tandem repeats of transcriptional response elements, depending on the reporter. Reporters used to screen for activity are outlined in Table 8, most of which were obtained from Cignal.

Table 8. List of tested luciferase reporters of original screen.

Reporter	Full Name	Pathway	Source
AARE	Amino-acid response element	Amino acid deprivation	Cignal
EGR1	Early growth response 1	EGR1 signaling	Cignal
Nanog	Nanog homeobox	Nanog signaling	Cignal
GLI	Glioma-associated oncogene	Hedgehog signaling	Cignal
XRE	Xenobiotic response element	AhR signaling	Cignal
ERSE	ER stress response	ER stress	Cignal
NFAT	Nuclear factor of activated T-cells	PKC / Ca^{2+} signaling	Cignal
RBP-Jk	Recombining binding protein suppressor of hairless	Notch signaling	Cignal
FOXO	Forkhead box	Pi3K / AKT signaling	Cignal
PPAR	Peroxisome proliferator-activated receptor	PPAR signaling	Cignal
STAT3	Signal transducer and activator of transcription 3	STAT3 signaling	Cignal
HIF-1	Hypoxia-inducible factor-1	Hypoxia	Cignal
SMAD	Mothers against decapentaplegic	TGFβ signaling	In-house

Ptgs2	Cyclooxygenase II	Cox2 promoter	In-house
Top Flash	Wnt / R-spondin	Wnt signaling	In-house
Col2-Sox9	Collagen type II / SRY-box 9	Col2 promoter	In-house
Runx2	Runt-related transcription factor 2	Osteoblast differentiation	In-house
Atf4	Activating transcription factor 4	Matrix mineralization	Dr. Gerard Karsenty (Columbia)
Nr4a2	Nuclear receptor subfamily 4 group A member 2	Inflammation and others	Dr. Jacques Drouin (IRCM)
MEF2	Myocyte enhancer factor 2	MEF2 signaling	Cignal

The results of the reporter screen in MLO-A5 cells are illustrated in Figure 2 and are representative of the induction noted in MC3T3 (data not shown). In the interest of space, only results from co-transfections with WT-BRIL or MALEP-BRIL are shown. Two reporters markedly stand out from the rest: NFAT-Luc and MEF2-Luc, which were found to be induced by both WT-BRIL and MALEP-BRIL.

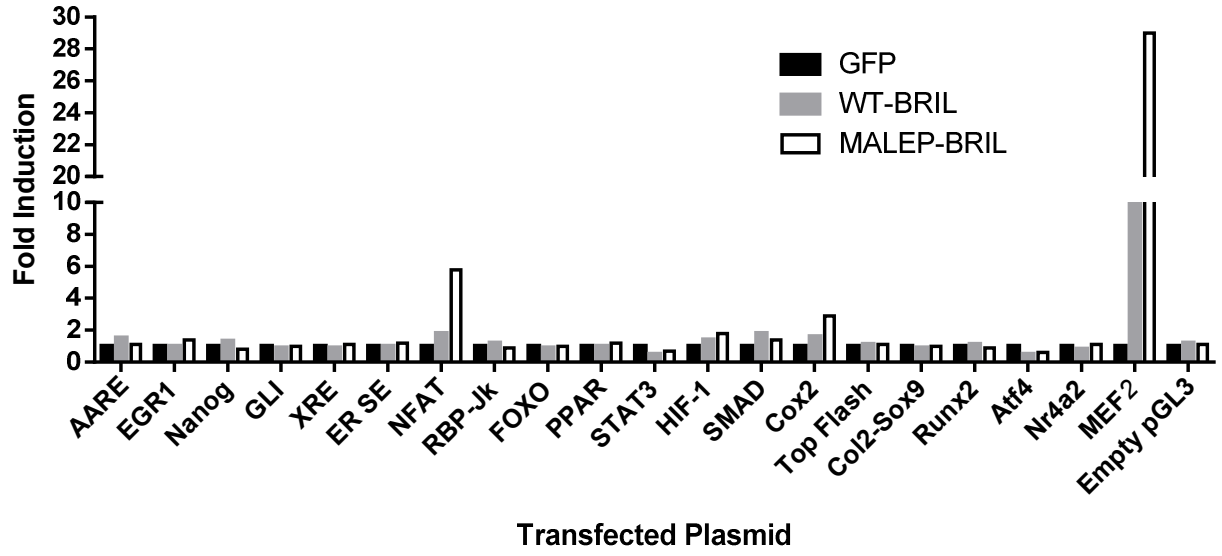

Figure 2. Original screen of luciferase reporter activity in transfected MLO-A5 cells. All results were normalized to GFP's average readout. Each transfection was carried out with 100ng of both the effector and reporter plasmids. Data represents average (N=1).

3.1.2. MEF2-Luc and NFAT-Luc reporters are induced by BRIL

The two reporters MEF2-Luc and NFAT-Luc were selected for further testing based on the data from the original screen as well as their relevance in osteoblasts and bone cells in general, detailed below. The inductions measured in the context of this project in the MEF2-Luc and NFAT-Luc reporters are shown in Figure 4A. Structures of the MEF2-Luc and NFAT-Luc plasmids are detailed in Figure 3. The MEF2-Luc is a reporter made of 6 MEF2 MADS-box transcription response elements, a minimal CMV promoter and a firefly luciferase reporter gene. The reporter was designed to measure transcriptional activity of all four MEF2 factors (MEF2A, MEF2B, MEF2C and MEF2D). Myocyte-specific enhancer factor 2, or MEF2, is a family of proteins that contain both MADS-box and MEF2 DNA-binding domains [66]. In osteoblasts, MEF2C is a transcription factor involved in osteoblast differentiation and gene regulation, thought to be upstream of bone-specific transcription factors Runx2 and Osterix [67]. The NFAT-Luc (a new construct from Addgene, which responded better to BRIL transfections than the reporter from Cignal) is a reporter made of 3 composite NFAT-AP1 (activator protein-1) response elements from the human interleukin-2 (IL-2) gene fused to its minimal human IL-2 promoter. Nuclear factor of activated T-cells (NFAT) is a transcription factor that shuttles between the cytoplasm (when phosphorylated) and the nucleus (when dephosphorylated), controlled by the action of calcineurin [68]. The NFAT signalling pathway is involved in osteoblasts by regulating bone mass, where overexpression in mice leads to higher bone mass [69].

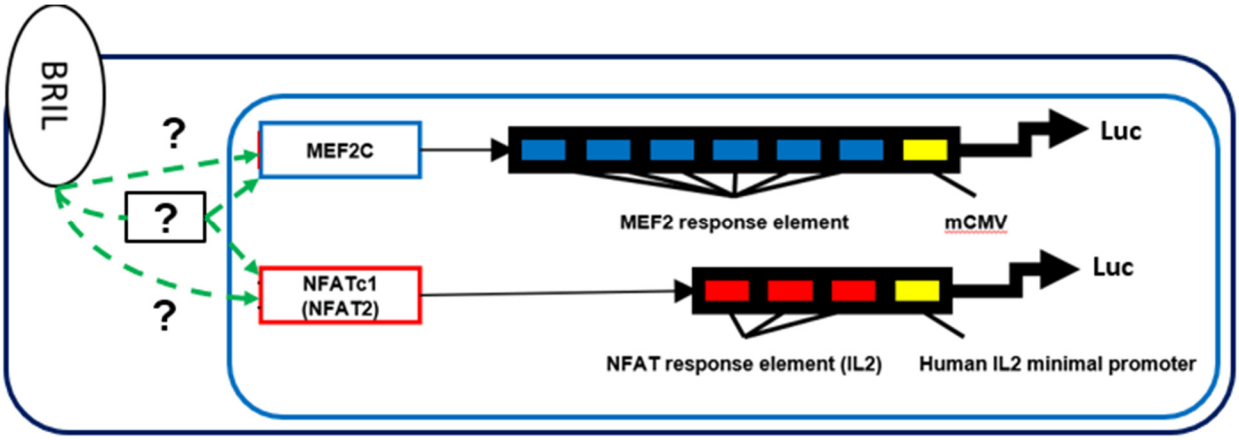

Figure 3. MEF2-Luc and NFAT-Luc reporter constructs. Schematic illustrating luciferase reporter structure as well as BRIL's potential mechanisms of action leading to reporter induction.

Significant inductions were recorded for both WT-BRIL and MALEP-BRIL forms as compared to both GFP and IFITM3 negative controls. The GFP serves as a control for the transfection procedure, while IFITM3 is closely related to BRIL in structure, and allows for the detection of BRIL-specific effects. WT-BRIL's (6- to 41-fold) and MALEP-BRIL's (4- to 43-fold) inductions were at similar levels to the positive control, MEF2C, which ranges from 8- to 40-fold. S40L-BRIL somewhat induces the reporter although not statistically significant, likely due to its lowered expression. The same can be seen on the NFAT-Luc reporter, where both WT-BRIL and MALEP-BRIL significantly induce the reporter ranging from 5- to 16-fold inductions, comparable to NFATc1 itself, which ranges from 7- to 26-fold. Figure 4B and 4C confirm protein expression and localization of the transfected forms of BRIL respectively. Western blots and immunofluorescent staining were also used to confirm presence of IFITM3, MEF2C and NFATc1 (data not

shown). However, no obvious difference was noted between the activity of three forms of BRIL on both MEF2-Luc and NFAT-Luc reporters.

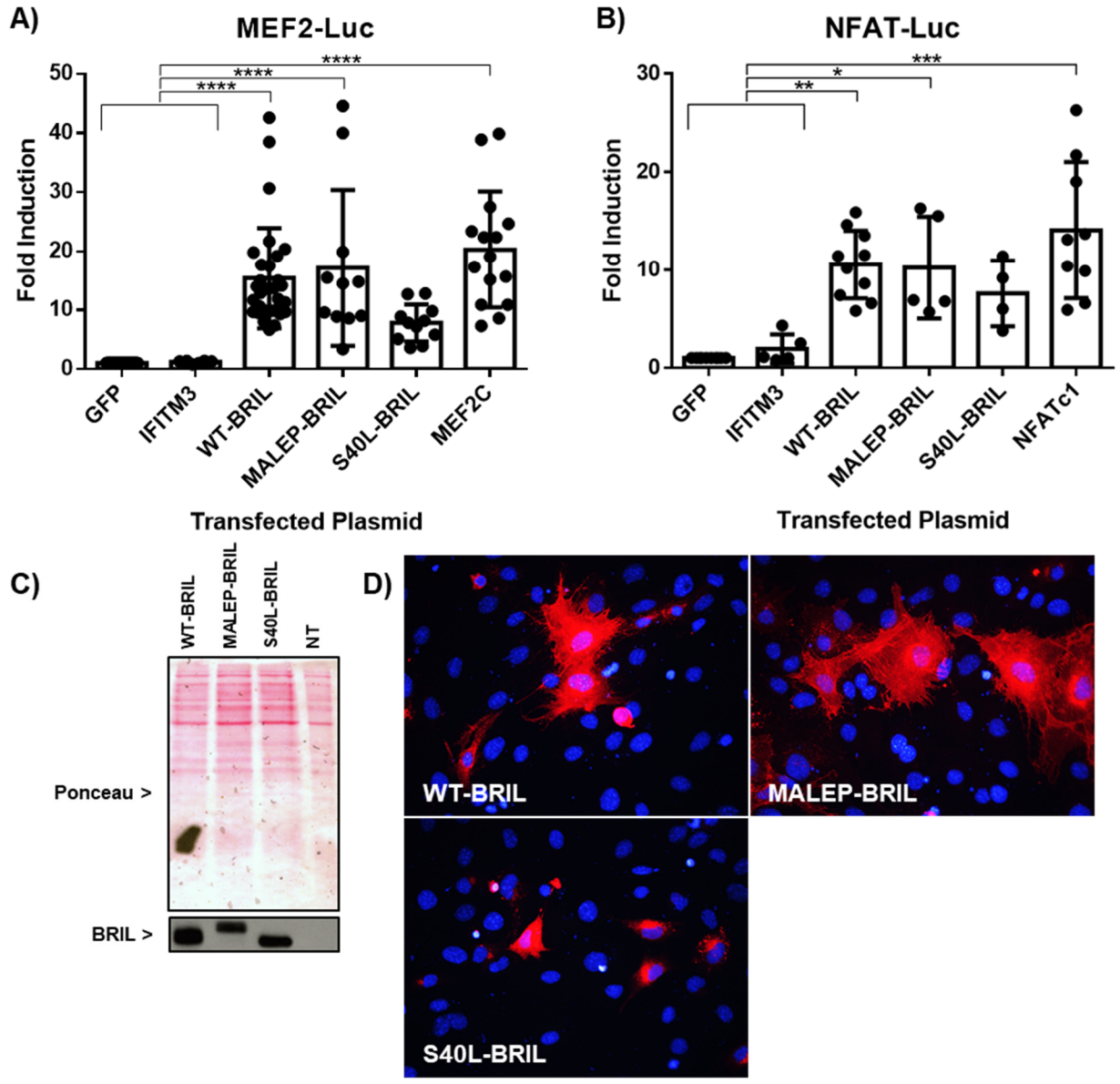

Figure 4. BRIL activity, expression and localization in MC3T3 cells. A)-B) Effect of BRIL forms on MEF2-Luc and NFAT-Luc readout in transfected MC3T3 cells. All results were normalized to GFP's average readout. Each transfection was carried out with 100ng of both the effector and reporter plasmids. Each data point represents one experiment, during which two repeats were performed. Data represents average ±SD

(MEF2-Luc: N=11-30 / NFAT-Luc: N=4-10). C) Western blot detection of the three forms of BRIL using anti-BRIL N-terminal antibody in transfected and naïve MC3T3 cells. (NT=Non-transfected). D) Immunofluorescent staining of transfected MC3T3 cells permeabilized using triton and anti-BRIL N-terminal antibody. Pictures are merged with DAPI stains and taken at 40X.

Considering the reporter readouts in response to simple BRIL transfections are caused by the activation of endogenous pathways, we opted to explore the effect of combined transfections with BRIL and pathway members related to each reporter; in this case, MEF2C for MEF2-Luc, and NFATc1 for NFAT-Luc. We noted apparent synergistic induction of the MEF2-Luc reporter when the WT-BRIL form is co-transfected with MEF2C, as readouts obtained are greater than additive (Figure 5). Luciferase assay results using the MALEP-BRIL and S40L-BRIL forms also showed similar synergy (data not shown). The same cannot be said of the NFAT-Luc reporter, where simple additive effects were observed in co-transfections of WT-BRIL and NFATc1.

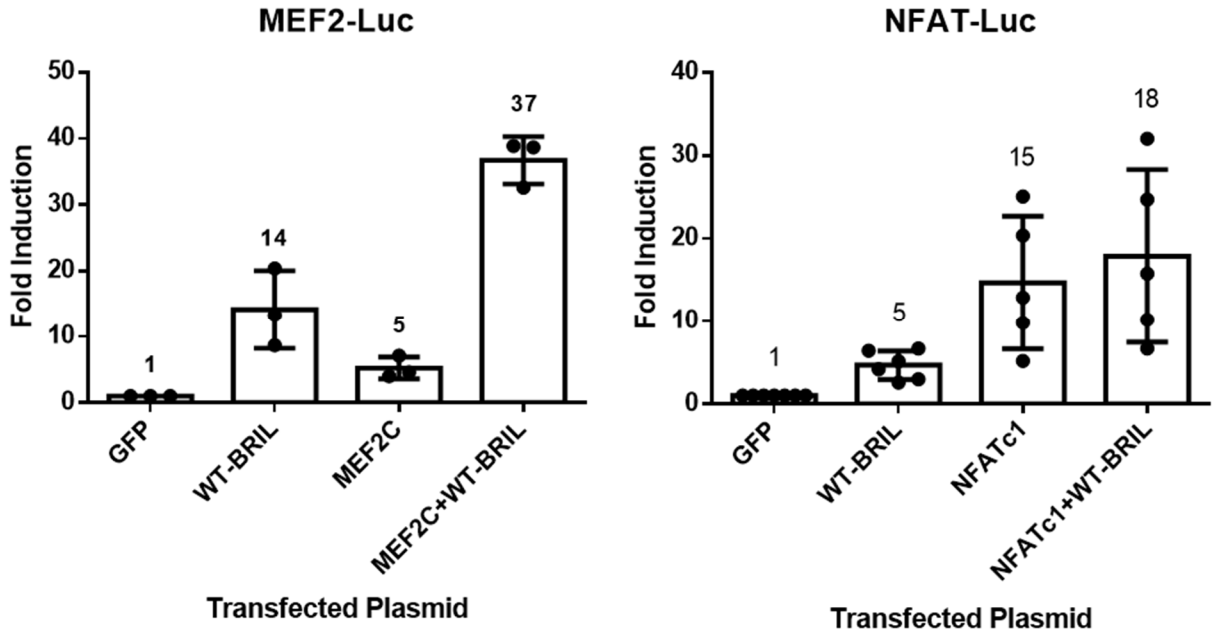

Figure 5. Co-transfection of WT-BRIL with MEF2C and NFATC1 have synergistic and additive effects respectively. Effect of WT-BRIL co-transfected with MEF2C or NFATc1 on MEF2-Luc or NFAT-Luc readout respectively in transfected MC3T3 cells. All results were normalized to GFP's average readout. Each transfection was carried out with 50ng of both effectors and 100ng of reporter plasmids. The GFP plasmid served as the other effector for WT-BRIL, MEF2C and NFATc1 transfections. Each data point represents one experiment, during which two repeats were performed. Data represents average ±SD (MEF2-Luc: N=3 / NFAT-Luc: N=5-8).

Having established that lower inductions were recorded using the NFAT-Luc reporter and the apparent lack of synergistic activity of BRIL and NFAT, the emphasis was first put primarily on manipulations of MEF2 activity in MC3T3 cells. Details on the various manipulations involving NFAT are detailed in section 3.4.

3.2. BRIL and MEF2 activity in MC3T3 cells

3.2.1. Kinetics of the MEF2-Luc reporter

In order to further examine possible differences in the ability of the different forms of BRIL to induce the MEF2-Luc reporter, I investigated the kinetics of induction. The luciferase readout was measured at 8-, 12- and 24-hours following co-transfection of the three forms of BRIL and the MEF2-Luc reporter. The kinetic of activity of the MEF2-Luc in the presence of the 2 mutant forms of BRIL (MALEP and S40L) was not significantly different from that induced by the WT-BRIL (Figure 6). The MEF-Luc reporter was significantly activated by the 3 forms over the GFP control, only 8h after transfection. Although the MALEP-BRIL appeared to be slightly more active than the WT-BRIL and S40L-BRIL at this 8h time-point, this was not observed by 12h and 24h. These results suggested that there was no selective advantage of one form over the other at preferentially inducing the MEF2-Luc reporter.

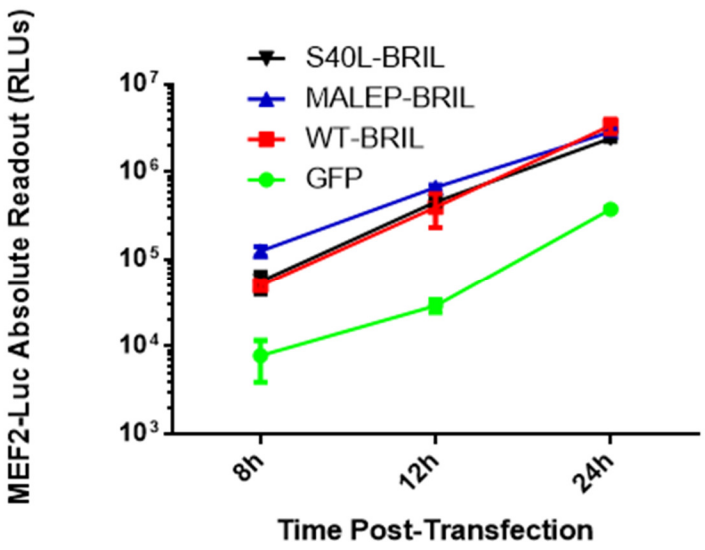

Figure 6. MEF2-Luc luciferase readout as measured at 8-, 12- and 24-hour time points following transfection in MC3T3 cells. All results were normalized to GFP's average readout. Each transfection was carried out with 100ng of both the effector and reporter plasmids. Y axis is in logarithmic scale, base 10. Data represents average (N=2).

3.2.2. BRIL and MEF2 expression in MC3T3 cells

In order to verify whether the observed MEF2-Luc reporter induction is caused by an increased transcriptional of the *Mef2* genes, rather than BRIL modulating a signaling pathway, we explored if and which specific member of the *Mef2* family (MEF2A, MEF2B, MEF2C and MEF2D) could contribute to the BRIL promoting activity. It was also important to conduct these experiments considering the MEF2-Luc reporter can be equally modulated by any of the MEF2 members. We first assessed whether BRIL could modulate their expression levels. This was tested by quantifying the relative expression levels of the *Mef2* transcripts in naïve and transfected MC3T3 cells by RT-qPCR. Figure

7 illustrates gene expression data of MC3T3 transfected with plasmids encoding the three BRIL forms and non-transfected cells as negative controls.

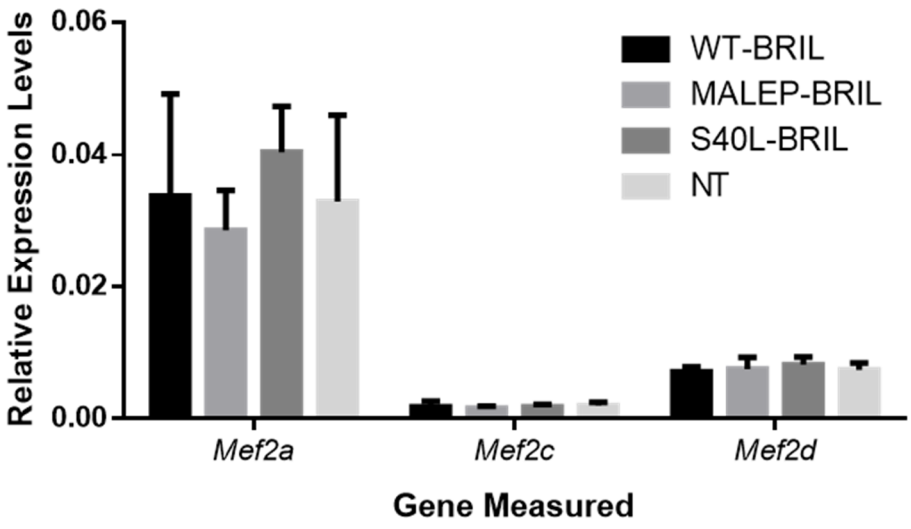

Figure 7. Quantitative PCR showing relative expression of *Mef2* family members in transfected and naïve MC3T3 cells. WT-BRIL, MALEP-BRIL and S40L-BRIL plasmids were transfected using 1µg of DNA. Relative expression normalized using β-actin (*Actb*). Data represents average ±SD (N=3). NT=Non-transfected.

Initial evaluations of levels of *Mef2* gene expression revealed *Mef2a* is highly expressed compared to all other forms, followed by *Mef2d* and *Mef2c*. *Mef2b* is not expressed in MC3T3 cells (data not shown). Forced expression of all three forms of BRIL had no significant effect on *Mef2* expression as compared to naïve non-transfected MC3T3. Considering *Mef2* gene expression was unaffected, and following the rationale that the MEF2-Luc reporter is designed to report all MEF2 family members, we also transfected MC3T3 with plasmids encoding MEF2A, MEF2C and MEF2D. This could give us a sense of which MEF2 family member is likely involved in the induction

following BRIL transfection. Co-transfections using a MEF2A plasmid showed an induction of the MEF2-Luc reporter similar to MEF2C, while the MEF2D plasmid results mirrored S40L-BRIL (some data shown (MEF2C and S40L-BRIL readouts) in Figure 4A).

In the following sections, the focus was put to possibly identify the mechanism(s) and intermediate(s) by which BRIL activated the MEF2-Luc reporter.

3.2.3. BRIL's link with the MEF2 protein family and one of its known repressors, HDAC4

Considering BRIL transfection had no effect on *Mef2* gene expression, as well as to narrow down the search for BRIL's link to MEF2, it was necessary to validate bona-fide activation of the pathway by investigating other known MEF2 regulatory proteins. I first explored whether histone deacetylase 4 (HDAC4) could modulate the response induced by BRIL. HDAC4 is known to directly interact with MEF2 and regulate its nuclear localization and activity [70, 71]. HDAC4 is part of class IIa of histone deacetylases that shuttles between the cytoplasm and nucleus in a signal-dependent manner [72]. HDAC4's shuttling is controlled by the phosphorylation-dependent binding to 14-3-3 proteins. When HDAC4 is phosphorylated at three serine residues (S246, S467 and S632), it promotes 14-3-3 binding and subsequently is retained in the cytoplasm [72]. The phosphorylation of S266, found within the nuclear localization signal of HDAC4, also retains the protein in the cytoplasm. When none of the serine residues are phosphorylated, HDAC4 remains in the nucleus, where it acts as a corepressor of several transcription factors, including the MEF2 family.

It was therefore of interest to clarify the potential role that BRIL may have on the repression induced by HDAC4. A plasmid encoding HDAC4 was consequently used to overexpress HDAC4 in MC3T3, aimed at potentially inhibiting MEF2 and thus the MEF2-Luc reporter induction caused by BRIL transfection. A mutated form of HDAC4 was also used, named HDAC4-mut, where the three phosphorylation sites S246, S467 and S632 are changed to alanine residues, forcing the protein to remain in the nucleus and thus constitutively active. We noted a dose-dependent inhibition of WT-BRIL with both HDAC4 and HDAC4-mut, the latter being much more potent as expected, whereby only an amount of 1.0ng and 0.1ng of transfected HDAC4 and HDAC4-mut plasmid respectively could quench half the induction caused by 70ng of WT-BRIL (Figure 8).

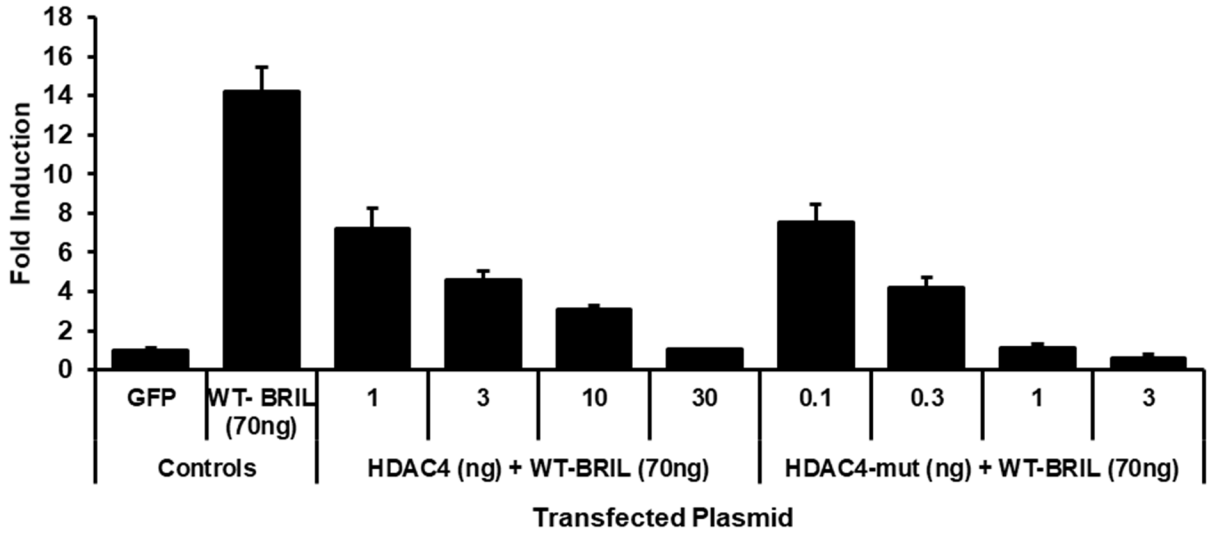

Figure 8. Dose-dependent inhibition of WT-BRIL by HDAC4 and HDAC4-mut in transfected MC3T3 cells. All results were normalized to GFP's average readout. Other than the GFP negative control (100ng), all transfections included 70ng of the WT-BRIL plasmid. Various quantities of HDAC4 and HDAC4-mut plasmids were co-transfected with WT-BRIL, and GFP plasmid in order to obtain a total of 100ng of DNA. Data represents average ±SE (N=1).

Results therefore show that it is possible to inhibit the induction of the MEF2-Luc reporter caused by WT-BRIL with very little of HDAC4. Therefore, it provides further evidence that the effect of BRIL on the MEF2-Luc reporter is readily mediated by one of the endogenous MEF2.

Next, we measured the MEF2-Luc activity after co-transfections with the three forms of BRIL to test whether they were equally sensitive to the inhibitory activity of HDAC4. All showed similar sensitivity to the repressive effect of HDAC4 and HDAC-mut (data not shown). These data indicate that the MEF2-Luc's activity in response to BRIL transfection can be prevented by the overexpression of HDAC4 but does not seem to differentiate between WT-BRIL and its two other mutant forms, MALEP-BRIL and S40L-BRIL.

It was also investigated whether any change could be observed in HDAC4's nucleo-cytoplasmic shuttling and expression levels in response to BRIL transfection. To do so, HDAC4 was co-transfected with all three forms of BRIL (or with an empty plasmid instead of GFP as it would have interfered with the immunofluorescence detection) as part of a co-immunolabeling experiment using separated antibodies targeting BRIL and HDAC4 (FLAG-tagged), in triton-permeabilized MC3T3 cells. In the case of co-transfections with BRIL, cells expressing both HDAC4 and BRIL were counted, and HDAC4's cellular localization was noted. As shown in Figure 9 the cell count distribution percentage showed HDAC4 distribution in the cytoplasm and the nucleus did not dramatically vary in response to BRIL expression. However, slight changes, although not statistically significant, were noted in terms of nuclear

localization. These may be considered biologically non-significant considering the activity of the MEF2-Luc reporter did not vary between different forms of BRIL. However, endogenous or even low quantities of transfected HDAC4 were not detectable by immunostaining.

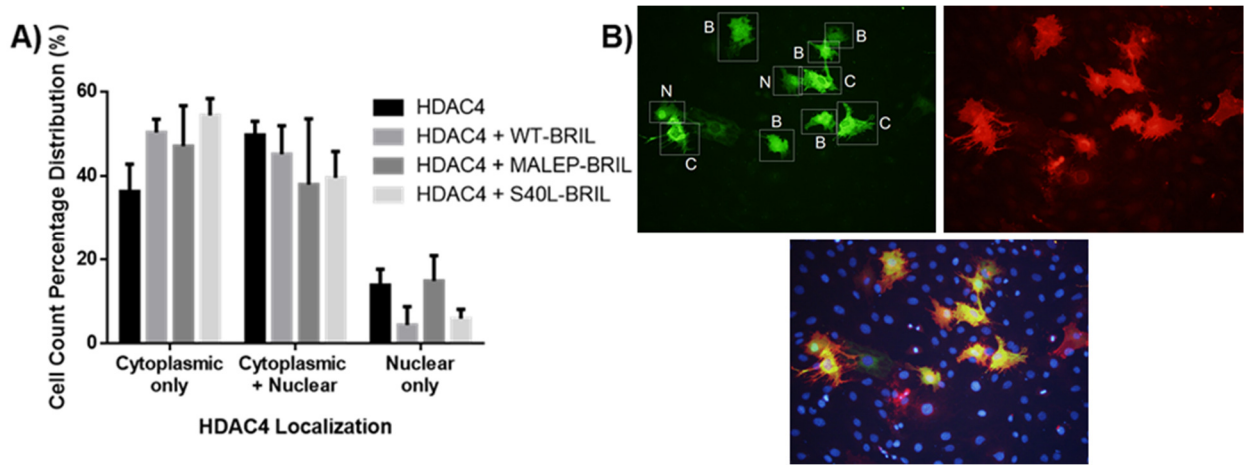

Figure 9. HDAC4 subcellular localization upon co-transfection with BRIL in MC3T3 cells. A) Cell count distribution percentage of immunofluorescent staining of triton-permeabilized transfected MC3T3 cells. Data represents average ±SD (N=3). B) Example of immunofluorescent staining using anti-BRIL N-terminal and anti-HDAC4 antibodies. Picture of HDAC4 and MALEP-BRIL co-transfection, taken at 20X, used for the cell count. Top left: Visualization of HDAC4 protein in green. Top right: Visualization of MALEP-BRIL protein in red. Bottom center: Merge of both HDAC4 and MALEP-BRIL with DAPI. B: Both cytoplasmic and nuclear. C: Cytoplasmic only. N: Nuclear only. Each transfection was carried out with 500ng of both effector plasmids (BRIL forms and HDAC4).

Furthermore, I also determined whether BRIL transfections could lead to changes in expression levels of *Hdac* family members. Based on the repressive effect of HDAC4 on the MEF2-Luc reporter, it could be predicted that the expression of one or more *Hdac* family member would be downregulated in response to BRIL transfection. This was measured by RT-qPCR and included the ubiquitously expressed and nuclear class I HDAC1, HDAC2 and HDAC3 as well as the class IIa HDAC4, HDAC5 and HDAC7 that shuttle between the cytoplasm and nucleus [73]. In wild-type MC3T3 cells, expressions are ranked as follows: *Hdac2* > *Hdac1* = *Hdac3* > *Hdac4* = *Hdac5* > *Hdac7* (Figure 10). However, no such downregulation was observed, as the expression of all the *Hdac* genes were not significantly affected by the presence of transfected WT-, MALEP- and S40L-BRIL.

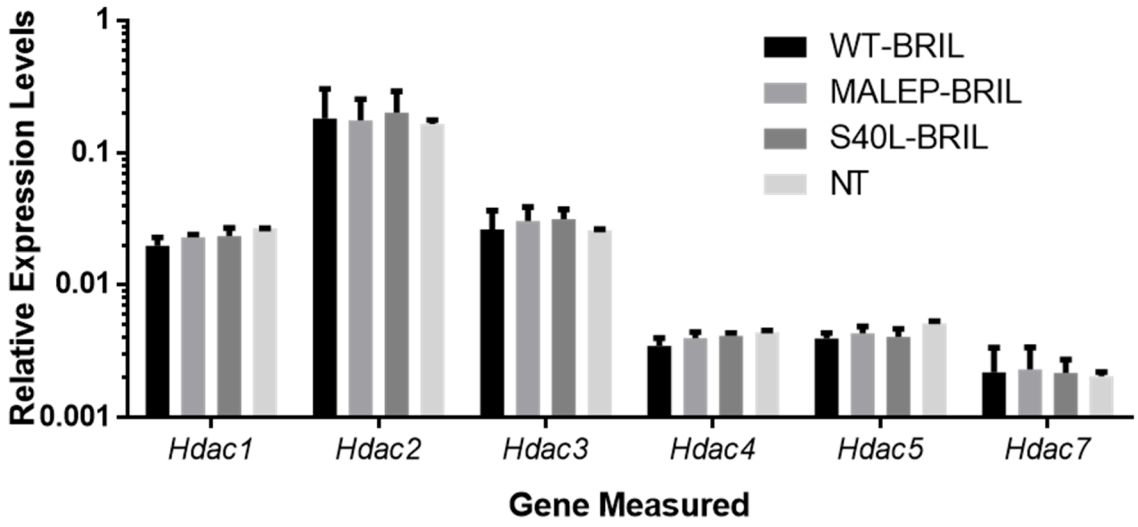

Figure 10. Quantitative PCR of *Hdac* family members in transfected and naïve MC3T3 cells. WT-BRIL, MALEP-BRIL and S40L-BRIL plasmids were transfected using 1µg of DNA. Relative expression based on β-actin (*Actb*). Y axis is in logarithmic scale, base 10. Data represents average ±SD (N=3). NT=Non-transfected.

Considering that HDAC is known to be controlled by its phosphorylation status, I next investigated whether BRIL could promote HDAC phosphorylation and hence prevent its inhibitory activity towards MEF2. HDAC4's phosphorylation status in response to BRIL transfection was examined using an anti-phospho-HDAC4 antibody detecting the phosphorylated serines S467 and S632, donated by Dr. Yang [72]. However, phospho-HDAC were difficult to discern by western blotting. Several non-specific bands were detected, so the results could not allow us to conclude unambiguously that BRIL could or not cause changes in the phosphorylation status of HDAC4 following co-transfection with the various forms of BRIL (data not shown).

It was therefore first concluded that there was no difference between the forms of BRIL in terms of temporal activation of the MEF2-Luc reporter, nor were there any significant variations in *Mef2* gene expression detected in response to BRIL transfections. Furthermore, small quantities of HDAC4 inhibit the induction of the MEF2-Luc by all forms of BRIL, further suggesting that BRIL's activity is mediated by endogenous MEF2s. However, we could not detect any variation in *Hdac* gene expression, HDAC4 localization or its phosphorylation status in response to BRIL transfections. Following these experiments, a focus was put on other avenues directly involving BRIL and its mutants, specifically its structure and function.

3.3. Structural and functional studies of BRIL mediating transcriptional activation of MEF2

3.3.1. N-terminal truncated forms of WT-BRIL

While establishing different elements and pathways BRIL may be involved in is important, studying the function of BRIL in relation to its structure is also valuable. Following several luciferase assays using a version of WT-BRIL with a Myc tag (used for other purposes such as affinity chromatography) or HA tag (used for immunofluorescence and Western blots) on the N-terminus, it was noted that the modified proteins did not lead to any luciferase activity when its plasmid was transfected with the MEF2-Luc reporter (Figure 11A). This led us to hypothesise that the function associated with the MEF2-Luc reporter could be linked to the N-terminal end of the protein, given that the addition of the Myc and HA tag interfered with the protein's effect. To address this possibility, truncated versions of WT-BRIL were produced whereby five or six amino acids were removed at the N-terminal of the protein (Δ2-6 / Δ7-12 / Δ19-24 / Δ25-30).

As illustrated by Figure 11A, co-transfections using the truncated WT-BRIL proteins with the MEF2-Luc reporter showed that the BRIL Δ2-6 was the most severely affected, and its luciferase readout dropped to the levels of the GFP negative control. The other truncated proteins did show reproducible and consistent slight decreases in activity, although not statistically significant. Western blot results demonstrate that BRIL Δ2-6 and BRIL Δ7-12 were expressed at levels comparable to WT-BRIL, while BRIL Δ19-24 and BRIL Δ25-30 expression was much lower (Figure 11B). An

immunofluorescent staining assay confirmed correct protein localization for all truncated forms of BRIL (Figure 11C).

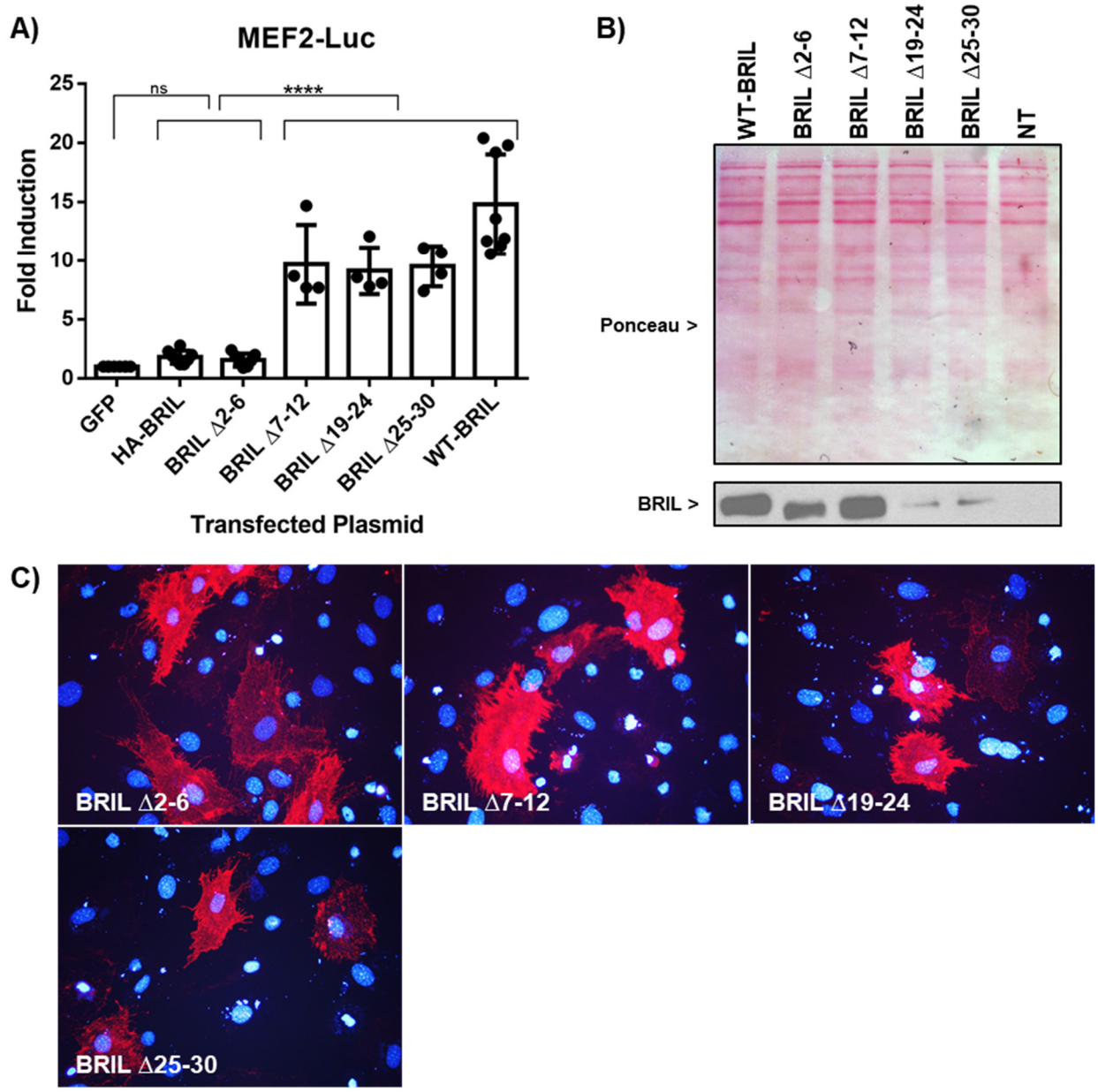

Figure 11. N-terminal five or six amino acid deletion in WT-BRIL in MC3T3 cells. A) Effect of truncated forms of WT-BRIL forms on MEF2-Luc in transfected MC3T3 cells. All results were normalized to GFP's average readout. Each transfection was carried out with 100ng of both the effector and reporter plasmids. Each data point represents

one experiment, during which two repeats were performed. Data represents average ±SD (N=4-8). B) Western blot detection of the four truncated forms of BRIL using anti-BRIL C-terminal antibody in transfected and naïve MC3T3 cells. NT=Non-transfected. C) Immunofluorescent staining of transfected MC3T3 cells permeabilized using triton and anti-BRIL C-terminal antibody. Pictures are merged with DAPI stains and taken at 40X.

Amino acid sequence alignments of the BRIL N-terminal segment (1-50) showed a stretch (1 to 9) of highly conserved amino acids MDTXYPRED throughout a series of species (Figure 12). Only primates have an alanine at position 4, while all other studied mammals and birds have a serine. However, more divergence can be observed from residues 10 to 30, suggesting that they may less likely be ‘functional’ in the MEF2-Luc readout, as determined from data of Figure 11.

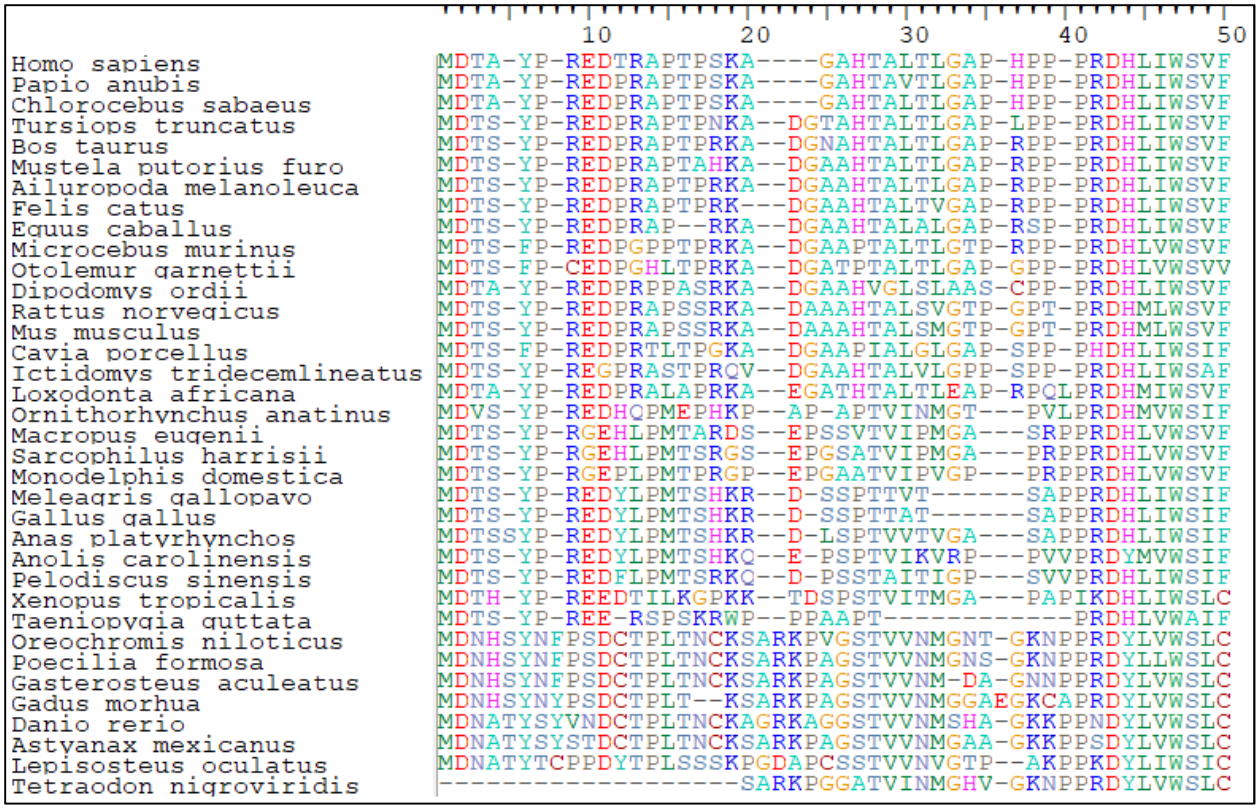

Figure 12. Protein sequence alignment of BRIL N-terminus. Alignments were generated by *ClustalW Multiple alignment*. The alignment only shows the first 50 amino acids.

Following the results demonstrating that the first N-terminal amino acids have a significant impact on BRIL's activity and are heavily conserved, the analysis was refined in an attempt to pinpoint more exactly what residues would be critical for BRIL's activity on the MEF2-Luc reporter.

3.3.2. Alanine-scanning and other amino acid substitutions of WT-BRIL

It was determined that the best course would be to study the residues using an alanine-scanning technique. This was done by substituting individual residues at

position 2 to 6 (D-T-S-Y-P) with alanine (Figure 13A). Luciferase readouts revealed that the amino acids with the greatest effect on BRIL's induction of the MEF2-Luc reporter are D2, T3 and Y5. It was also expected that the S4 alanine substitution would have no impact since primates have an alanine at position 4 of their BRIL protein. Considering the potential functional implication of the aspartic acid at position 2, we included mutants D2E and D2N to verify if position 2 was dependent on the charge and/or structure, respectively. The aspartic acid to glutamic acid (D2E) change would preserve the acidic charge, while the aspartic acid to asparagine (D2N) would preserve the structure (same size for residues D/N) but not the charge. Both mutations failed at re-establishing BRIL's normal induction of the MEF2-Luc reporter (Figure 13A). Figure 13B and 13C confirm near-normal protein expression and localization of the transfected forms of BRIL respectively. The experiments highlighted the critical nature of the primary BRIL sequence responsible for the activation of a cascade leading to MEF2.

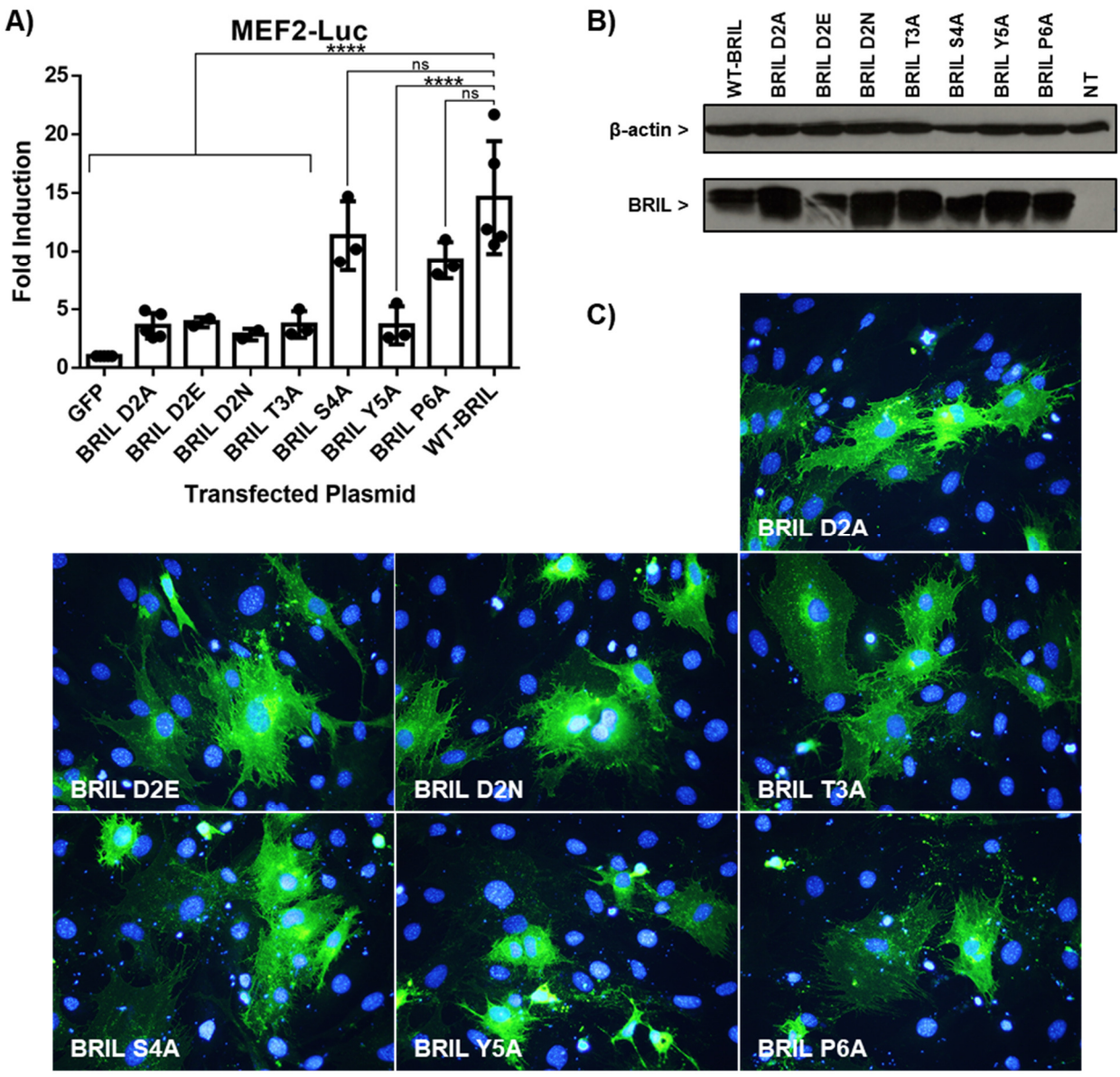

Figure 13. Effect of alanine scanning and other amino acid substitutions of WT-BRIL in transfected MC3T3 cells. A) Effects of WT-BRIL alterations on MEF2-Luc in transfected MC3T3 cells. All results were normalized to GFP's average readout. Each transfection was carried out with 100ng of both the effector and reporter plasmids. Each data point represents one experiment, during which two repeats were performed. Data represents average ±SD (N=3-5). B) Western blot detection of the seven mutated forms of BRIL using anti-BRIL N-terminal antibody in transfected and naïve MC3T3 cells.

NT=Non-transfected. C) Immunofluorescent staining of transfected MC3T3 cells permeabilized using triton and anti-BRIL N-terminal antibody. Pictures are merged with DAPI stains and taken at 40X.

3.3.3. N-terminal truncated and alanine substitution of MALEP-BRIL

Similar to the experiments conducted above with the WT-BRIL form, various amino acid deletions and substitutions in the MALEP-BRIL protein were explored and the subsequent outcomes are presented on Figure 14. Results obtained mirrored the effects seen with the WT-BRIL protein, where deletion of the amino acids 2-6 and the alanine substitution of D2 most severely affected MEF2-Luc's readout (Figure 14A). Again, protein expression and localization of the transfected forms of BRIL are confirmed in Figure 14B and 14C respectively.

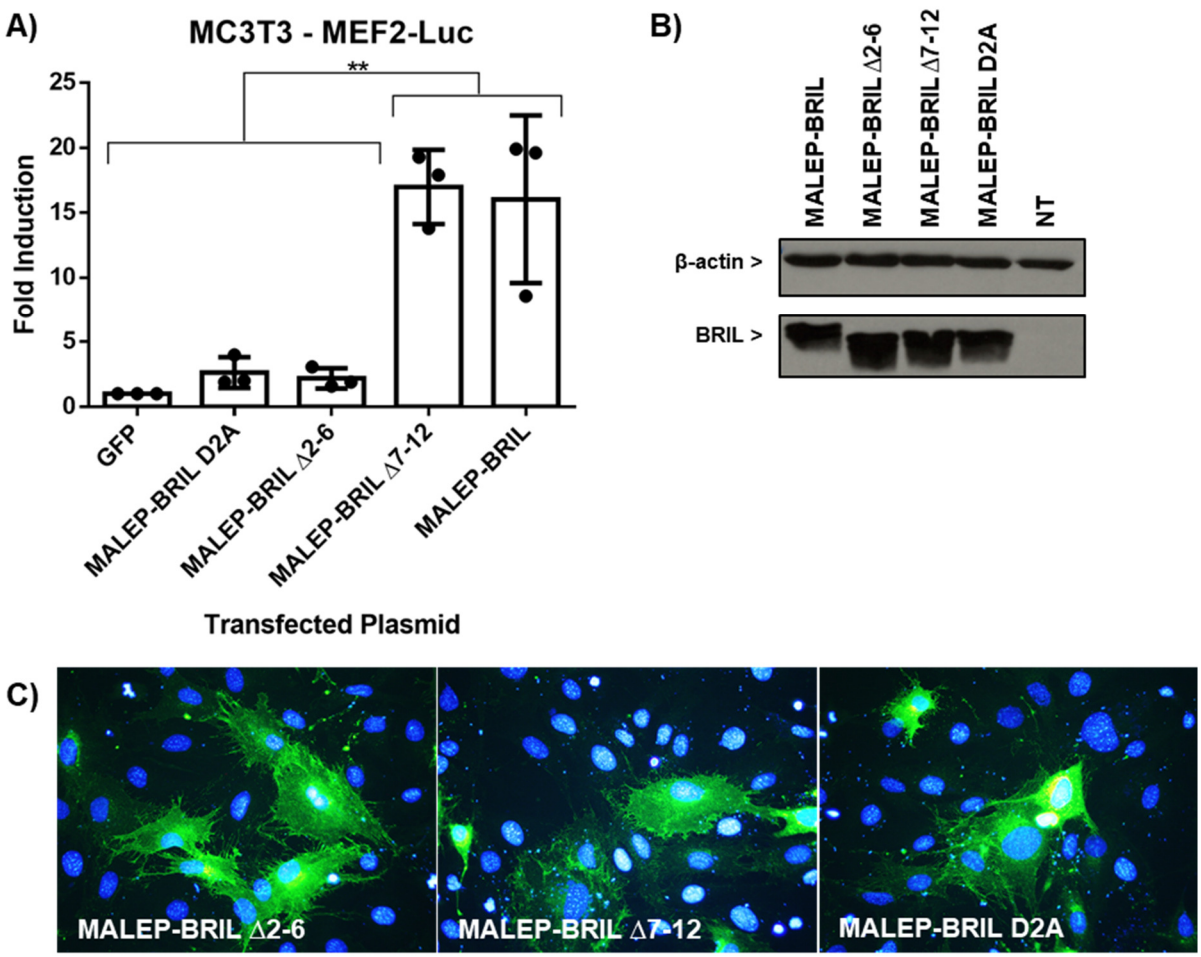

Figure 14. Effect of alanine scanning and five or six amino acid deletions of MALEP-BRIL in transfected MC3T3 cells. A) Effects of MALEP-BRIL alterations on MEF2-Luc in transfected MC3T3 cells. All results were normalized to GFP's average readout. Each transfection was carried out with 100ng of both the effector and reporter plasmids. Each data point represents one experiment, during which two repeats were performed. Data represents average ±SD (N=3). B) Western blot detection of the three mutated forms of MALEP-BRIL using anti-BRIL C-terminal antibody in transfected and naïve MC3T3 cells. NT=Non-transfected. C) Immunofluorescent staining of transfected MC3T3 cells permeabilized using triton and anti-BRIL C-terminal antibody. Pictures are merged with DAPI stains and taken at 40X.

3.3.4. Other mutations affecting WT-BRIL localization and topology

Next, it was investigated in more details whether the subcellular localization of BRIL was important for its ability to induce the MEF2-Luc reporter. It is known that the S40L-BRIL is trapped in the ER-Golgi and that it constantly gives lower activation fold than WT and MALEP forms. For this purpose, I used a series of other variants that were previously tested and shown also not to reach the plasma membrane [21]: the L101R mutant remains in the cytoplasm since the mutation disrupts the alpha-helix necessary for the transmembrane domain of the protein; the C-terminal KDEL-tagged form, which is a canonical ER-retention motif, is retained in the ER; the alanine-substituted cysteines at positions C52A, C53A and C52A-C53A inhibit palmitoylation leading to retention in the ER-Golgi; the K118-STOP form reaches the plasma membrane but has its extracellular C-terminal tail removed; and the OSTN-BRIL fused protein and A22N-BRIL form with an inserted glycosylation site adopt a different topology, where both the N-terminus and C-terminus are outside the cell. Overall, BRIL's induction of the MEF2-Luc reporter seemed heavily impacted by the L101R, KDEL and C52A-C53A mutations, reducing the inductions to the negative control's level, shown in Figure 15A. However, when only one palmitoylation site is disrupted, as is the case of C52A and C53A, or when the C-terminal of the protein is removed, the reduction is considerably less drastic. However, protein expression presented in Figure 15B show that BRIL L101R is virtually non-expressed, while all other mutated forms are expressed at lower levels than the WT-BRIL protein.

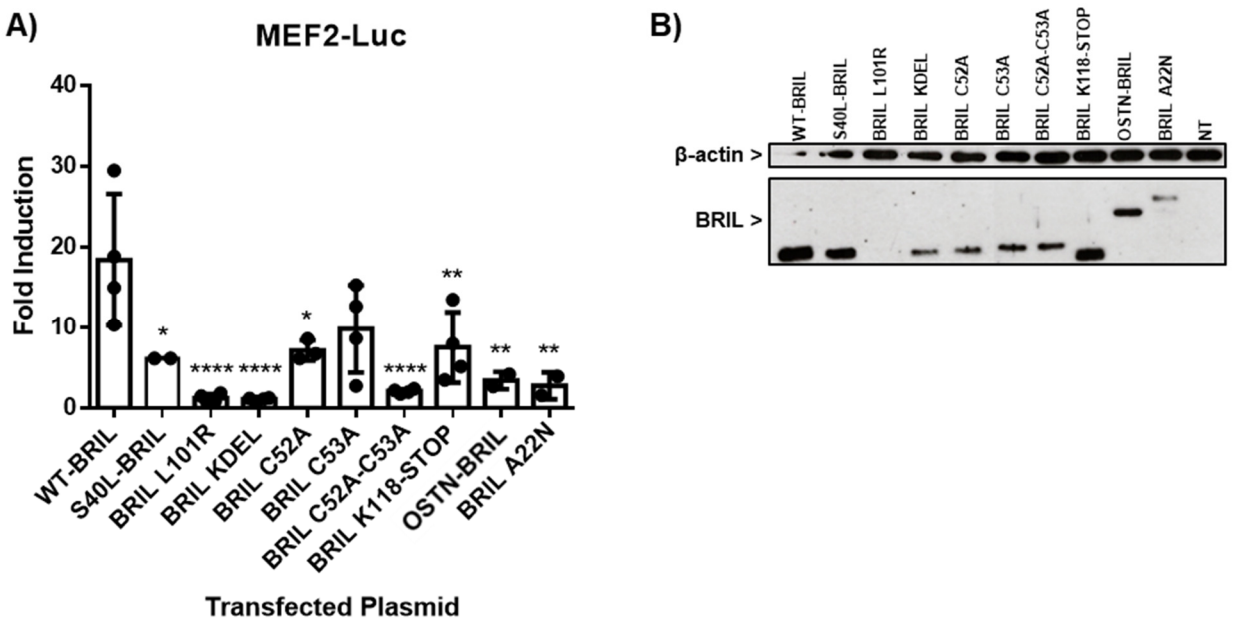

Figure 15. Effect of other WT-BRIL mutations affecting its localization and topology in transfected MC3T3 cells. A) Effects of WT-BRIL alterations on MEF2-Luc in transfected MC3T3 cells. All results were normalized to GFP's average readout. Each transfection was carried out with 100ng of both the effector and reporter plasmids. Each data point represents one experiment, during which two repeats were performed. Data represents average ±SD (N=2-4). B) Western blot detection of the mutated forms of WT-BRIL in transfected and naïve MC3T3 cells. NT=Non-transfected.

These results show in part that BRIL's plasma membrane localization and type II topology are important to its function leading to the MEF2-Luc induction.

3.3.5. Localization of S40L-BRIL is not re-established with S40D-BRIL mutant

The potential phosphorylation of the S40 position in the BRIL protein was also taken into consideration. Based on the Denmark Technical University (DTU)

Bioinformatics NetPhos 3.1 phosphorylation prediction tool, a strong score suggested the S40/S60 and S42/S62 positions of the human and mouse BRIL protein respectively are possible sites of a phosphorylation event. However, we focused on the S40L-BRIL mutant given its clinical importance. The S40-BRIL mutant could therefore possibly prevent phosphorylation events to occur in the WT-BRIL and affect its localization to the plasma membrane. Therefore, a plasmid harboring an S40D-BRIL form was constructed, where an aspartic acid was used as a phosphomimetic. An immunofluorescent staining of triton-permeabilized MC3T3 cells was performed, where WT-BRIL, S40L-BRIL and the S40D-BRIL form were transfected separately, allowing for localization comparisons (Figure 16). Results showed that the S40D-BRIL mutant localized in the ER-Golgi, similar to S40L-BRIL, suggesting that potential phosphorylation of residue S40 would not be causing S40L-BRIL's mis-localization (Figure 16). It must be pointed out that the localization shown in Figure 16 for the S40L and S40D mutants differ substantially form the WT. A reticular intracellular pattern and no clear plasma membrane staining is visible for S40L and S40D, while the WT-BRIL labels the cell contour extending out to all filopodia, and Golgi.

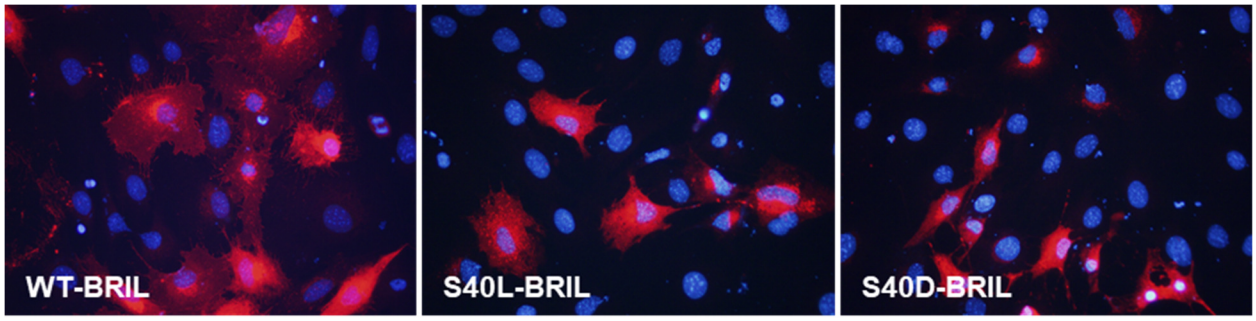

Figure 16. S40D-BRIL localizes to the ER-Golgi, similar to S40L-BRIL. Immunofluorescent staining of transfected MC3T3 cells permeabilized using triton and anti-BRIL N-terminal antibody. Pictures are merged with DAPI stains and taken at 40X.

Similarly, an immunofluorescent staining of non-permeabilized MC3T3 cells using an anti-C-terminal antibody yielded no signal for both S40L- and S40D-BRIL, demonstrating both do not properly localize to the plasma membrane in the type II topology (data not shown).

3.3.6. Summary of structure-function studies

Following these results, the role of WT-BRIL's N-terminus as a regulator of the MEF2-Luc reporter has been narrowed to amino acids D2, T3 and Y5. In terms of MALEP-BRIL, deletion of the amino acids 2-6 and substitutions affecting D2 yield results similar to WT-BRIL. Furthermore, BRIL's subcellular localization is likely important to its function following luciferase and immunofluorescence assays.

3.4. BRIL and NFAT activity in MC3T3 cells

3.4.1. BRIL and NFAT expression in MC3T3 cells

As mentioned in section 3.1.2., it was found that the NFAT-Luc reporter responded to BRIL transfection in MC3T3 cells. Readouts following transfection of all forms of BRIL were 8- to 15-fold, slightly lower but comparable to those of our transfected NFATc1 plasmid, serving as positive control. Considering that the NFAT-Luc reporter is designed to report the activity of all isoforms of NFATc, we explored the possibility that the activation was caused by the increase in transcription of the endogenous *Nfat* genes. Based on previous reports detailing the involvement of NFATc1 and NFATc2 in osteoblasts, we decided to narrow down the evaluation of endogenous gene expression to *Nfatc1* and *Nfatc2* genes. We first assessed whether

BRIL overexpression could modulate their expression levels. This was tested by quantifying the relative expression levels of the *Nfatc* transcripts in naïve and transfected MC3T3 cells by RT-qPCR. Figure 17 illustrates gene expression data of MC3T3 transfected with the three BRIL proteins and non-transfected cells as negative controls.

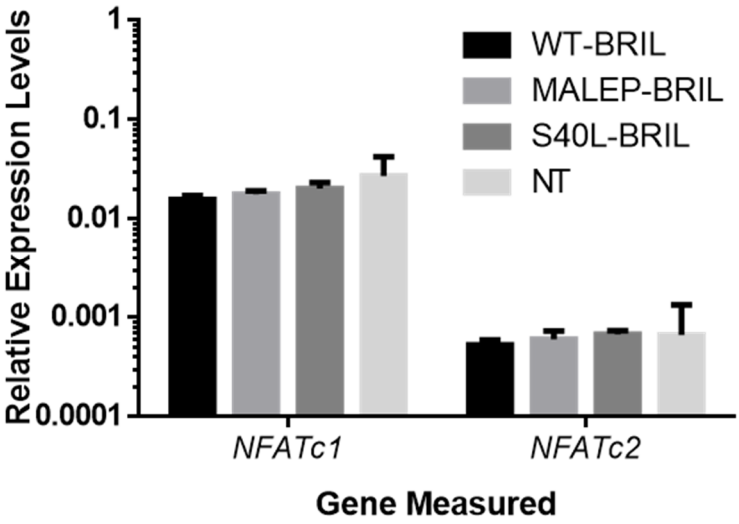

Figure 17. Quantitative PCR of *Nfatc* family members in transfected and naïve MC3T3 cells. WT-BRIL, MALEP-BRIL and S40L-BRIL plasmids were transfected using 1µg of DNA. Relative expression based on β-actin (*Actb*). Y axis is in logarithmic scale, base 10. Data represents average ±SD (N=3). NT=Non-transfected.

Overall, non-transfected MC3T3 cells expressed NFATc1 at levels 20-fold higher than NFATc2. Statistical analyses revealed *Nfatc1* and *Nfatc2* expression was not influenced by the presence of transfected BRIL. Considering NFATc1's expression level is higher in endogenous MC3T3 than NFATc2, BRIL's activity is probably mediated through NFATc1.

3.4.2. Modulation through NFAT pathway members and chemical inhibition by FK506

Next, we focused on identifying the possible involvement of NFAT pathway members as well as the calcineurin chemical inhibitor FK506. The Ca^{2+}-calcineurin-NFAT canonical signaling pathway begins with calcium (Ca^{2+}) binding to the regulatory subunit β of calcineurin to activate its phosphatase activity [68]. The catalytic subunit α of calcineurin then removes phosphate residues from NFATc1, which exposes nuclear localization sequences on the NFATc1 N-terminus. NFATc1's dephosphorylation subsequently promotes its nuclear entry, where it acts as a transcription factor for several genes. FK506, a known immunosuppressive drug, binds first to intracellular FKBP12 proteins, which in tern bind to calcineurin, preventing Ca^{2+} binding and subsequent activation.

In the context of this project, we opted to carry out co-transfections using plasmids encoding the catalytic subunit α of calcineurin (Cn-A) and a known negative regulator of calcineurin, named regulator of calcineurin 1 (RCAN1) [74]. RCAN1 is known to be induced directly by NFATc1 and provides a negative feedback mechanism to turn off the signalling. These plasmids were co-transfected with the WT-BRIL plasmid, and on both MEF2-Luc and NFAT-Luc reporters. Preliminary data, which only include one to three transfection experiments depending on the molecule tested, demonstrate possible effects of all three Cn-A, RCAN1 and FK506 (Figure 18). Specifically, when co-transfected with WT-BRIL, Cn-A demonstrated a greater than additive effect on both MEF2-Luc and NFAT-Luc readouts (Figure 18A and 18B). In contrast, RCAN1 inhibited WT-BRIL's induction of both reporters in co-transfection experiments. The addition of FK506 also substantially reduced the induction of WT-

BRIL (as well as MALEP-BRIL and S40L-BRIL; data not shown) on both reporters (Figure 18C and 18D). However, it is important to note that our negative control's (GFP) readout also diminished on both reporters following the addition of FK506, while the induction of NFATc1 on the NFAT-Luc reporter remained the same in response to FK506. The low experimental repeats can explain the variability seen in the results, but also gives us a glimpse into possible involvement of NFAT pathway members in BRIL's relationship with both MEF2 and NFAT. Altogether manipulation of the NFAT pathway tended to confirm that BRIL can indeed signal to increase NFAT and MEF2, perhaps through some common mechanisms.

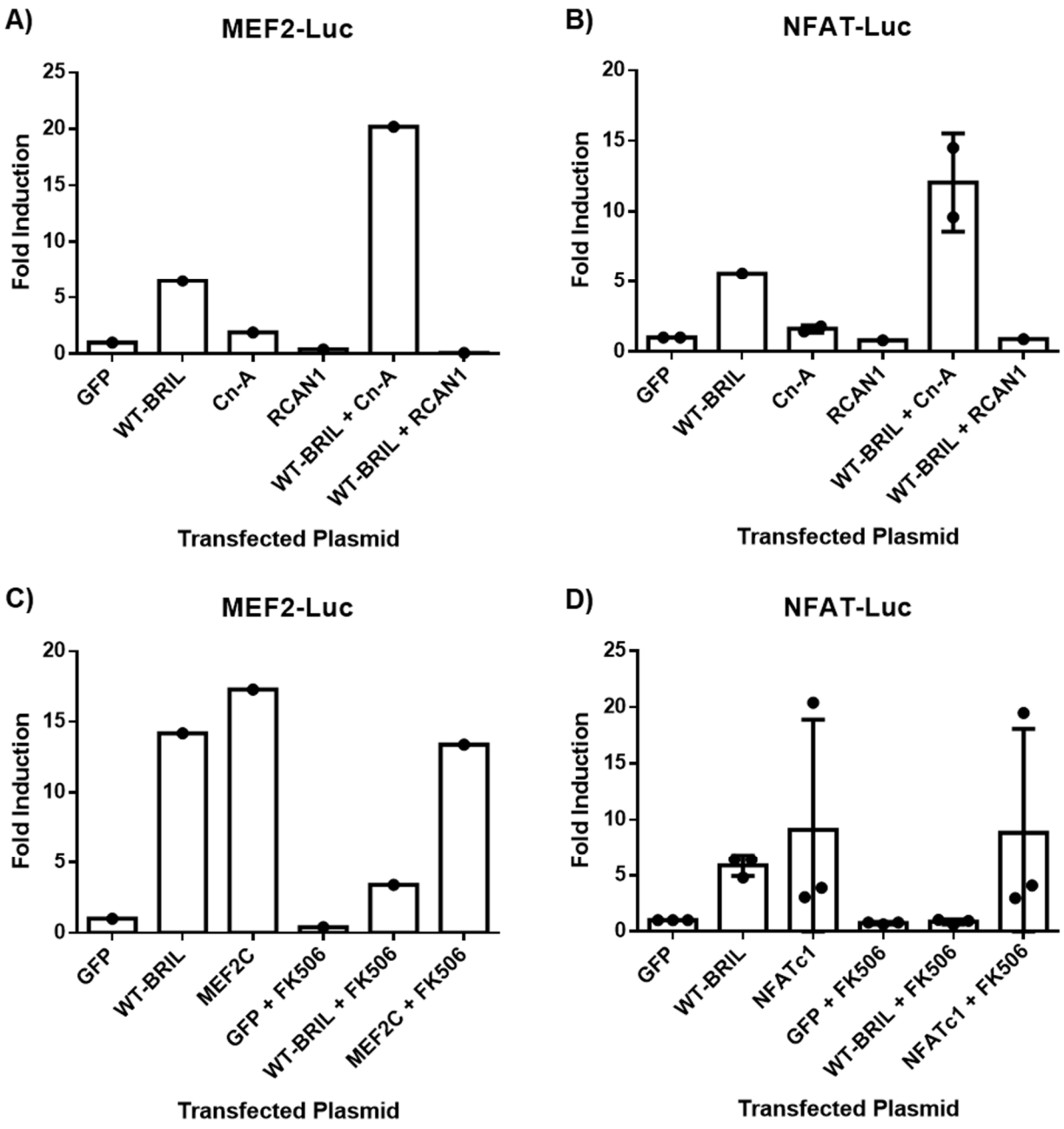

Figure 18. NFAT pathway members and calcineurin chemical inhibitor FK506 influence both MEF2-Luc and NFAT-Luc reporter readouts in transfected MC3T3 cells. Effect of co-transfecting WT-BRIL and Cn-A or RCAN1 on A) MEF2-Luc and B) NFAT-Luc. Each transfection was carried out with 50ng of both effectors and 100ng of reporter plasmids. The GFP plasmid served as the other effector for all transfection

denoted with only one plasmid. Effect of FK506 (10nM) on C) MEF2-Luc and D) NFAT-Luc readouts following WT-BRIL, MEF2C or NFATc1 transfections. Each transfection was carried out with 100ng of both effector and reporter plasmids. All results were normalized to GFP's average readout. Each data point represents one experiment, during which two repeats were performed. Data represents average ±SD, when applicable (N=1-3).

3.4.3. N-terminal modifications of WT- and MALEP-BRIL on NFAT-Luc

Similar transfection and luciferase assays involving mutants generated in section 3.3.1 to 3.3.3. were conducted in MC3T3 with the NFAT-Luc reporter. Figure 19A, 19B and 19C outline the results obtained from co-transfections of NFAT-Luc and five or six amino acid deletions of WT-BRIL, alanine scanning and other substitutions of WT-BRIL and similar alterations in MALEP-BRIL respectively.

Modulation of WT- and MALEP-BRIL's forms showed few significant results. First, co-transfections using the truncated WT-BRIL proteins with the NFAT-Luc reporter showed no significant differences with both WT-BRIL and GFP controls, and large inter-experimental variations were noted. When alanine scanning was carried out in WT-BRIL, luciferase readouts revealed that the amino acids with the greatest effect on BRIL's induction are D2, T3 and Y5, mirroring results from the MEF2-Luc reporter. However, no significant difference could be established between WT-BRIL and the D2A, D2N, D2E, T3A and Y5A mutants. In terms of modifications of the MALEP-BRIL form, the MALEP-BRIL Δ7-12 mutant induced the NFAT-Luc reporter significantly higher than the GFP negative control. However, large inter-experimental variations could not

establish significant variation between the positive control, MALEP-BRIL, and any other the alanine scanned or truncated forms. Therefore, contrary to the MEF2-Luc reporter, the role of BRIL's N-terminus with the NFAT-Luc reporter remains to be clarified.

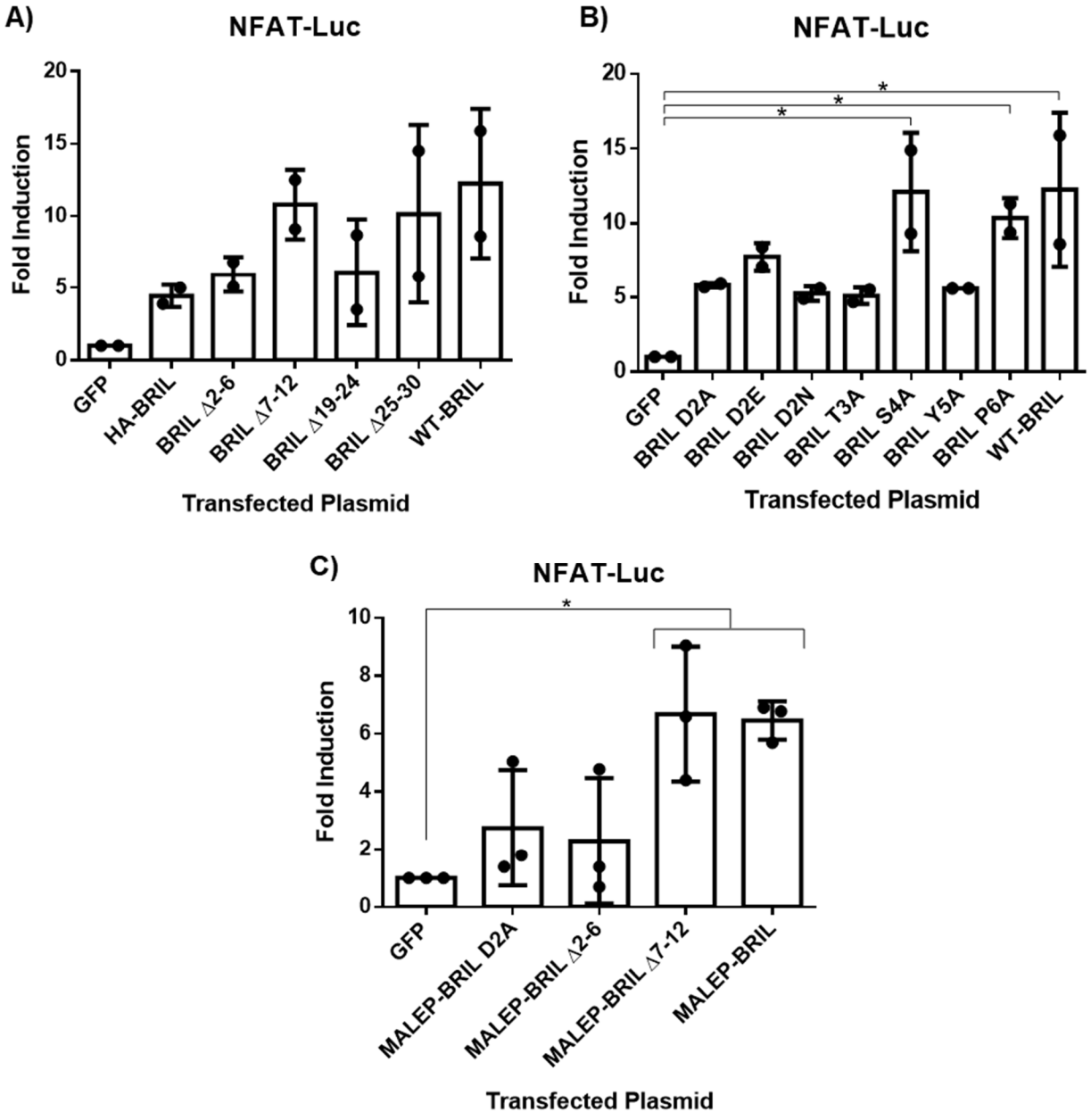

Figure 19. N-terminal truncated and alanine substitution of WT- and MALEP-BRIL on NFAT-Luc in transfected MC3T3 cells. A) N-terminal five or six amino acid

deletions in WT-BRIL. B) Effect of alanine scanning and other amino acid substitutions of WT-BRIL. C) Effect of alanine scanning and five or six amino acid deletions of MALEP-BRIL. All results were normalized to GFP's average readout. Each transfection was carried out with 100ng of both the effector and reporter plasmids. Each data point represents one experiment, during which two repeats were performed. Data represents average ±SD (N=2-3).

3.5. BRIL in MLO-A5 cell lines

3.5.1. MALEP-BRIL's induction MEF2-Luc and NFAT-Luc in MLO-A5 cells is enhanced in comparison to other forms

MLO-A5 are murine osteocyte-like cells and an alternate line to conduct BRIL overexpression experiments and test for the form-specific effects of BRIL on luciferase-reporters. The rationale for using the MLO-A5 is that they could serve as a more suitable cell line to monitor expression of sclerostin (*Sost*), an osteocytic-specific gene known to be a direct transcriptional target of MEF2C [75] and that they are more amenable to genetic modification without appreciable phenotypic drift (Dr. Linda Bonewald, personal communication) than are MC3T3. We therefore tested both MEF2-Luc and NFAT-Luc reporters in transfection assays with all forms of BRIL.

As shown in Figure 20A, both reporters were activated by BRIL but in a more selective manner than in MC3T3. First, WT-BRIL's induction of MEF2-Luc is more variable, ranging from 8- to 52-fold, while the NFAT-Luc reporter is induced from 1.5- to 6-fold. Furthermore, MALEP-BRIL shows signs of distinctly heightened induction on both reporters (ranging from 29- to 116- fold and 8- to 21-fold on MEF2-Luc and NFAT-

Luc respectively), while S40L-BRIL shows little to no induction comparable to the IFITM3 negative control. Western blots and immunofluorescent staining confirmed expression and localization of all proteins whose plasmids were transfected, though protein expression of the S40L-BRIL was significantly lower than the two other forms (Figure 20B-C).

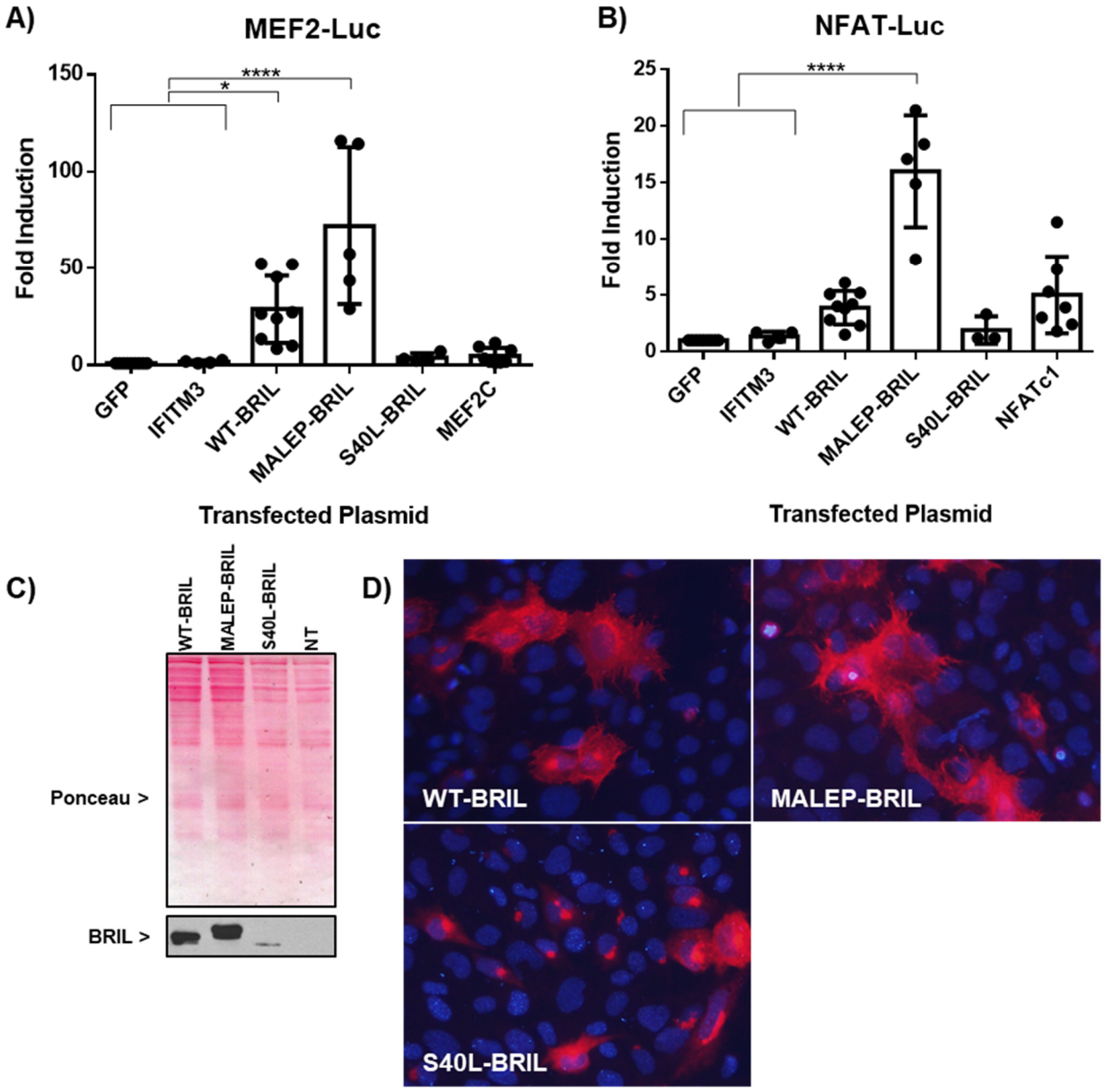

Figure 20. BRIL activity, expression and localization in MLO-A5 cells. A)-B) Effect of BRIL forms on MEF2-Luc and NFAT-Luc readout in transfected MLO-A5 cells. All

results were normalized to GFP's average readout. Each transfection was carried out with 100ng of both the effector and reporter plasmids. Each data point represents one experiment, during which two repeats were performed. Data represents average ±SD (MEF2-Luc: N=5-9 / NFAT-Luc: N=3-9). C) Western blot detection of the three forms of BRIL using anti-BRIL N-terminal antibody in transfected and naïve MLO-A5 cells. (NT=Non-transfected). D) Immunofluorescent staining of transfected MLO-A5 cells permeabilized using triton and anti-BRIL N-terminal antibody. Pictures are merged with DAPI stains and taken at 40X.

3.5.2. Gene expression in MLO-A5 in response to BRIL transfections

The various forms of BRIL also did not significantly induce changes in the endogenous mRNA levels for *Mef2*s (A, B, C, and D) and *Nfatc1-2* expression in MLO-A5 (not shown). We decided to expand the array of genes tested for expression alteration by including *Ptgs2* and *Nr4a3*, the two genes previously established as being upregulated in a MALEP-BRIL knock-in model [59]. Prostaglandin-endoperoxidase synthase 2, or *Ptgs2*, encodes cyclooxygenase 2 (COX2), is the inducible enzyme catalyzing the first step conversion arachidonic acid to prostaglandins (PGs) and a mediator of inflammation [76]. COX2 is crucial for regeneration after fracture repair [77]. The buildup of PGs outside the cell leads to stimulation of corresponding receptors that signal using the accumulation of the secondary messenger cyclic adenosine monophosphate (cAMP) and consequently activates protein kinase A (PKA), leading to the downstream regulation of factors like NR4A3. NR4A3 is a member of a family of three nuclear orphan receptors (along with NR4A1 and NR4A2) and transcriptional

regulators which have pleiotropic functions and are activated by several pathways including the PKA pathway [78]. All three NR4A are known to be expressed in bone [79, 80]. Other genes tested included *Serpinf1* (PEDF) for its link with BRIL in OI type V and atypical type VI, as well as its role as the gene whose mutation causes OI type VI. *Sost* was also included for its role as a late-differentiation osteoblast marker, as well as for its relationship with MEF2. *Sost* expression and parathyroid hormone (PTH)-driven inhibition were suggested as being mediated by MEF2A, MEF2C and MEF2D in bone cells [81]. No significant variation was observed in *Serpinf1* expression between BRIL forms (Figure 21), while *Sost* was not expressed in proliferating MLO-A5 (data not shown). However, *Ptgs2* and *Nr4a3* were both significantly upregulated when MALEP-BRIL was transfected as compared to other forms of BRIL in MLO-A5 cells, as shown in Figure 21.

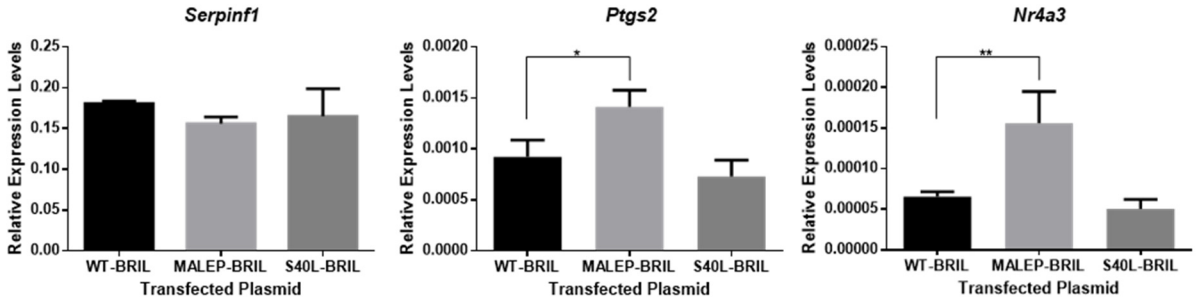

Figure 21. Quantitative PCR of various markers in transfected and naïve MLO-A5 cells. WT-BRIL, MALEP-BRIL and S40L-BRIL plasmids were transfected using 1µg of DNA. Relative expression based on β-actin (*Actb*), and subsequently normalized for a matched non-transfected control. Data represents average ±SD (N=3).

Concordant with the recorded upregulation of *Ptgs2*, the Ptgs2-Luc reporter harboring 1.13kb of the mouse *Ptgs2* promoter (that included binding sites for CRE, NF-

kB, RUNX2, C/EPB, NFAT and AP1, illustrated in Figure 22A) was significantly induced by the transfection of MALEP-BRIL (Figure 22B). In order to discriminate which portion of the promoter is responsive to BRIL, thereby also elucidating which binding elements and factor is most likely responsible for activating the *Ptgs2* gene, we generated plasmids harboring large deletions in the Ptgs2-Luc reporter, gradually shortening to promoter region to include less and less binding elements. The preliminary results tend to suggest that the proximal elements, between -253 and -195 (including the NFAT site) were less prone to BRIL induction (Figure 22C).

On the other hand, no induction was recorded for the NR4A2-Luc luciferase reporter, which features three NR4A2 binding elements (data not shown). Although the NR4A2 binding elements are not ideal for detecting NR4A3 activity, it nevertheless serves as a close surrogate for NR4A3.

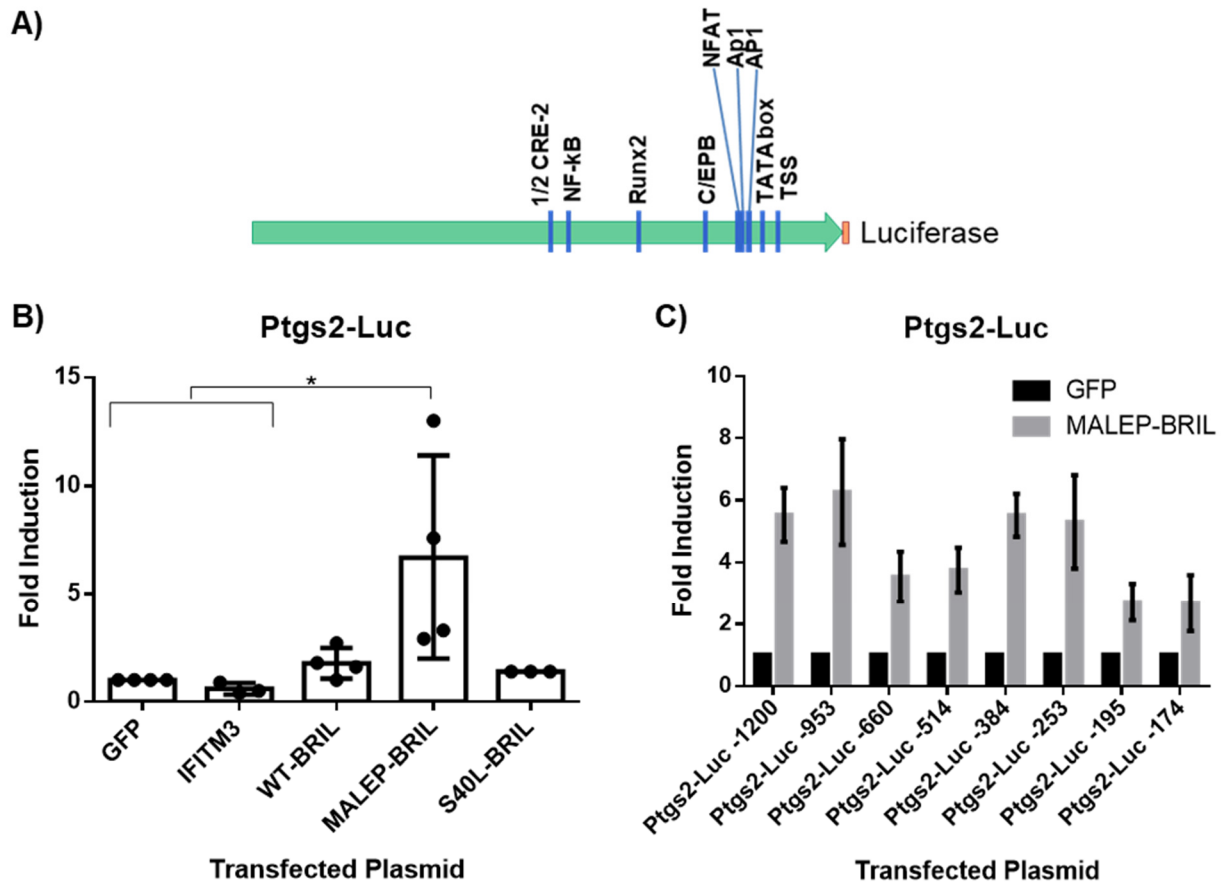

Figure 22. Structure and inductions of Ptgs2-Luc in response to BRIL transfection in MLO-A5 cells. A) Structure of the Ptgs2-Luc reporter based on the sequence of the mouse *Ptgs2* promoter. B) Luciferase fold induction readouts of Ptgs2-Luc. Each data point represents one experiment, during which two repeats were performed. Data represents average ±SD (N=3-4). C) Luciferase fold induction readouts of Ptgs2-Luc truncated forms. Data represents average ±SE (N=2). All results were normalized to GFP's average readout. Each transfection was carried out with 100ng of both the effector and reporter plasmids.

3.6. BRIL in other cell lines

3.6.1. BRIL in other cell lines

In order to better understand the cellular context which permits BRIL from acting on the previously mentioned luciferase reporters, assays were carried out in various cell lines, such as SaOS-2 (human osteosarcoma), UMR106 (rat osteosarcoma), NIH3T3 (mouse fibroblast) and HEK293 (human embryonic kidney). Inductions of MEF2-Luc by both WT-BRIL and MALEP-BRIL was also detected in SaOS-2 and UMR106 (Figure 23), which both express BRIL endogenously. However, HEK293 and NIH3T3 cell lines do not express BRIL endogenously. The MEF2-Luc reporter was not induced by BRIL in HEK293 cells, while there was some variation recorded in NIH3T3 cells (Figure 24). Inductions of BRIL forms ranged from 1.8- to 2.3-fold, WT-BRIL being the highest. Although some variation was noted between WT-BRIL and the GFP and IFITM2 controls, the MEF2C positive control's induction largely surpassed all other transfected plasmids, casting doubt on the biological significance of the observed induction by WT-BRIL. These results suggest that BRIL's activity is mainly limited to cells of bone origin. Induction of the NFAT-Luc reporter remains limited to MC3T3 and MLO-A5 cells, as readouts in other cell lines were found at the levels of our negative controls, GFP and other IFITM family members.

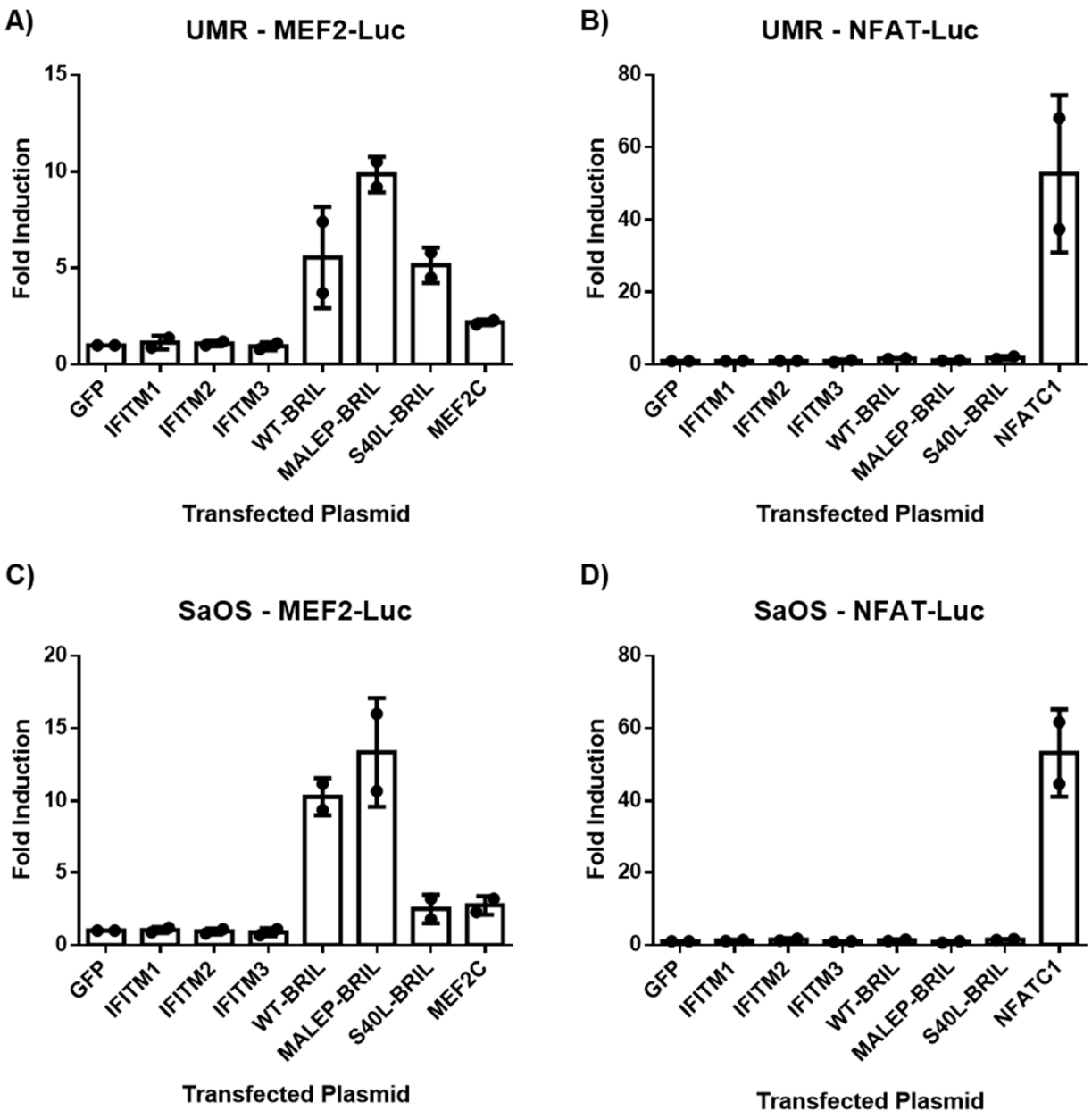

Figure 23. BRIL in other cells of bone origin. Effect of BRIL forms on MEF2-Luc (A) and NFAT-Luc (B) readout in transfected UMR106 rat osteosarcoma cells. Effect of BRIL forms on MEF2-Luc (C) and NFAT-Luc (D) readout in transfected SaOS human osteosarcoma cells. All results were normalized to GFP's average readout. Each transfection was carried out with 100ng of both the effector and reporter plasmids. Each

data point represents one experiment, during which two repeats were performed. Data represents average ±SD (N=2).

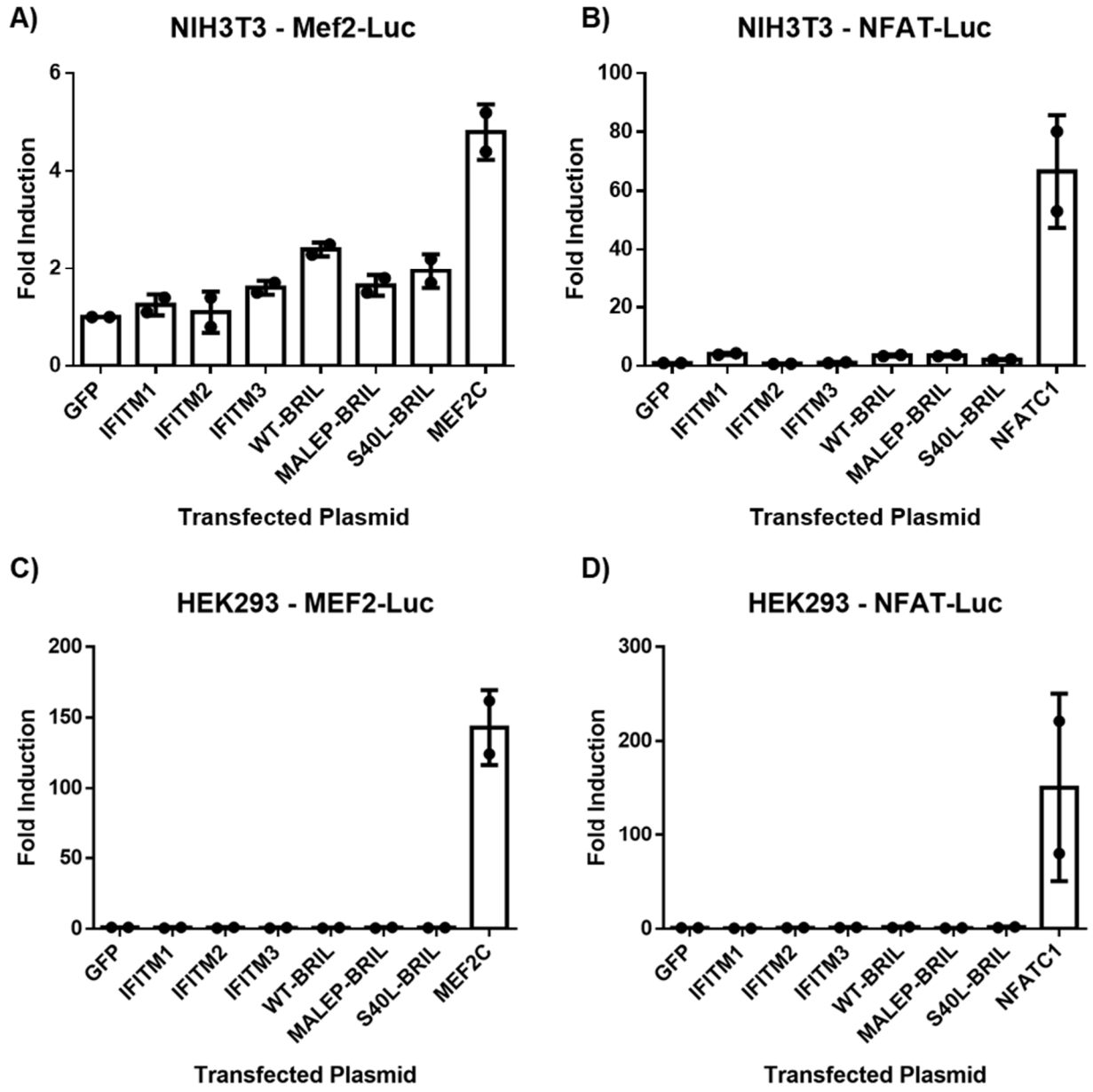

Figure 24. BRIL in other cells of non-bone origin. Effect of BRIL forms on MEF2-Luc (A) and NFAT-Luc (B) readout in transfected NIH3T3 human fibroblast cells. Effect of BRIL forms on MEF2-Luc (C) and NFAT-Luc (D) readout in transfected HEK293 human embryonic kidney cells. All results were normalized to GFP's average readout. Each

transfection was carried out with 100ng of both the effector and reporter plasmids. Each data point represents one experiment, during which two repeats were performed. Data represents average ±SD (N=2).

Chapter 4: DISCUSSION

4.1. BRIL is likely involved with MEF2 and NFAT

The main objective of the project was to determine the mechanism by which the mutant forms MALEP-BRIL and S40L-BRIL differs from the normal function of WT-BRIL, thereby causing OI type V and atypical type VI respectively. As previously mentioned, it was hypothesized that the two mutant forms of BRIL that lead to OI operate through gain-of-function mechanisms and that they are likely different based on their palmitoylation status and their subsequent cellular localization as well as their expression levels. Furthermore, based on previous works by Patoine et al. [21], both mutants are likely operative from within the intracellular compartment (whether it be the plasma membrane for MALEP-BRIL or the cytoplasmic side of the Golgi apparatus). The purpose of elucidating the mechanisms by which these mutants act was to provide insight into the mechanism causing OI type V and atypical type VI respectively in humans.

In order to possibly identify an intracellular signalling pathway that could be affected by expression of the two mutant forms of BRIL as compared to the WT form, most transient co-transfections were conducted in the MC3T3 and MLO-A5 osteoblast lines. A wide non-biased screen comprising 21 different luciferase reporters, activated by a diverse set of signalling pathways culminating on different transcription factors, was performed in HEK293, MC3T3 and MLO-A5 cells. With the previously mentioned premise, it was hypothesized that the two BRIL mutants (MALEP and S40L) could lead to a differential and/or selective activation of a pathway over the WT form. Following the screen of luciferase reporters, it was established that BRIL had the greatest inductions

on the MEF2-Luc and NFAT-Luc reporters in both MC3T3 and MLO-A5 cells, but that the effects were cell-context dependent. For instances, there were no significant differences brought about by the three different forms of BRIL overexpressed in MC3T3, and that apparently did not support our hypothesis of a dominant negative effect for the two mutant forms. However, in the MLO-A5, the MALEP-BRIL was always significantly more active than the two other forms. This could point to differences in the endogenous cell machinery in the two cell lines which is more permissible in the MLO-A5. Although the nature of those differences has not formally been deciphered, it could be due to the 'differentiation' status of the two cell types, MC3T3 and MLO-A5 being committed to osteoblast and osteocyte, respectively. Irrespective of the possible different mechanisms operating, the data presented herein are the very first ever to be reported for an 'activity' or a 'readout' stimulated by BRIL expression. This is based on and confirmed by gene and protein expression, cellular localization and luciferase assays. It is however important to note that MC3T3 and MLO-A5 cells have a very low transient transfection efficacy, whereby only an estimated 5-10% of cells truly incorporated and expressed the transfected plasmids. This is true for all transfected plasmids, regardless of their content and nature. Low transfection efficacy could potentially explain the apparent lack of effects seen in experiments following transfections. For example, if out of a total of 100 cells, only 10 were successfully transfected, and if a certain gene was upregulated 5-fold in transfected cells, the effect would be recorded as a 1.4-fold increase. This dramatic example shows that low transfection efficacy can severely dampen observed effects in endogenous gene regulation, protein expression or other assays. On the other hand, it also strengthens the detected effects on the luciferase

readouts, noted throughout this project, meaning small amounts of BRIL or other plasmids are responsible for the significant results. For example, if we noted a 1.5- and 2.4-fold upregulations of *Ptgs2* and *Nr4a3* respectively when transfection MALEP-BRIL at 10% transfection efficacy, the fold induction would be around 6- and 15-fold if 100% of the cells were transfected. Although HEK293 cells offered better transfection efficacy (around 50%), MC3T3 and MLO-A5 cells were nevertheless selected since these offered a more realistic cellular context considering BRIL is endogenously expressed in those bone cells. Similarly, outlined in section 3.6., BRIL functions on the MEF2-Luc reporter selectively in cells of bone origin, though NFAT-Luc inductions are limited to MC3T3 and MLO-A5 osteoblastic cells. The osteosarcoma cells UMR106 and SaOS-2 also differ in their expression of endogenous BRIL, whereby UMR106 constitutively express BRIL in proliferation, while SaOS-2 need to be further differentiated for them to express BRIL. Although BRIL transfections induce the MEF2-Luc reporter in osteosarcoma cells (which may suggest that the cellular machinery necessary for BRIL's function is found in these cells), no link has been reported between the presence of OI type V or atypical type VI and the increased incidence of osteosarcomas [82]. Additionally, several repeated attempts were done to stably overexpress all three forms of BRIL in MC3T3 and MLO-A5 cells using lentiviral vectors and subsequent resistant marker selection with puromycin. Stable cell lines would have been an important tool to measure endogenous gene expression in response to BRIL overexpression. However, at any given trial, homogenous cell populations expressing BRIL could not be obtained given the low percentage of cells expressing BRIL despite being resistant to puromycin. The difficulty surrounding the access to and manipulation of primary human osteoblasts

derived from OI patients also limited the availability of such cells for experimentation. Single-cell RNA sequencing could potentially offer a way to bypass the issue of low transfection and infection efficacy using MC3T3 and MLO-A5 cell populations. Despite the high cost of single-cell RNA sequencing, endogenous gene expression variations could be measured to reflect the true impact of overexpressing the different BRIL forms.

Involvement of both MEF2 and NFAT in BRIL's activity has been established through various experiments and results. First, the WT-BRIL protein seems to interact synergistically with the MEF2C transcription factor. The implied synergy is based on the results demonstrating greater-than-additive inductions of the MEF2-Luc reporter when co-transfecting both WT-BRIL and MEF2C. No such synergy was noted on the NFAT-Luc reporter, suggesting the relationship between BRIL and NFAT may be less direct than that of BRIL and MEF2. It is however important to note that the NFAT-Luc reporter contains an NFAT-AP1 composite response element, which has been denoted a weak binding site for the individual NFATC and AP1, respectively. However, they cooperatively activate when both bind its respective element [83]. The presence of NFAT alone in most co-transfections with the NFAT-Luc reporter may explain the lower induction of the reporter as well as the lack of synergy observed with BRIL. Second, we showed that HDAC4 readily participates by directly inhibiting MEF2 activity in response to BRIL transfection. Considering HDAC4's relationship with the MEF2 family members, this strengthens the hypothesis that BRIL does indeed act via MEF2 activity. Third, preliminary results demonstrated that the induction on the NFAT-Luc reporter following BRIL transfections could be enhanced by co-transfected Cn-A or inhibited by RCAN1. The modulation caused by NFAT pathway members (which are known to be involved

with NFAT itself) suggests that BRIL's induction of the NFAT-Luc reporter is likely related to the NFAT protein. Fourth, the addition of FK506, a known chemical suppressor of the Ca^{2+}-Calmodulin-NFAT pathway, in preliminary experiments demonstrated strong inhibitory effects on BRIL's induction of both MEF2-Luc and NFAT-Luc reporters. This may suggest a common upstream mechanism by which BRIL acts, which trickle down to MEF2 and NFAT activation, and will be discussed later.

The inductions of both MEF2-Luc and NFAT-Luc are interesting and pertinent given the fact that both MEF2 and NFAT have been known to have roles in osteoblasts. First, MEF2C is a transcription factor involved in osteoblast differentiation and gene regulation, thought to be upstream of bone-specific transcription factors Runx2 and Osterix [67]. These two factors are widely accepted as master osteogenic factors that allow the differentiation of mesenchymal stem cells to osteoblasts. Specifically, MEF2C binds directly to a Runx2 enhancer leading to its osteoblast-specific expression in mice [84]. However, little is known on the nature of the relationship between MEF2C and Osterix. The role of MEF2C has also been explored in osteocytes, where Dmp1-Cre-mediated Mef2c knockout led to increased bone mass in mice, through the regulation of two Wnt signaling modulators, Sfrp2 and Sfrp3 [85]. Second, the Ca^{2+}-Calcineurin-NFAT signalling pathway is involved in osteoblasts by regulating bone mass [69]. Overexpression of a nuclear-restricted form of NFAT in mice lead to higher bone mass, osteoblast overgrowth and enhanced proliferation. Other reports have suggested the inhibition of expression of osteoblast gene markers and function, and consequently a negative effect on bone formation and density following NFAT overexpression in osteoblasts of ROSA mice [86]. This was corroborated by the increase of osteoblast

differentiation and bone formation both *in vitro* and *in vivo* by pharmacologically inhibiting calcineurin b1 (upstream of NFAT) in osteoblasts [87]. Lee et al. [88] detailed the involvement of NFATc3 in the regulation of RANKL in osteoblasts, whereby NFATc3 directly binds to the RANKL promoter to stimulate RANKL expression. These findings pose a limitation to our results, as inclusion of NFATc3 in co-transfections and expression analyses may have offered further insight into NFAT and BRIL relationship. Additionally, both MEF2 and NFAT factors are controlled by their phosphorylation status and are active in the nucleus [68, 71].

4.2. Focus on the MEF2-Luc and BRIL's relationship with MEF2 and HDAC4

HDAC4 was investigated for its known inhibitory effect on MEF2 activity when present in the nucleus, which in turn is controlled by the phosphorylation status of S246, S467 and S632. *In vitro*, it has been reported that HDAC4 upregulates osteocalcin in osteoblasts [89]. *In vivo*, osteoblast-specific *HDAC4* deletion in mice yields a mild skeletal phenotype characterized by smaller vertebrae, shorter tibia and overall decreased bone volume, cortical thickness and area [90]. Additionally, these mice had elevated levels of *Mmp13* and *CTX*, markers of bone resorption, as well as *Sost*, a negative regulator of bone formation. We found that HDAC4's repression of the induction of MEF2-Luc's activity is evident but does not seem to differentiate between WT-BRIL and its two other mutant forms, MALEP-BRIL and S40L-BRIL. It is therefore likely that HDAC4 does not interact with BRIL, but rather directly with MEF2C. Based on the results presented, though also based on general RT-qPCR from an entire cell population with limited transfection efficacy, we can hypothesise the improbability that

the regulation by BRIL involves a variation in transcription of any of the HDAC classes I and IIa. Some slight changes in nuclear distribution of HDAC4 were noted following transfection of BRIL, though these may be considered biologically non-significant considering the activity of the MEF2-Luc reporter did not vary between different forms of BRIL. It is also possible that HDAC4 levels were too high to properly respond to BRIL, considering that small amounts of HDAC4 are required to inhibit BRIL's induction of the MEF2-Luc reporter.

Other possibilities were considered to explain the consequences of BRIL on MEF2 activation. BRIL could potentially affect the stability, phosphorylation status and/or subcellular localization of endogenous MEF2. However, we could not detect endogenous MEF2A and MEF2C proteins in MC3T3 cells by immunofluorescent staining nor by Western blotting. When transfected, MEF2A and MEF2C were almost exclusively restricted to the nucleus, regardless of their co-transfection with an empty plasmid or BRIL. Experiments to detect MEF2 stability and phosphorylation status were not attempted, though these may be potential avenues to explore in future projects.

4.3. Potential BRIL mechanism is likely indirect

The mechanism by which BRIL acts has also been clarified through evidences presented in this project. However, the offered hypotheses on BRIL's mechanism remain largely speculative. First, quantitative analyses of both MEF2 and NFAT gene expression revealed that neither varied dramatically in response to BRIL transfections, suggesting that BRIL has no direct effect on either transcription factor. It is again important to note that the low transfection efficacy could be responsible for diluted

observations in terms of gene expression. However, considering the same BRIL transfection (with limited efficiency) allowed us to detect gene expression changes in *Ptgs2* and *Nr4a3*, if MEF2 and NFAT genes were dramatically upregulated, it is unlikely these would remain undetected by qPCR. Second, there was no difference between BRIL forms in terms of temporal induction of the MEF2-Luc and NFAT-Luc reporters (data not shown) suggesting all forms induce MEF2 and NFAT similarly. Third, and as previously mentioned, the observed inhibitory effect of FK506 on BRIL's inductions of both reporters suggests a common upstream mechanism involving BRIL. A commonality of the effects of BRIL on MEF2 and NFAT is furthermore strengthened by the preliminary results showing co-transfections of BRIL and Cn-A or RCAN1 have synergistic and inhibitory effects respectively. Several reports feature a link between MEF2 and NFAT pathways, though the link is often established in other cell types other than bone cells. For example, MEF2 has been shown to be required for calcineurin signaling in developing skeletal muscle, specifically for myogenic differentiation [91, 92]. Likewise, some reports show a direct link between the Ca^{2+}-calcineurin/calmodulin pathway and MEF2, similar to the link with NFAT itself [93-96]. Our results, along with the established relationship between Ca^{2+}-calcineurin-NFAT and MEF2 and NFAT, allow us to hypothesise that the Ca^{2+}-calcineurin-NFAT and/or Ca^{2+}-calmodulin could be the most upstream cascade activated by BRIL, culminating in both MEF2 and NFAT transcription factors. Future endeavours could undertake experiments to measure or manipulate intracellular calcium levels to elicit physiological responses in cells transfected with BRIL (using calcium ionophores or thapsigargin, a known inhibitor of sarco/endoplasmic reticulum Ca^{2+} ATPase).

Furthermore, as previously mentioned, considering BRIL is localized at the plasma membrane and that the MEF2 and NFAT transcription factors are active in the nucleus, this suggests that the nature of the induction is likely indirect, whereby one or several factors lie between BRIL and MEF2 and/or NFAT. Given that both transcription factors rely on their phosphorylation status for their entry and subsequent activity in the nucleus, it is possible intermediate factors with phosphorylation functions lie between BRIL and MEF2/NFAT. MEF2 is involved in various kinase activity in leukemic and neuronal cells, notably the mitogen-activated protein kinase (MAPK) signaling pathways (which include the extracellular signal-regulated kinase (ERK), c-Jun N-terminal kinase (JNK) and p38 MAPK pathways) as well as cAMP-dependent PKA pathway [97-101]. Specifically, in osteoblasts, the PKA pathway is involved with PTH-driven HDAC4 regulation, which in turn influences MEF2C activity [102]. In NFAT's case, it has been shown that cAMP promotes 14-3-3 binding to and phosphorylation of NFAT, which consequently negatively regulates NFAT transcriptional activity in BHK fibroblasts [103]. Although the specifics of the interaction between BRIL and other factors remain unclear, it is also possible to hypothesise that BRIL may influence major phosphorylation pathways like PKA, which have been shown to be related to MEF2 and NFAT.

In any case, further studies will be required to exactly pinpoint the link between BRIL and MEF2/NFAT. BRIL's protein-protein interactome could be investigated using several methods, notably affinity chromatography and co-immunoprecipitation assays *in vitro*, or even yeast 2 hybrid *in vivo*. Data from these types of experiments could help determine what factor can interact with BRIL in the context of osteoblasts and MEF2/NFAT.

4.4. Structural alterations of BRIL and subsequent function effects

Valuable information was also provided by the experiments carried out on the truncated version of BRIL. When the first few amino acid (D-T-S-Y-P) in the BRIL protein are interfered with by deletion, its function that leads to high MEF2-Luc readout is inhibited. This is less clear in terms of the NFAT-Luc reporter, but similar trends have been observed. High amino acid conservation also leads to the same conclusion: the functional role of BRIL is most likely reliant on the N-terminus. The BRIL's N-terminus' role as an inducer of the MEF2-Luc and NFAT-Luc activity was further narrowed to specific amino acids found within the first of the protein, specifically D2, T3 and Y5. Through D2E and D2N substitutions, it was determined the nature of the charge and structure of the aspartic acid at position 2 were not factors important for the function of BRIL on the MEF2-Luc. The phosphorylation status of both the threonine at position 3 and tyrosine at position 5 may also be a factor influencing BRIL's activity, given the DTU Bioinformatics NetPhos 3.1 phosphorylation prediction tool scored both amino acids T3 (on human and mouse BRIL sequences) and Y5 (on mouse BRIL sequence) as potential phosphorylation candidates. Both T3 and Y5 are also heavily conserved throughout evolution with few exceptions, suggesting the nature of the amino acids are important at position 3 and 5. Since any single substitution causes abolition of BRIL's induction of the MEF2-Luc, it is possible a combination of various phosphorylated amino acids be necessary for BRIL's normal function. Currently, the phosphorylation status of BRIL is unknown, and could be assessed in future studies using mass spectrometry. The same deletion of amino acids 2-6 and alanine substitution of D2 in MALEP-BRIL were found to have a complete abrogation of induction of the MEF2-Luc reporter. This

suggests that the addition of the MALEP amino acids at the N-terminal does not replace or disturb the function of the DTSYP amino acids. The role of the C-terminal end of BRIL was also addressed using the BRIL K118-STOP mutant, which lacks the extracellular tail of the protein. While its induction of the MEF2-Luc reporter was diminished, so was its protein expression. Considering some reporter activity was still observed, it is unlikely the C-terminal tail of the protein is involved in the MEF2-Luc induction, though these results could warrant further investigation. Furthermore, BRIL's subcellular localization is likely important to its function, as revealed by the reduction or lack of induction in most instances when the protein cannot correctly localize to the plasma membrane. Specifically, the failure of BRIL forms KDEL, C52A-C53A, OSTN-BRIL to localize to the plasma membrane in a type II orientation are of note. This suggests that the N-terminus of BRIL must correctly localize the plasma membrane and must be within the cytoplasm in order to induce MEF2 activity. Therefore, it can be suggested that BRIL interacts with another membrane protein or complex leading to its induction of MEF2, and potentially NFAT though tests on the NFAT-Luc reporter have not been done. When we turn to S40L-BRIL, we show that the S40D-BRIL mutant also localizes to the ER-Golgi compartment. This suggests that the potential phosphorylation of residue S40 would unlikely be causing S40L-BRIL's mis-localization. However, the data accumulated so far does not allow us to attribute a potential gain-of-function for either the MALEP- or the S40L-BRIL that would be distinct from the WT-BRIL.

4.5. BRIL in MLO-A5 cells

The MLO-A5 cell line has enabled us to study previously established luciferase reporters in a new cellular context, revealing significantly distinct inductions of all three forms of BRIL. The MLO-A5 cell line looks promising to specifically study the MALEP-BRIL mutant, as inductions it causes are significantly and consistently higher than WT-BRIL, which is not seen in MC3T3. *Sost* expression would however not be possible to monitor as a surrogate of BRIL activity (given their similar pattern of expression in osteoblasts) considering it is not expressed in the undifferentiated MLO-A5 in which we perform the transfection. Quantitative PCR and luciferase reporter screens in MLO-A5 cells yielding *Ptgs2* upregulation and inductions of Ptsg2-Luc respectively have opened new avenues to explore a new pathway involving BRIL. The promoter of the *Ptgs2* gene has been well mapped and characterized, with the identification of many binding sites for different transcription factors regulating its expression, outlined in Figure 22A, including NFAT/AP1 binding elements [104]. Following transfection of truncated forms of the Ptgs2-Luc reporter, preliminary data suggests that the proximal elements of the *Ptgs2* promoter are less active. However, this remains to be confirmed with more repetitions. Additional experiments could include co-transfections using luciferase reporters harboring only one *Ptgs2* promoter element at a time, in an attempt to determine which specific element and associated factor may be responsible for the induction caused by BRIL transfection.

A link can be drawn between the knock-in (KI) mouse model of OI type V by Rauch et al. [59], where mice expression the MALEP-BRIL form of the protein had increased expression of *Ptgs2*. It was hypothesized that this was linked to an

inflammatory response, often associated with *Ptgs2*. In bone, COX2 is crucial for regeneration following fracture repair and could be indirectly involved in the differentiation of mesenchymal stem cells and osteoblastogenesis, though it is dispensable for bone formation as KO mice present no evident skeletal issues [77, 105, 106]. COX2 was also found to be involved in role of PTH-driven bone formation suppression [107]. Therefore, the roles of COX2 seem to act in opposition of each other, similar to the paradoxical bone fragility and increased bone formation phenotypes seen in OI type V patients. The results surrounding *Ptgs2* upregulation in MLO-A5 cells following MALEP-BRIL transfection could help draw a link between *in vitro* and *in vivo* models of OI type V, considering these same markers are upregulated in the in vivo mouse model.

Some links have been reported between Ptgs2, MEF2 and NFAT. MEF2 has been reported to be involved in gastrin-mediated *Ptgs2* expression, where activation of AP-1 and MEF2 further stimulates the *Ptgs2* promoter and increases the expression of *Ptgs2* mRNA and COX2 protein [108]. A paper by Hernandez et al. [109] has shown that NFAT appears to have a role in VEGF-induced angiogenesis through COX2 induction. Though these interactions may not be directly applicable to the context of BRIL's activity in osteoblast, it may offer some avenues to explore for future studies. Most importantly, Huang et al. [110] demonstrated a role for the Ca^{2+}-calcineurin-NFAT pathway in the PTH induction of COX2 in osteoblasts. The same publication also presents evidence of cross-talk between the cAMP-PKA pathway and the previously mentioned factors. Further investigation into the relationship between factors in these pathways and the subsequent involvement of BRIL in their function will be required.

This may be achieved by modulating the hypothetically involved pathways and recording the variations in inductions of the various reporters used in this project.

Chapter 5: CONCLUSIONS

Overall, it is now possible to include MEF2, NFAT and COX2 as candidates for downstream targets of BRIL. Though BRIL does not affect gene or protein expression, it may well affect, directly or indirectly, the three stated factors that have been shown to be involved in osteoblasts at different levels. Additionally, the study of BRIL's function is now narrower, limited to specific amino acids at the N-terminus and in the cellular context of bone cells. The disparities between WT-BRIL and its two mutant forms MALEP-BRIL and S40L-BRIL were clarified. MALEP-BRIL's structural alterations yielded similar results to WT-BRIL, but induction of MEF2-Luc, NFAT-Luc and Ptgs2-Luc are uniquely high in MLO-A5 cells. S40L-BRIL remains more elusive and will require more investigation related to its cellular localization and its mechanism leading to atypical OI type VI. Considering many questions remain in regard to the BRIL protein in general and its two mutant forms, further elucidating these functions could serve as new avenues to therapeutic applications for OI type V and atypical type VI.

Chapter 6: REFERENCES

1. Moffatt, P., et al., *Engineered viruses to select genes encoding secreted and membrane-bound proteins in mammalian cells.* Nucleic Acids Res, 2002. **30**(19): p. 4285-94.
2. Moffatt, P., et al., *Bril: A novel bone-specific modulator of mineralization.* Journal of Bone and Mineral Research, 2008. **23**(9): p. 1497-1508.
3. Hanagata, N., et al., *Phenotype and gene expression pattern of osteoblast-like cells cultured on polystyrene and hydroxyapatite with pre-adsorbed type-I collagen.* J Biomed Mater Res A, 2007. **83**(2): p. 362-71.
4. Hanagata, N., et al., *Characterization of the osteoblast-specific transmembrane protein IFITM5 and analysis of IFITM5-deficient mice.* Journal of Bone and Mineral Metabolism, 2011. **29**(3): p. 279-290.
5. Kuroda, S., et al., *Mechanical stress induces bone formation in the maxillary sinus in a short-term mouse model.* Clin Oral Investig, 2013. **17**(1): p. 131-7.
6. Friedman, R.L., et al., *Transcriptional and posttranscriptional regulation of interferon-induced gene expression in human cells.* Cell, 1984. **38**(3): p. 745-55.
7. Alber, D. and P. Staeheli, *Partial inhibition of vesicular stomatitis virus by the interferon-induced human 9-27 protein.* J Interferon Cytokine Res, 1996. **16**(5): p. 375-80.
8. Zhang, Z., et al., *Evolutionary dynamics of the interferon-induced transmembrane gene family in vertebrates.* PLoS One, 2012. **7**(11): p. e49265.
9. Hickford, D., et al., *Evolution of vertebrate interferon inducible transmembrane proteins.* BMC Genomics, 2012. **13**: p. 155.

10. Almen, M.S., et al., *Genome wide analysis reveals association of a FTO gene variant with epigenetic changes.* Genomics, 2012. **99**(3): p. 132-7.

11. Siegrist, F., M. Ebeling, and U. Certa, *The small interferon-induced transmembrane genes and proteins.* J Interferon Cytokine Res, 2011. **31**(1): p. 183-97.

12. Bailey, C.C., et al., *IFITM-Family Proteins: The Cell's First Line of Antiviral Defense.* Annu Rev Virol, 2014. **1**: p. 261-283.

13. Huang, I.C., et al., *Distinct patterns of IFITM-mediated restriction of filoviruses, SARS coronavirus, and influenza A virus.* PLoS Pathog, 2011. **7**(1): p. e1001258.

14. Lu, J., et al., *The IFITM proteins inhibit HIV-1 infection.* J Virol, 2011. **85**(5): p. 2126-37.

15. Brass, A.L., et al., *The IFITM proteins mediate cellular resistance to influenza A H1N1 virus, West Nile virus, and dengue virus.* Cell, 2009. **139**(7): p. 1243-54.

16. Kasaai, B., M.H. Gaumond, and P. Moffatt, *Regulation of the bone-restricted IFITM-like (Bril) gene transcription by Sp and Gli family members and CpG methylation.* J Biol Chem, 2013. **288**(19): p. 13278-94.

17. Li, L. and J.R. Davie, *The role of Sp1 and Sp3 in normal and cancer cell biology.* Ann Anat, 2010. **192**(5): p. 275-83.

18. Sinha, K.M. and X. Zhou, *Genetic and molecular control of osterix in skeletal formation.* J Cell Biochem, 2013. **114**(5): p. 975-84.

19. Robbins, D.J., D.L. Fei, and N.A. Riobo, *The Hedgehog signal transduction network.* Sci Signal, 2012. **5**(246): p. re6.

20. Jheon, A.H., et al., *Characterization of a novel KRAB/C2H2 zinc finger transcription factor involved in bone development.* J Biol Chem, 2001. **276**(21): p. 18282-9.

21. Patoine, A., et al., *Topological mapping of BRIL reveals a type II orientation and effects of osteogenesis imperfecta mutations on its cellular destination.* J Bone Miner Res, 2014. **29**(9): p. 2004-16.

22. Weston, S., et al., *A membrane topology model for human interferon inducible transmembrane protein 1.* PLoS One, 2014. **9**(8): p. e104341.

23. Bailey, C.C., et al., *Interferon-induced transmembrane protein 3 is a type II transmembrane protein.* J Biol Chem, 2013. **288**(45): p. 32184-93.

24. Omasits, U., et al., *Protter: interactive protein feature visualization and integration with experimental proteomic data.* Bioinformatics, 2014. **30**(6): p. 884-6.

25. Shao, S. and R.S. Hegde, *Membrane protein insertion at the endoplasmic reticulum.* Annu Rev Cell Dev Biol, 2011. **27**: p. 25-56.

26. Rabu, C., et al., *Biogenesis of tail-anchored proteins: the beginning for the end?* J Cell Sci, 2009. **122**(Pt 20): p. 3605-12.

27. Galat, A., *Peptidylprolyl cis/trans isomerases (immunophilins): biological diversity--targets--functions.* Curr Top Med Chem, 2003. **3**(12): p. 1315-47.

28. Harding, M.W., et al., *A receptor for the immunosuppressant FK506 is a cis-trans peptidyl-prolyl isomerase.* Nature, 1989. **341**(6244): p. 758-60.

29. Siekierka, J.J., et al., *A cytosolic binding protein for the immunosuppressant FK506 has peptidyl-prolyl isomerase activity but is distinct from cyclophilin.* Nature, 1989. **341**(6244): p. 755-7.

30. Kang, C.B., et al., *FKBP family proteins: immunophilins with versatile biological functions.* Neurosignals, 2008. **16**(4): p. 318-25.

31. Hanagata, N. and X. Li, *Osteoblast-enriched membrane protein IFITM5 regulates the association of CD9 with an FKBP11-CD81-FPRP complex and stimulates expression of interferon-induced genes.* Biochem Biophys Res Commun, 2011. **409**(3): p. 378-84.

32. Tsukamoto, T., et al., *Role of S-palmitoylation on IFITM5 for the interaction with FKBP11 in osteoblast cells.* PLoS One, 2013. **8**(9): p. e75831.

33. Lietman, C.D., et al., *A transgenic mouse model of OI type V supports a neomorphic mechanism of the IFITM5 mutation.* J Bone Miner Res, 2015. **30**(3): p. 489-98.

34. Patoine, A., et al., *The osteogenic cell surface marker BRIL/IFITM5 is dispensable for bone development and homeostasis in mice.* Plos One, 2017. **12**(9): p. 24.

35. Lange, U.C., et al., *Normal germ line establishment in mice carrying a deletion of the Ifitm/Fragilis gene family cluster.* Mol Cell Biol, 2008. **28**(15): p. 4688-96.

36. Firth, H.V., et al., *DECIPHER: Database of Chromosomal Imbalance and Phenotype in Humans Using Ensembl Resources.* Am J Hum Genet, 2009. **84**(4): p. 524-33.

37. Robinson, M.E., et al., *Osteogenesis Imperfecta: Skeletal Outcomes After Bisphosphonate Discontinuation at Final Height.* J Bone Miner Res, 2019.

38. Marini, J.C., et al., *Osteogenesis imperfecta.* Nat Rev Dis Primers, 2017. **3**: p. 17052.

39. Marom, R., et al., *Pharmacological and biological therapeutic strategies for osteogenesis imperfecta.* Am J Med Genet C Semin Med Genet, 2016. **172**(4): p. 367-383.

40. Sillence, D.O., A. Senn, and D.M. Danks, *Genetic heterogeneity in osteogenesis imperfecta.* J Med Genet, 1979. **16**(2): p. 101-16.

41. Tournis, S. and A.D. Dede, *Osteogenesis imperfecta - A clinical update.* Metabolism, 2018. **80**: p. 27-37.

42. Thomas, I.H. and L.A. DiMeglio, *Advances in the Classification and Treatment of Osteogenesis Imperfecta.* Curr Osteoporos Rep, 2016. **14**(1): p. 1-9.

43. Glorieux, F.H., et al., *Type V osteogenesis imperfecta: a new form of brittle bone disease.* J Bone Miner Res, 2000. **15**(9): p. 1650-8.

44. Rauch, F., et al., *Osteogenesis imperfecta type V: marked phenotypic variability despite the presence of the IFITM5 c.– 14C> T mutation in all patients.* Journal of medical genetics, 2013. **50**(1): p. 21-24.

45. Shapiro, J.R., et al., *Phenotypic variability of osteogenesis imperfecta type V caused by an IFITM5 mutation.* J Bone Miner Res, 2013. **28**(7): p. 1523-30.

46. Vieira, R.L., et al., *Hyperplastic callus formation in osteogenesis imperfecta type V mimicking osteosarcoma: 4-year follow-up with resolution.* Skeletal Radiol, 2006. **35**(6): p. 402-5.

47. Cheung, M.S., F.H. Glorieux, and F. Rauch, *Natural history of hyperplastic callus formation in osteogenesis imperfecta type V.* J Bone Miner Res, 2007. **22**(8): p. 1181-6.

48. Cho, T.J., et al., *A single recurrent mutation in the 5'-UTR of IFITM5 causes osteogenesis imperfecta type V.* Am J Hum Genet, 2012. **91**(2): p. 343-8.

49. Semler, O., et al., *A mutation in the 5'-UTR of IFITM5 creates an in-frame start codon and causes autosomal-dominant osteogenesis imperfecta type V with hyperplastic callus.* Am J Hum Genet, 2012. **91**(2): p. 349-57.

50. Farber, C.R., et al., *A novel IFITM5 mutation in severe atypical osteogenesis imperfecta type VI impairs osteoblast production of pigment epithelium-derived factor.* J Bone Miner Res, 2014. **29**(6): p. 1402-11.

51. Guillen-Navarro, E., et al., *Two mutations in IFITM5 causing distinct forms of osteogenesis imperfecta.* Am J Med Genet A, 2014. **164A**(5): p. 1136-42.

52. Hoyer-Kuhn, H., et al., *A nonclassical IFITM5 mutation located in the coding region causes severe osteogenesis imperfecta with prenatal onset.* J Bone Miner Res, 2014. **29**(6): p. 1387-91.

53. Chandler, N., et al., *Rapid prenatal diagnosis using targeted exome sequencing: a cohort study to assess feasibility and potential impact on prenatal counseling and pregnancy management.* Genet Med, 2018. **20**(11): p. 1430-1437.

54. Rodriguez Celin, M., S. Moosa, and V. Fano, *Uncommon IFITM5 mutation associated with severe skeletal deformity in osteogenesis imperfecta.* Ann Hum Genet, 2018. **82**(6): p. 477-481.

55. He, Y., et al., *A prenatal case of osteogenesis imperfecta diagnosed with next-generation sequencing.* J Obstet Gynaecol, 2017. **37**(6): p. 809-810.

56. Dagdeviren, D., et al., *Dental and craniofacial characteristics caused by the p.Ser40Leu mutation in IFITM5.* Am J Med Genet A, 2019. **179**(1): p. 65-70.

57. Corradi, M., et al., *The recurrent causal mutation for osteogenesis imperfecta type V occurs at a highly methylated CpG dinucleotide within the IFITM5 gene.* J Pediatr Genet, 2014. **3**(1): p. 35-9.

58. Reich, A., et al., *Type V OI primary osteoblasts display increased mineralization despite decreased COL1A1 expression.* J Clin Endocrinol Metab, 2015. **100**(2): p. E325-32.

59. Rauch, F., et al., *Crispr-Cas9 engineered osteogenesis imperfecta type V leads to severe skeletal deformities and perinatal lethality in mice.* Bone, 2018. **107**: p. 131-142.

60. Gregoire, S. and X.J. Yang, *Association with class IIa histone deacetylases upregulates the sumoylation of MEF2 transcription factors.* Mol Cell Biol, 2005. **25**(6): p. 2273-87.

61. Monticelli, S. and A. Rao, *NFAT1 and NFAT2 are positive regulators of IL-4 gene transcription.* Eur J Immunol, 2002. **32**(10): p. 2971-8.

62. Wang, A.H., et al., *HDAC4, a human histone deacetylase related to yeast HDA1, is a transcriptional corepressor.* Mol Cell Biol, 1999. **19**(11): p. 7816-27.

63. Clipstone, N.A., D.F. Fiorentino, and G.R. Crabtree, *Molecular analysis of the interaction of calcineurin with drug-immunophilin complexes.* J Biol Chem, 1994. **269**(42): p. 26431-7.

64. Liu, Q., J.C. Busby, and J.D. Molkentin, *Interaction between TAK1-TAB1-TAB2 and RCAN1-calcineurin defines a signalling nodal control point.* Nat Cell Biol, 2009. **11**(2): p. 154-61.

65. Clipstone, N.A. and G.R. Crabtree, *Identification of calcineurin as a key signalling enzyme in T-lymphocyte activation.* Nature, 1992. **357**(6380): p. 695-7.

66. Pon, J.R. and M.A. Marra, *MEF2 transcription factors: developmental regulators and emerging cancer genes.* Oncotarget, 2016. **7**(3): p. 2297-312.

67. Stephens, A.S., et al., *Myocyte enhancer factor 2c, an osteoblast transcription factor identified by dimethyl sulfoxide (DMSO)-enhanced mineralization.* J Biol Chem, 2011. **286**(34): p. 30071-86.

68. Crabtree, G.R. and S.L. Schreiber, *SnapShot: Ca2+-calcineurin-NFAT signaling.* Cell, 2009. **138**(1): p. 210, 210 e1.

69. Winslow, M.M., et al., *Calcineurin/NFAT signaling in osteoblasts regulates bone mass.* Dev Cell, 2006. **10**(6): p. 771-82.

70. Cohen, T.J., et al., *The deacetylase HDAC4 controls myocyte enhancing factor-2-dependent structural gene expression in response to neural activity.* FASEB J, 2009. **23**(1): p. 99-106.

71. Dong, C., et al., *Myocyte enhancer factor 2C and its directly-interacting proteins: A review.* Prog Biophys Mol Biol, 2017. **126**: p. 22-30.

72. Li, L. and X.J. Yang, *Molecular and Functional Characterization of Histone Deacetylase 4 (HDAC4).* Methods Mol Biol, 2016. **1436**: p. 31-45.

73. Seto, E. and M. Yoshida, *Erasers of histone acetylation: the histone deacetylase enzymes.* Cold Spring Harb Perspect Biol, 2014. **6**(4): p. a018713.

74. Arron, J.R., et al., *NFAT dysregulation by increased dosage of DSCR1 and DYRK1A on chromosome 21.* Nature, 2006. **441**(7093): p. 595-600.

75. Kato, Y., et al., *Establishment of an osteoid preosteocyte-like cell MLO-A5 that spontaneously mineralizes in culture.* J Bone Miner Res, 2001. **16**(9): p. 1622-33.

76. Blackwell, K.A., L.G. Raisz, and C.C. Pilbeam, *Prostaglandins in bone: bad cop, good cop?* Trends Endocrinol Metab, 2010. **21**(5): p. 294-301.

77. Zhang, X., et al., *Cyclooxygenase-2 regulates mesenchymal cell differentiation into the osteoblast lineage and is critically involved in bone repair.* J Clin Invest, 2002. **109**(11): p. 1405-15.

78. Rodriguez-Calvo, R., M. Tajes, and M. Vazquez-Carrera, *The NR4A subfamily of nuclear receptors: potential new therapeutic targets for the treatment of inflammatory diseases.* Expert Opin Ther Targets, 2017. **21**(3): p. 291-304.

79. Pirih, F.Q., et al., *Parathyroid hormone induces the nuclear orphan receptor NOR-1 in osteoblasts.* Biochem Biophys Res Commun, 2003. **306**(1): p. 144-50.

80. Pirih, F.Q., et al., *Parathyroid hormone induces the NR4A family of nuclear orphan receptors in vivo.* Biochem Biophys Res Commun, 2005. **332**(2): p. 494-503.

81. Leupin, O., et al., *Control of the SOST bone enhancer by PTH using MEF2 transcription factors.* J Bone Miner Res, 2007. **22**(12): p. 1957-67.

82. Maiya, S., et al., *Osteosarcoma occurring in osteogenesis imperfecta tarda.* Int Orthop, 2002. **26**(2): p. 126-8.

83. Macian, F., C. Lopez-Rodriguez, and A. Rao, *Partners in transcription: NFAT and AP-1.* Oncogene, 2001. **20**(19): p. 2476-89.

84. Kawane, T., et al., *Dlx5 and mef2 regulate a novel runx2 enhancer for osteoblast-specific expression.* J Bone Miner Res, 2014. **29**(9): p. 1960-9.

85. Kramer, I., et al., *Mef2c deletion in osteocytes results in increased bone mass.* J Bone Miner Res, 2012. **27**(2): p. 360-73.

86. Sesler, C.L. and M. Zayzafoon, *NFAT signaling in osteoblasts regulates the hematopoietic niche in the bone microenvironment.* Clin Dev Immunol, 2013. **2013**: p. 107321.

87. Yeo, H., et al., *Conditional disruption of calcineurin B1 in osteoblasts increases bone formation and reduces bone resorption.* J Biol Chem, 2007. **282**(48): p. 35318-27.

88. Lee, H.L., et al., *High extracellular calcium-induced NFATc3 regulates the expression of receptor activator of NF-kappaB ligand in osteoblasts.* Bone, 2011. **49**(2): p. 242-9.

89. Makinistoglu, M.P. and G. Karsenty, *The class II histone deacetylase HDAC4 regulates cognitive, metabolic and endocrine functions through its expression in osteoblasts.* Mol Metab, 2015. **4**(1): p. 64-9.

90. Nakatani, T., et al., *The Deletion of Hdac4 in Mouse Osteoblasts Influences Both Catabolic and Anabolic Effects in Bone.* J Bone Miner Res, 2018. **33**(7): p. 1362-1375.

91. Friday, B.B., et al., *Calcineurin initiates skeletal muscle differentiation by activating MEF2 and MyoD.* Differentiation, 2003. **71**(3): p. 217-27.

92. Boubali, S., et al., *Calcium/calmodulin-dependent protein kinase II regulates IL-10 production by human T lymphocytes: a distinct target in the calcium dependent pathway.* Mol Immunol, 2012. **52**(2): p. 51-60.

93. Duran, J., et al., *Ca(2+)/Calmodulin-Dependent Protein Kinase II and Androgen Signaling Pathways Modulate MEF2 Activity in Testosterone-Induced Cardiac Myocyte Hypertrophy.* Front Pharmacol, 2017. **8**: p. 604.

94. Zhang, M., et al., *Calcium/calmodulin-dependent protein kinase II couples Wnt signaling with histone deacetylase 4 and mediates dishevelled-induced cardiomyopathy.* Hypertension, 2015. **65**(2): p. 335-44.

95. Li, S., et al., *Structural and Mechanistic Bases of Nuclear Calcium Signaling in Human Pluripotent Stem Cell-Derived Ventricular Cardiomyocytes.* Stem Cells Int, 2019. **2019**: p. 8765752.

96. Li, J., et al., *Muscle A-kinase-anchoring protein-beta-bound calcineurin toggles active and repressive transcriptional complexes of myocyte enhancer factor 2D.* J Biol Chem, 2019. **294**(7): p. 2543-2554.

97. Han, J., et al., *Activation of the transcription factor MEF2C by the MAP kinase p38 in inflammation.* Nature, 1997. **386**(6622): p. 296-9.

98. Wang, X., et al., *ERK5 pathway regulates transcription factors important for monocytic differentiation of human myeloid leukemia cells.* J Cell Physiol, 2014. **229**(7): p. 856-67.

99. Chen, X., et al., *MEF2 signaling and human diseases.* Oncotarget, 2017. **8**(67): p. 112152-112165.

100. Wang, X., et al., *Regulation of neuroprotective activity of myocyte-enhancer factor 2 by cAMP-protein kinase A signaling pathway in neuronal survival.* J Biol Chem, 2005. **280**(17): p. 16705-13.

101. Daems, C., et al., *MEF2 Cooperates With Forskolin/cAMP and GATA4 to Regulate Star Gene Expression in Mouse MA-10 Leydig Cells.* Endocrinology, 2015. **156**(7): p. 2693-703.

102. Nakatani, T. and N.C. Partridge, *MEF2C Interacts With c-FOS in PTH-Stimulated Mmp13 Gene Expression in Osteoblastic Cells.* Endocrinology, 2017. **158**(11): p. 3778-3791.

103. Chow, C.W. and R.J. Davis, *Integration of calcium and cyclic AMP signaling pathways by 14-3-3.* Mol Cell Biol, 2000. **20**(2): p. 702-12.

104. Fishilevich, S., et al., *GeneHancer: genome-wide integration of enhancers and target genes in GeneCards.* Database (Oxford), 2017. **2017**.

105. Robertson, G., et al., *Alteration of femoral bone morphology and density in COX-2-/- mice.* Bone, 2006. **39**(4): p. 767-72.

106. Choudhary, S., et al., *Prostaglandin E2 acts via bone marrow macrophages to block PTH-stimulated osteoblast differentiation in vitro.* Bone, 2013. **56**(1): p. 31-41.

107. Choudhary, S., et al., *Cyclooxygenase-2 suppresses the anabolic response to PTH infusion in mice.* PLoS One, 2015. **10**(3): p. e0120164.

108. Guo, Y.S., et al., *Gastrin stimulates cyclooxygenase-2 expression in intestinal epithelial cells through multiple signaling pathways. Evidence for involvement of ERK5 kinase and transactivation of the epidermal growth factor receptor.* J Biol Chem, 2002. **277**(50): p. 48755-63.

109. Hernandez, G.L., et al., *Selective inhibition of vascular endothelial growth factor-mediated angiogenesis by cyclosporin A: roles of the nuclear factor of activated T cells and cyclooxygenase 2.* J Exp Med, 2001. **193**(5): p. 607-20.

110. Huang, H., et al., *Parathyroid hormone induction of cyclooxygenase-2 in murine osteoblasts: role of the calcium-calcineurin-NFAT pathway.* J Bone Miner Res, 2010. **25**(4): p. 819-29.